UNIVERSITA' DEGLI STUDI DI MILANO

SCUOLA DI DOTTORATO DI RICERCA IN SCIENZE BIOCHIMICHE, NUTRIZIONALI E METABOLICHE

DIPARTIMENTO DI CHIMICA, BIOCHIMICA E BIOTECNOLOGIE PER LA MEDICINA

DOTTORATO DI RICERCA IN BIOCHIMICA, CICLO XXIV

TESI DI DOTTORATO DI RICERCA

STRUCTURAL PROPERTIES AND INTERACTIONS AT THE SURFACE OF BIOMIMETIC AGGREGATES

RONDELLI, VALERIA MARIA

Tutor:
Prof. Sandro SONNINO
Prof. Laura CANTU'

Coordinatore del dottorato:
Prof. Francesco BONOMI

Anno Accademico 2010/2011

CONTENTS

1. INTRODUCTION

General aspects of biological membranes

Living cells must contain all that is needed to survive and reproduce themselves. This depends on the existence of membranes. Membranes are self-aggregating objects that can form lamellar structures, with a thickness between 60 and 100 Å. They entrap cellular compartments with different composition. While varying from cell to cell, their mean composition is kept: a cell membrane is composed for 40% by lipids and for 60% by proteins.

1.1. Membranes functionality

- **Structural Role**

Plasma membranes define the individuality of the cells, separating them from the environment and controlling the composition of the in and out regions. They are in fact highly selective permeability barriers, they can regulate the molecular composition of the medium and intracellular ions, they contain selective transport systems, which allow the controlled inward and outward flow of specific molecules. In eukaryotic cells also intracellular membranes are present, thinner than the plasma membrane. They define cell organelles such as mitochondria or lysosomes. In the intracellular space membranes may also form bicontinuous structures, such as in the Golgi apparatus. This structural arrangement increases the surface area available for certain functions while in a confined space.

- **Dynamic Role**

Membranes are dynamic structures, capable of movements that enable the cell and subcellular structures to modify their shape and to move. The plasma membrane is extremely soft with respect to fluctuations or shape changes, but it is virtually incompressible for side stress. This unique combination of dynamic properties allows cells to travel long distances without loss of material. Some important mechanisms of compositional regulation or macromolecular transport across the membrane depend on specific dynamic properties. For example, endocytosis requires the invagination of a segment of the membrane containing a small volume of extracellular fluid. Then the so formed vesicle is detached, while the membrane melts to weld at the site of invagination. Similarly, cells can release macromolecules outside, through the exocytosis process. In

Figure 1 examples of these processes are shown. Budding and fusion of vesicles is involved.

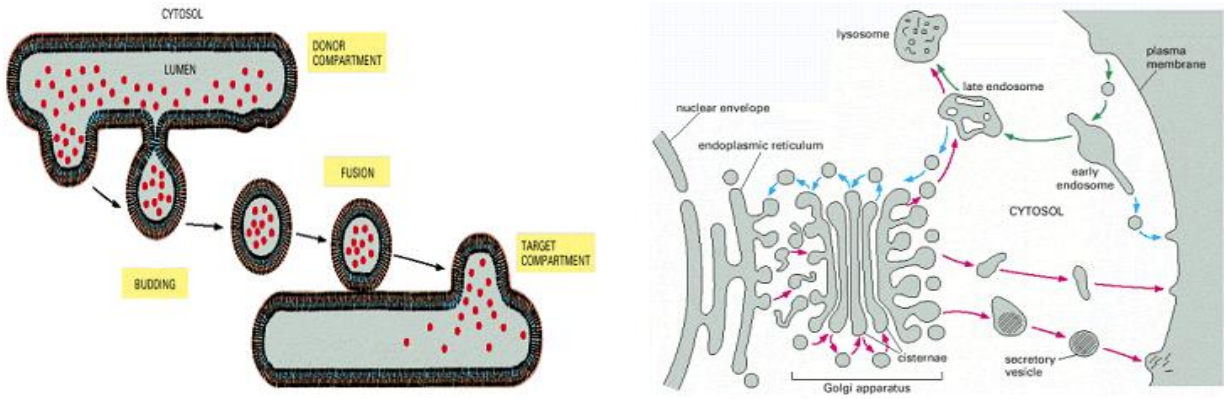

Figure 1. Right side: schematic view of an intracellular transport route from the endoplasmic reticulum to the cell membrane mediated by vesicles. Left side: phenomena of invagination, fusion and fission are sketched.

These phenomena, responding to specific needs of the cell, are based on a local change of elasticity or because of surface tension effects between regions of different curvature. When a shape change occurs, the elastic energy of the cell membrane is involved.

- **Functional Role**

By controlling the flow of substrates, ions, etc. from one compartment to another, membranes modulate the concentration of substances, influencing the metabolic pathways. Membranes also regulate the flow of information between cells and their environment through specific receptors for external signals.

1.2. Membranes composition: relation to the specific role

Lipids and proteins are the main components of membranes, but their amount greatly varies in different membranes. The membranes also contain a small amount of polysaccharides, in the conjugated forms of glycoproteins or glycolipids.

- **Lipids**

The three main classes of membrane lipids are phosphoglycerids, sphingolipids and cholesterol. Cholesterol has a hydrophobic compact structure, while phosphoglycerids

and sphingolipids are amphiphilic molecules. Each tissue has a particular composition in lipids. The composition of fatty acids of sphingolipids and phosphoglicerids is tissue-dependent. Often a greater variability is observed between membranes of different tissues as compared to similar membranes of tissues belonging to different species, indicating the existence of a relationship between composition and function. The myelin membranes, for example, which work as insulating sheaths of nerve axons, have a low protein content (18%), while they are rich in lipids, in particular they have a high proportion of glycosphingolipids. Cardiolipin is located only in the inner mitochondrial membrane, and few internal membranes are poor in sphingolipids and cholesterol. The lipid composition can alter membrane fluidity.

- **Proteins**

Proteins are responsible for most of membrane processes. They can have transport, catalytic, structural and recognition functions. In the plasma membrane proteins are about the 50%, while intracellular membranes have a higher protein content due to their higher enzymatic activity. For example, in membranes involved in energy transfer processes, such as the inner mitochondrial membrane, the protein content is up to 75%.

- **Carbohydrates**

Carbohydrates are found in membranes as glycoproteins or glycolipids. These molecules are present only in the outer plasma membrane or the luminal side of the endoplasmic reticulum. In particular, gangliosides are glycosphingolipids, amphiphilic molecules where the hydrophobic domain is a lipid (ceramide), while the hydrophilic is composed by saccharidic groups. In gangliosides at least one of these sugar rings is a sialic acid, that is it contains a –COOH group, dissociating in $–COO^-$ and H^+. When isolated from membranes, gangliosides are usually prepared as Na^+ salts. In aqueous solution, gangliosides may dissociate, leaving the negatively charged sugar.

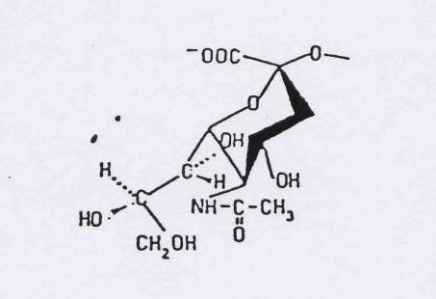

Figure 2: sialic acid structure**.**

Glycosphingolipids are fundamental components of cellular membranes and, especially in nervous tissues, a significant amount of them (~10%) is constituted by gangliosides. Gangliosides differ from one another in both the hydrophobic and the hydrophilic groups. Their classification is based on their hydrophilic head.

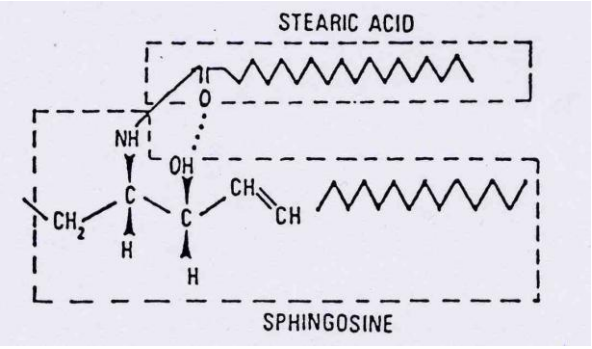

Figure 3: structure of ceramide.

As for the sugar backbone they are classified as:
series 1: glucose, galactose, N-acetylgalactosamine, galactose
series 2: glucose, galactose, N-acetylgalactosamine
series 3: glucose, galactose
series 4: galactose
The sialic is linked to a galactose unit or to another sialic. As for the number of sialic acid residues they are classified as monosialic (M), disialic (D), trisialic (T). The lowercase letters “a” and “b” refer to the different spatial arrangement that sialic can have, typically parallel or serial. The number of sialic acids is very important because it corresponds to the maximum charge of the head, although they may be only partially dissociated. Moreover their spatial arrangement is very important for steric reasons.

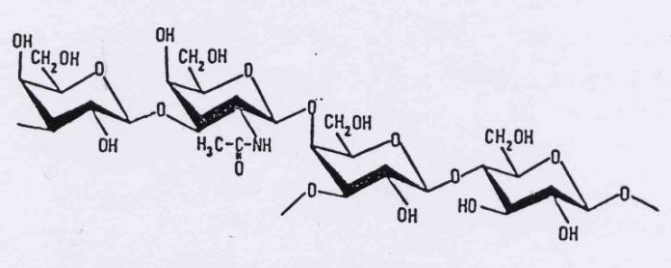

Figure 4: structure of the main sugar chain of the heads.

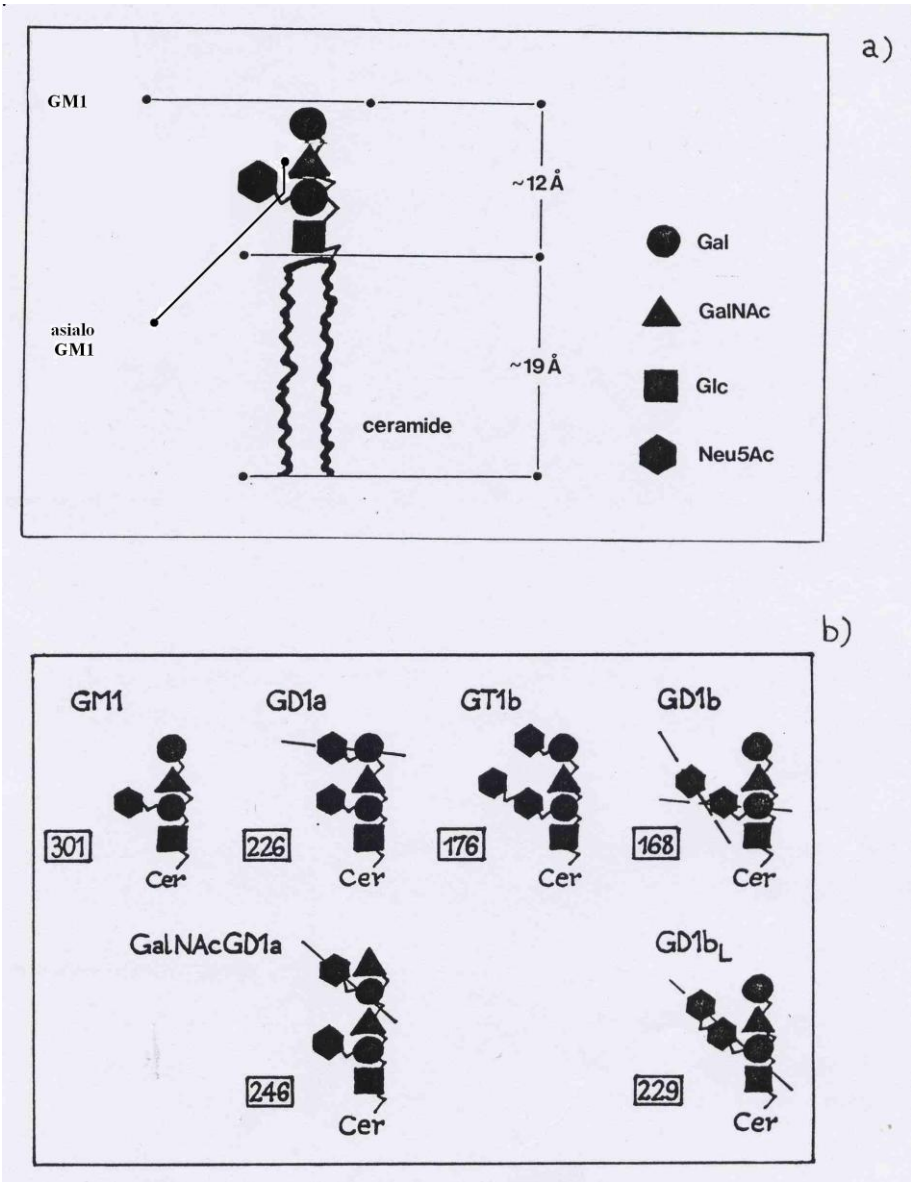

Figure 5: Structure of various sugar molecules varying the number and configuration of the sugars.

In this thesis work we focused mainly on GM1 and GD1a gangliosides.

Most gangliosides fulfill the conditions necessary to form micelles in aqueous solutions (in normal conditions), except for GM3 and GM4 that form vesicular bilayers due to their

reduced head size. Moreover, in the presence of sufficient amounts of other lipids, they can form extended mixed bilayers.

Let us dwell briefly on the characteristics that gangliosides are likely to confer to the cell membrane where they are embedded:

a) The presence in the molecule of both hydrophobic and hydrophilic charged moieties, makes gangliosides suited to interact with a variety of different substances.

b) Because of Coulomb repulsion, the presence of negative charge in the heads requires a big area, increasing locally the liquid character and the compressibility of the membrane.

c) The ionic character of gangliosides influences the surface potential of the membrane, raising its value.

d) Both the ceramide and the saccharide headgroup have a dipole momentum. The total momentum of the molecule is strongly influenced by the presence of one or more dissociated sialic acids and by their position. The extent of dissociation and type of ganglioside therefore bring about significant changes in the dipole moment of the surface of the membrane, reflecting in the intermolecular interaction energies of the constituents of the membrane itself.

e) Gangliosides are inserted in the membrane with the lipid tails normal to the surface. Like the other components they have a certain translational and rotational mobility that contributes to membrane fluidity. An increased fluidity has been observed in the presence of gangliosides, proportional to their lateral mobility, connected to the structure of the polar head. Fluidity increases by increasing the number of sialic acids and decreasing the length of the oligosaccharide chain. The influence of gangliosides on the flow properties of the membrane can be understood by considering their aggregation behavior.

f) Gangliosides are arranged in the outer layer of the membrane, thus presenting a totally asymmetrical distribution, functional to their role.

Gangliosides display both a strong hydrophobic character, due to the presence of an extended double lipid chain, and a strong hydrophilic character as well, increasing with the increase of the number of sugar rings. Gangliosides are a particular class of amphiphiles in which the packing properties can be attributed to the geometrical characteristics of the headgroup, which requires a large space to accommodate the sugars and their water of hydration. The greater the area of the interface, the smaller the aggregates, with a lower number of aggregation.

Table 1: Main structural parameters obtained for various gangliosides**.**

	Molecular weight	Number of sugars	Aggregation number	Area at the interface ($Å^2$)	Packing parameter	Hydrodinamic radius (Å)	Charge (q_e)
GM2	1398	4	451	92	0.440	66	100
GM1	1560	5	301	95.4	0.428	58.7	48
GD1a	1851	6	226	98.1	0.416	58	60

The size of the hydrophobic moiety was calculated to be l_c = 23.64 Å, V = 963 $Å^3$. The value of l_c was used parametrically in the evaluation of the monomeric area at the interface (depending on the model of Israelachvili) while the value l = l_c = 18.91 • 0.8 Å was taken as the length of the semi-minor axis of the core of globular micelles in a hydrodynamic simulation. The extension of the hydrophilic layer was evaluated by following the instructions of Maggio, giving a value of 4 Å for each group in a straight-chain sugar, reduced by a factor of 0.85 for flexibility.

1.2.1. Membrane structure

The presence, the amount and their lateral distribution within the layers of membrane is related to their specific activity. The fluid mosaic model of Singer and Nicolson can help to outline the organization of the membrane layers. This model describes the membrane as a two-dimensional solution of oriented proteins and lipids. The basic structure consists of a lipid bilayer, where the hydrophobic chains of the individual molecules are shielded from contact with the aqueous solvent by the polar heads.

Because the structure of the lipid bilayer is dictated by the physico-chemical properties of the participating molecules, we point out some characteristics of the membrane structure in relation to the arrangement and composition of its components.

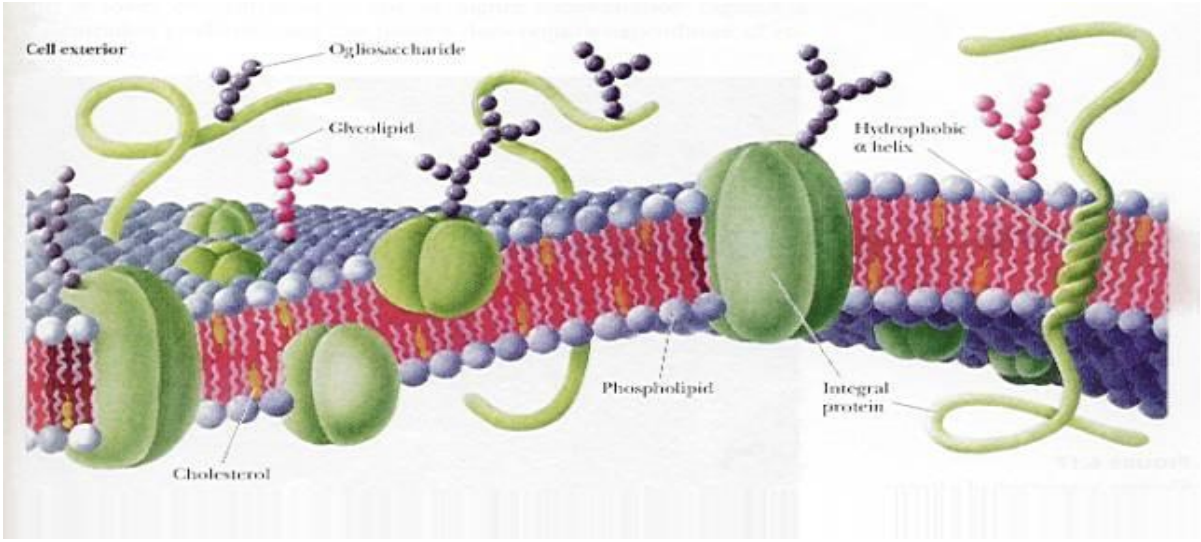

Figure 6: Fluid mosaic membrane model

- **Lipid-protein interaction**

Membrane proteins are linked by more or less strong interactions with the lipid bilayer: the type of interaction and localization of proteins reveal a high degree of organization of the membrane. For example, proteins involved in the transport of electrons in the inner membrane of mitochondria are organized in functional units, both laterally and across the membrane. In addition, proteins show an orientation within and across the lipid bilayer, such as in the case of enzymes, which need to expose the catalytic site to one of the two sides of the membrane. In the case of proteins that cross the membrane, the structure is stabilized by the interactions between the non-polar tails of lipids and the hydrophobic domains of these proteins. We should therefore assume mechanisms of selective lipid-protein interactions. These mechanisms must take into account the physics of the system, the interaction forces that can actually be established between specific molecules. For example: if the size of the hydrophobic domain of the protein and the average thickness of the lipid bilayer should not be compatible, we have to imagine a stretching of lipid chains to let the protein fit the bilayer, as shown in Figure 7 [Sackmann].

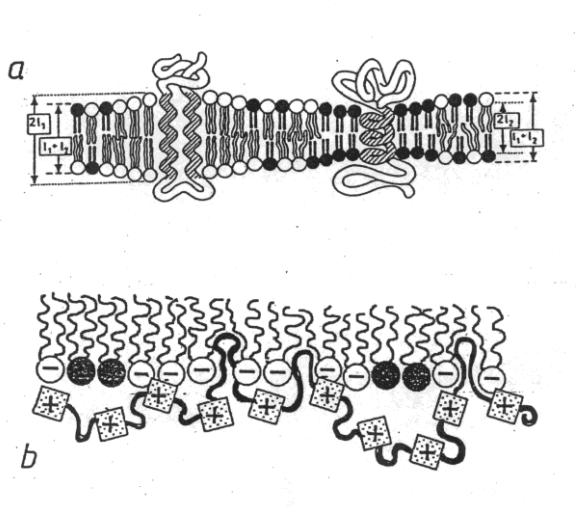

Figure 7: Mechanisms of lipid-protein specific interactions.

a) interaction due to the compatibility between the lipid layer thickness and the length of the hydrophobic region of the protein.

b) electrostatic interaction between a filamentous protein and bilayer.

It is evident from the figure 7 that a suitable arrangement of lipid molecules with different hydrophobic chain length will lead to the attractive interaction between the protein and the membrane throughout the thickness of the hydrophobic domain, creating a very stable structure. So even the arrangement of lipid molecules around the protein cannot be random, but it is dictated by specific requirements for compatibility.

Another mechanism of interaction of proteins with the lipid membrane is electrostatic. Many peripheral proteins may show this type of interaction. In this case, it is necessary to assume an appropriate collection of membrane lipids, dictated by the need to achieve a particular surface charge distribution in the region of the protein interaction domains. In Figure 7b an example of this mechanism of selective interaction between a filamentous protein (eg spectrin) and the bilayer is shown.

- **Asymmetry and spontaneous curvature**

Membranes are structurally and functionally asymmetric, in fact they show differences both in composition and enzyme activity. For example, the pump that regulates the concentration of Na + and K + into cells, consists of a transport system oriented in such a way to transport K + inside and and Na + outside of the membrane. The distribution of lipids is asymmetric. Probably the asymmetry is generated during the biosynthesis of the membrane and is maintained thanks to the very long characteristic times required for molecules to move from one side to the other of the membrane (flip-flop). In particular we want to emphasize the total asymmetry of carbohydrates, either in the form of glycoproteins and of glycolipids. In fact, these molecules are arranged only on the outer side of the membrane with the hydrophilic portion that extends into the extracellular

space. This special distribution is linked to the role of these molecules in the processes of recognition, adhesion and as receptors.

From the structural point of view, an important effect of the asymmetry of the two lipid layers is the possibility to have a spontaneous curvature. The outer layer of the membrane can be made up of molecules that on average show a greater tendency to the formation of a convex closed structure, more than the inner layer (according to laws based on the needs of individual monomers). This phenomenon stabilizes the closed structure of the membrane. Moreover, even within the pseudo-two-dimensional system of a single layer of the membrane, it is possible to make local phase separations between regions with different spontaneous curvature. This is the case, for example, with lipids with different hydrophobic length, or a different presence of glycolipids or proteins. The ability to create regions with different spontaneous curvature is at the basis of all phenomena of invagination, merging, channel formation etc.. For example, in the process of endocytosis, the vesicle detaching from the membrane has a different composition with respect to the parent membrane. Spatial selection of components is essential for the dynamic roles of the membrane.

- **Fluidity**

The interactions among lipids and between lipids and proteins are very complex and dynamic. Thanks to the fluidity of the membrane, both the lipid molecules and the proteins can move laterally. The degree of fluidity depends on temperature and on the composition of the fatty acid chains. The lipid chains can be "ordered" (C-C bonds in the *trans* conformation) or "disordered" (some links in *gauche* conformation). The transition from the gel-chains to the fluid-chains state occurs above a particular temperature, T_m, called melting temperature. The transition temperature depends on the length of the chains and on their degree of instauration.

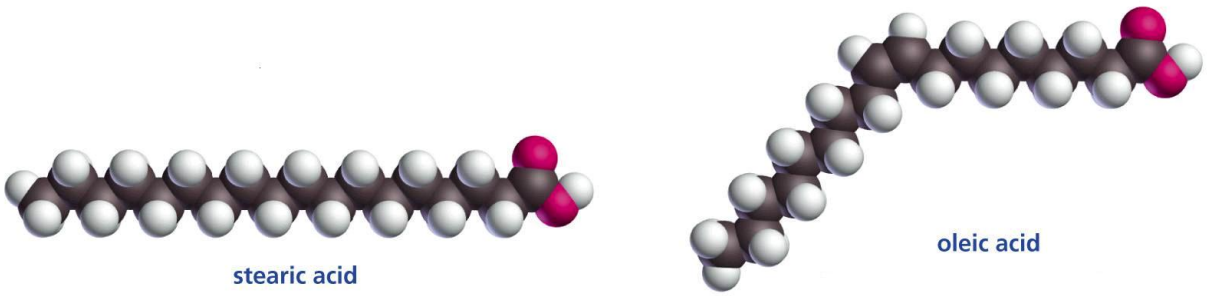

Figure 8: chains configurations with or without double cis bond.

Obviously, the presence of a kink in the chains causes “disorder” and therefore a lowering of the transition temperature. T_m increases with the length of the chains. Thus the fluidity of a membrane changes if the lipid composition changes (for example, if the degree of unsaturation of the chains changes). The individual lipid molecules can diffuse along the layer of the membrane in association with other specifically interacting molecules, for example through electrostatic or lipid-protein interactions. Areas with different degrees of fluidity can then be created, with islands of molecules that diffuse in the fluid layer. Once again we emphasize the importance of the physical properties of the system: the creation of zones with different fluidity is given by a partial phase separation between domains with different transition temperature. It is analogous to the movement of a solid body in a fluid surface. The ability to regulate membrane fluidity is essential both for the dynamic role of the membrane, and for the functional one (enzymes also can diffuse more or less rapidly in the layer). It is also interesting to study the elastic properties of membranes, because their motions create fluctuations in areas with a higher or lower density of molecules.

1.2.2. Self-aggregation mechanism

Amphiphilic molecules show a significant spatial separation of their solubility characteristics, as they are formed by an hydrophobic (one or two hydrocarbon chains) and a hydrophilic part (called the headgroup). In aqueous solution, they tend to form aggregated structures in order to shield the hydrophobic parts from contact with the hydrophilic solvent. The characteristic of the different structures that are formed (shown

in figure 9) are determined by several factors among which the most important are steric and thermodynamic.

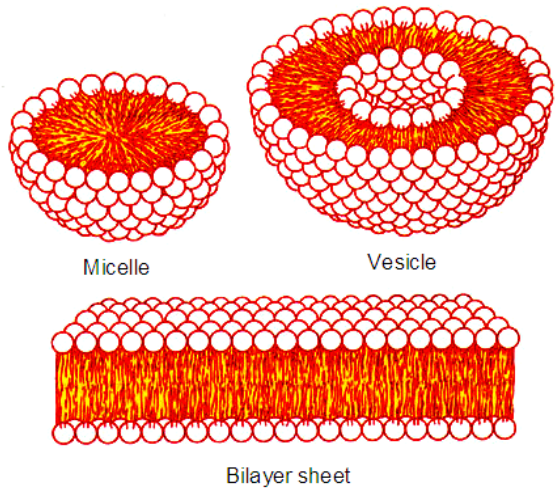

Figure 9: Organized structures formed by amphiphilic molecules in water. Single chain amphiphils form micelles while those with double chain usually form bilayers.

The aggregation of molecules in well-defined structures, such as micelles or bilayers or vesicles, derives from the interaction between the hydrophobic chains, which prefer to cluster, and the hydrophilic nature of the headgroups, which forces them to stay in contact with water. These two competing effects give rise to the idea of "opposite forces": one that tends to decrease, the other to increase the area in contact with the solvent. All this leads to the concept of *optimum surface area* for heads, corresponding to minimum interaction energy. We can use geometric considerations to determine the possible structures of the aggregates. These depend on the volume of the hydrocarbon chain and its maximum possible extension. While in some cases this analysis allows to unequivocally predict the form of aggregates, sometimes it gives alternative structures, such as both micelles and vesicles. The key factor in these cases is entropy. This tells us that structures with a large aggregation number, although energetically or geometrically possible, are entropically not favored.

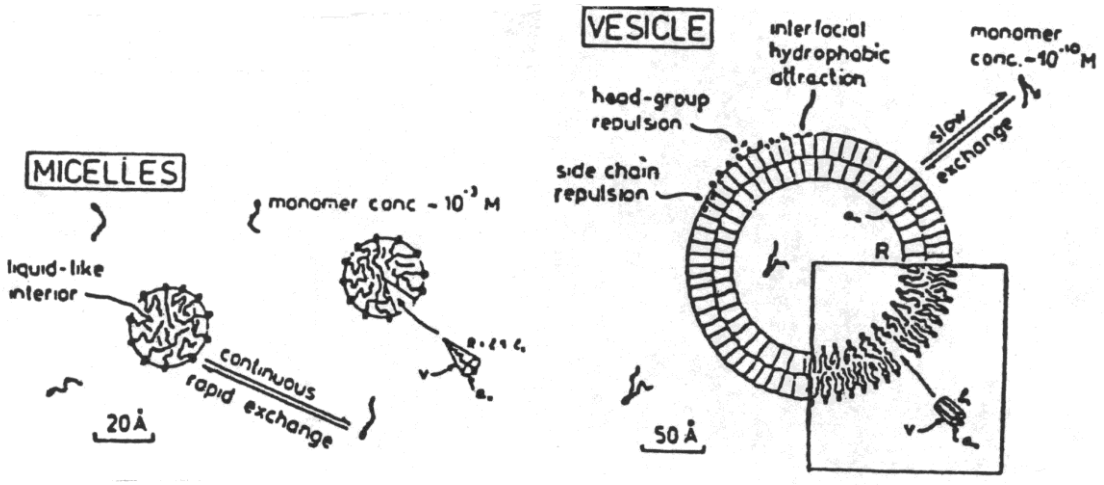

Figure 10: Schematic representation of the formation of micelles and vesicles in water. The entropy favors structures with low aggregation number.

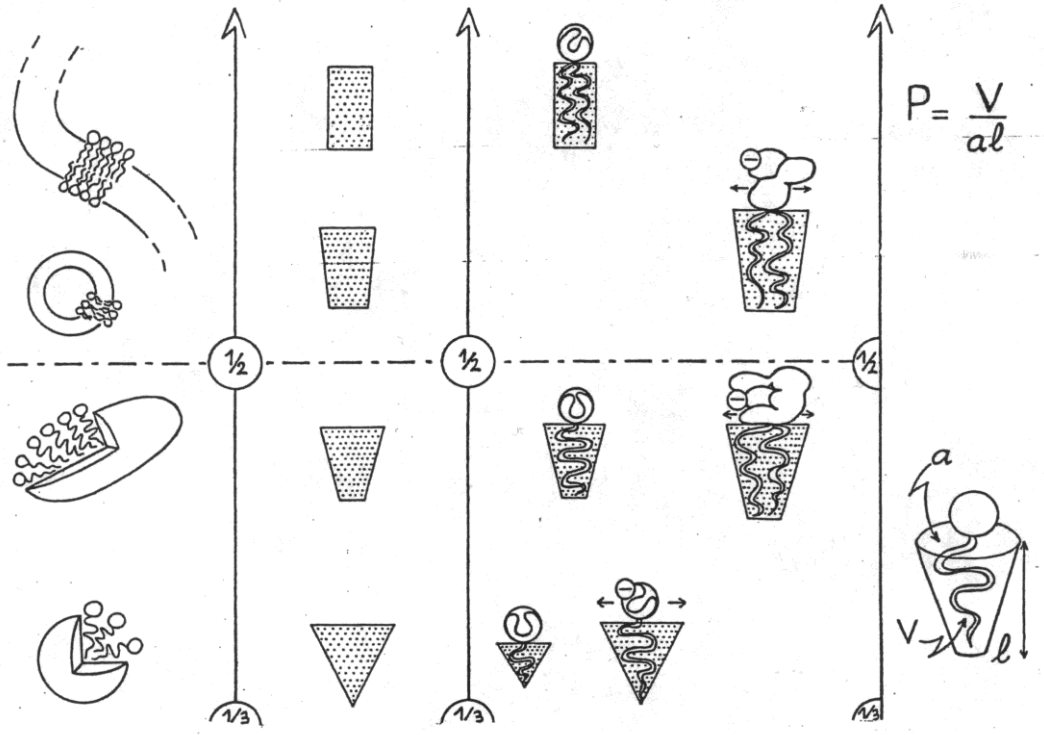

Figure 11: From left to right: different structures for amphiphilic molecules determined by the variation of packing parameter P. This parameter depends on the characteristics of the monomer, for example the complexity of the head, possibly charged, the presence of one or two hydrophobic tails.

1.3. Role of lipids in membranes

A long lived controversy concerns whether proteins or lipids are the major players in governing the structure of biological membranes. On one side, the huge presence of proteins in biological membranes is underlined, with their multi-scale molecular complexity. Proteins cover, cross and decorate membranes on both faces. On this basis, they are claimed to organize the membrane structure by sorting suitable lipids to populate their environment, originating the membrane compositional unevenness. On the other side, the role of lipids is underlined. Biological membranes exist thanks to the aggregational properties of complex lipids. Moreover, with their cooperative behaviour lipids reach the complexity of a “non-covalently-bound macromolecule”, much bigger and adaptive than a protein. Even a simple pure phospholipid single-component model membrane is well known to respond to environmental stimuli, like pressure or temperature, modulating, through cooperativity, a variety of features like fluidity, elasticity, permeability, surface stiffness and crowding. Collections of even simple phospholipids are sophisticated enough to allow not only for phase transitions, but also for phase coexistence and phase- sensitivity to spatial confinement [Corti et al. (2006) (2007)]. In complex biomembranes, the lipid matrix has to match very different requirements. The ordered structure of the lipid bilayer is overall very stable, compatibly with its primary function as a physical barrier. However, biological membranes need to act as well as the active interface between the different environments that they separate from each other, thus they need to be highly dynamic in their structural properties both in space and in time. In this, they can also sustain and promote the protein functions, for example, by modulating lateral and transverse barriers, providing adaptive solubility media, cooperating in membrane punctual or extensive deformations.

Spontaneous aggregates with different curvature and topology can be obtained not only with multicomponent systems , but also with monocomponent glycosphingolipid systems [Cantu et al. (1997a) (2000); Boretta et al. (1997)]. So, not only mixing of different lipids, but also local demixing of mixed lipids within the same aggregate gives rise to diverse additional features [Cantu et al. (1997b)]. Local lipid demixing is observed in model systems [Jorgensen and Mouritsen (1995); Knoll et al. (1991)], and it has been hypothesised long time ago to occur also in biomembranes [Lee et al. (1974); Wunderlich et al. (1975) (1978); Karnovsky et al. (1982); Simons and van Meer (1988); Israelachvili (1977); Jain and White, (1977)]. Hunting the raft has constituted a topic for research and

discussion much before the development of suitable experimental techniques to unequivocally assess its existence.

Biological membranes are out-of-equilibrium complex systems [Mayor and Rao (2004)], thus sometimes a fundamental question arises, whether model artificial systems are adequate for an appropriate description. A membrane model system can be achieved by extracting a lipid mixture from the native biomembrane or by mixing purified individual components and if built up starting from individual components. In both cases, they are unavoidable limitations connected with the system preparation. In fact, many studies on domains in biological membranes rely on the putative resistance of lipid raft components to the solubilization by non-ionic detergents. Detergent-resistant membrane preparations might reflect the properties of lipid rafts in living cells [Sonnino and Prinetti (2008)], however they are undoubtedly systems driven to equilibrium by the specific experimental conditions used for detergent extraction systems. On the other hand, simple membrane models are forcedly strongly over-simplified. One of the major limitations is that they rarely take in consideration a very important feature of biological membranes, i.e., their asymmetry. Asymmetric distribution of lipid components across the bilayer is particularly marked in plasma membranes, highly enriched in the strongly asymmetric sphingolipids and cholesterol. In a typical plasma membrane, sphingolipids and phosphatidylcholine are the major components of the outer layer, while phosphatidylserine and phosphatidylethanolamine are mainly present at the cytoplasmic face. The cytoplasmic leaflet is also more enriched in cholesterol. In addition, while the spontaneous flip-flop of glycero- and sphingo- lipids from one to the other layer are strongly unfavoured and can only occur as energy-dependent events, cholesterol can freely and rapidly move from intracellular stores to the inner leaflet and diffuse to the outer layer, or vice versa, introducing a further dynamical aspect [Wood et al. (2011); Schroeder et al. (1991)].

Cholesterol and sphingolipids show cooperative effects of many biological processes, not limiting to lipid-driven membrane organization (for example, both they are synergically acting to regulate the function of transmembrane receptors [Fantini and Barrantes (2009)]). Remarkably, it is getting clear that their concentrations at different cellular sites are subjected to a tight regulation in a very narrow range [Van Meer et al. (2008)].

Cholesterol preferentially associates with ordered acyl chains of complex lipids, due to the tight packing of the planar smooth-face of the sterol ring against the extended acyl chains of l_o phase lipids, both glycerol- and sphingolipids [Quinn (2010); Mouritsen (2010)]. Cholesterol forms a liquid-ordered phase in phospholipid bilayers in the

presence of sphingomyelin, that mixes more ideally with cholesterol than with a phosphatidylcholine with the same acyl chain [Snyder and Freire (1980); Sankaram and Thompson (1990)], and in sphingomyelin vesicles [Ferraretto et al. (1997)]. In the l_o phase, the sterol molecules are tightly intercalated between the ordered acyl chains of the bilayer-forming lipid [Brown and London (2000); Sonnino et al. (2006)].

A higher affinity of cholesterol for sphingolipids than for glycerolipids has been often invoked as one of the main forces driving to membrane hierarchical organization [Van Meer (2011a)]. Cholesterol forms a ordered, homogeneous phase with C_{16}-ceramide at a molar ratio of 60:40 mol% in monolayers [Scheffer et al. (2005)]. Such cholesterol/ceramide ordered domains can be observed at specific subcellular localizations in living cells [Goldschmidt-Arzi et al. (2011)]. Remarkably, these domains can be recognized by antibodies that are highly sensitive to ordered arrangement of molecules within the domain, i.e., to the two- dimensional structure of the molecular aggregate, that is, in turn, very sensitive to its molecular composition, being in particular influenced by the length of the ceramide fatty acyl chain [Scheffer et al. (2007)].

One of the important consequences of the uneven distribution of lipids along the membrane plane is the modulation of the membrane's tri-dimensional structure, leading to local deformation of membranes from the flat geometry, like budding or formation of invaginations. In this insight, it has been recently proposed that membrane curvature can greatly contribute to the reduction of line tension (the energy required to maintain a border between a membrane domain and the surrounding membrane environment) [Baumgart et al. (2003)], thus representing a general principle explaining the segregation of lipids and proteins in cellular membranes [Tian and Baumgart (2009)]. Curvature on the mesoscale has also been proposed as a structural motif on the membrane, exploited for curvature-based recognition of large macromolecules [McMahon and Gallop (2005)].

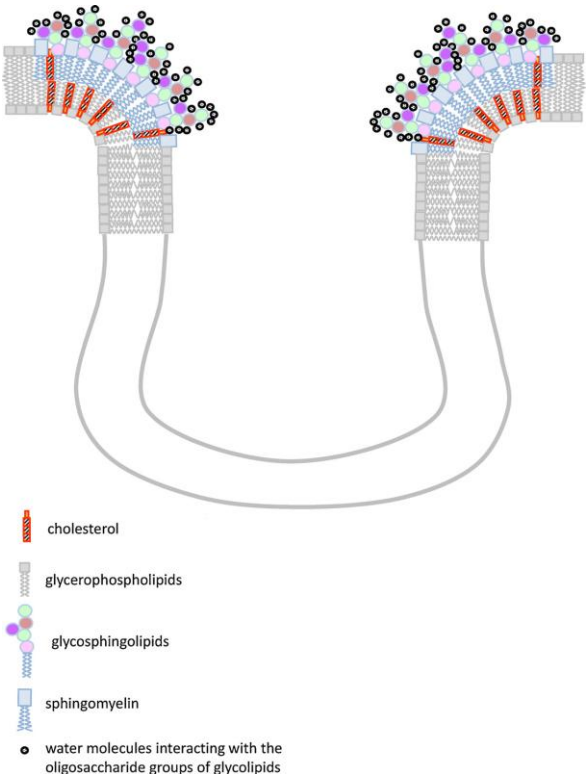

Figure 12: Arrangement of inner and outer layer membrane lipid components in a region with a saddle geometry, e.g., the edge of a caveola or of an endocytic vesicle. Caveolae- associated lipid rafts are likely present at the rim of the vesicle, giving their enrichment in gangliosides that confers a positive curvature to the membrane microenvironment. Lipid rafts are strongly enriched in outer layer lipids, such as gangliosides and phosphatidylcholine, and in cholesterol [Prinetti et al. (2000)], usually more enriched in the inner layer [Wood et al. (2011)].

The ability to draw ordered motifs on the surface of a hosting membrane is likely to constitute a major contribution of gangliosides to promoting morphological rearrangement of adhering macromolecules via structural templating. For example, this ability is at the basis of the gangliosides' role in the induction of amyloid fibril formation [Matsuzaki et al. (2010)] in Alzheimer's disease, i.e., the formation of those insoluble Aβ aggregates that are extracellularly deposited, forming the amyloid plaques.

2. MATERIALS AND METHODS

2.1. X-rays Scattering

The structural characterization of polymer solutions, macromolecules and molecular aggregates is facilitated by the development of techniques based on scattering of electromagnetic radiation and particles. The Small Angle Scattering of X-ray (SAXS) is an established technique to the analysis of the structure and fluctuations on the nanoscale. The small-angle diffusion of X-ray originates from the spatial non-uniformity of electron density within the material. The amount of structural information that can be achieved depends on the degree of supramolecular order in the sample, for example in the case of dilute solutions of macromolecules, it is possible to determine the shape and the radius of the disperse particles. As other scattering techniques using neutrons or visible radiation, even X-ray scattering is a non-invasive structural technique. Modern synchrotrons provide a high flow and well collimated flux, and this fact has led to the SAXS technique to be unique for its high spatial and temporal resolution and the small volumes required: we can perform experiments on samples diluted in the millisecond time scale. The technique of scattering is not a direct method of imaging: to have structural information we are required to do a rigorous analysis based on fitting methods.

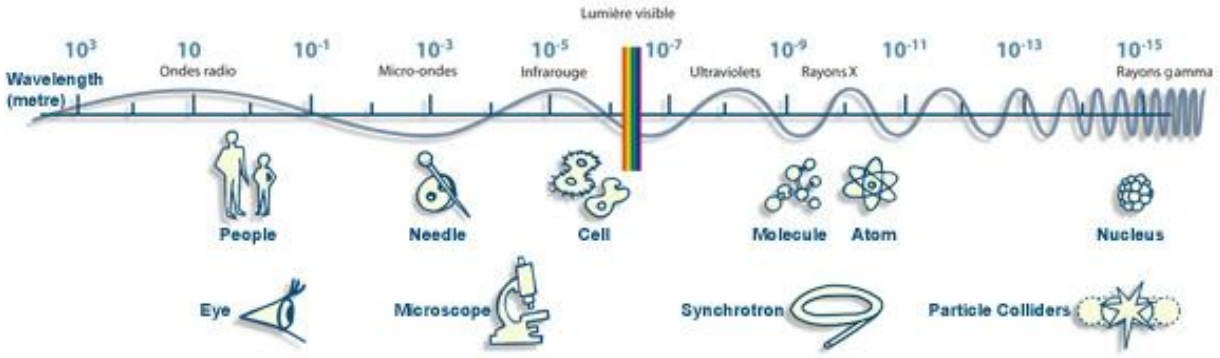

Figure 13: different kinds of radiation and relative possible application fields

The basic formalism of small-angle scattering is similar for light, X-rays and neutrons. The important difference resides in the type of interaction between radiation and the means: the scattered light originates from the change in refractive index, while the neutrons are diffused from atomic nuclei, the contrast term for X-ray is given by the

spatial fluctuations of electron density within the material. The typical experimental set up for a SAXS experiment is shown in figure 14.

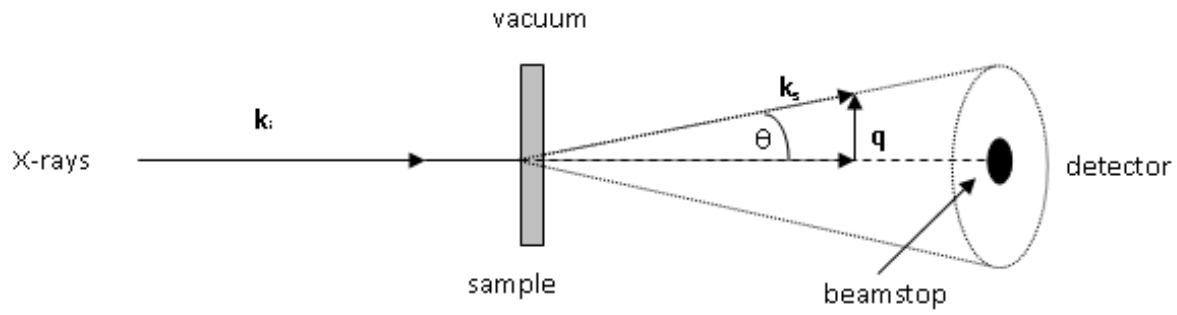

Figure 14: schematic representation of a scattering experiment

A beam of monochromatic and well collimated X-rays, hurts a sample, and the scattered radiation is collected from a two-dimensional detector. The transmitted beam is completely absorbed by a beamstop, positioned in front of the detector, and the entire path before and after the sample is in vacuum, in order to prevent absorption and scattering by air. The number of scattered photons as a function of the angle is measured. For a given sample, the amount of photons depends on the number of incident photons per second and per unit area (photon flux) and on the sample-detector distance. X-ray scattering is produced by electrons (Thomson scattering), and is independent of the wavelength of X-rays, except if nearby the absorption threshold of the material constituting the sample.

2.1.1. The radiation-matter interaction

The physical principles of scattering are the same for both the low angle and the wide angle diffraction, and apply to X-rays, neutrons and light, although, depending on the type of radiation considered, the interaction is different. A beam of particles with a certain energy, which interacts with matter, is comparable to an electric field associated with the incident wave. This field induces dipole oscillations of atoms. For X-rays the energy is so high to excite all the atomic electrons. The accelerated charges generate secondary waves that propagate in space, giving rise to interference phenomena. At large distances (far field approximation) one can measure the total scattering amplitude, given by the intensity of the scattered radiation from the sample.

For monochromatic radiation all the secondary waves have the same frequency but, having traveled different paths, will have, in general, different phases. Being high-energy radiation, the frequency is high, so it is possible to record only the spread intensity (the square of the amplitude of oscillation of the field) and its dependence on the angle of diffusion. Let's introduce some basic concepts: the scattering length and the density of scattering.

The scattering length

When an incident beam of X-ray encounters the electronic cloud of an atom of the sample, the physical parameter introduced to assess the magnitude of scattering is the scattering length. This quantity, expressed in centimeters, "weighs" the contribution of the total intensity, depending on the type of atom hit by the radiation, that is the number Z of electrons of the atom. Therefore, the scattering length provides a quantitative representation of the intensity of the interaction of electromagnetic radiation with the diffuser element, and is given by:

$$b = b_0 Z \qquad (2.1)$$

$$b_0 = 0.282 \cdot 10^{-12} cm \qquad (2.2)$$

b is therefore always positive and easy to be determined.

Density of scattering length

In a sample with molecules consisting of different atoms we can define an average scattering length, linear combination of the scattering lengths of the individual atoms that make up the molecule. For the purposes of calculating the diffuse intensity, it is important the *scattering length density*, more commonly called *scattering density*. This quantity is the ratio between the sum of the scattering lengths of atoms that make up the molecule and its volume.

$$\rho_0 = b_{tot} / V_0 \qquad (2.3)$$

X-rays scattering

An X-ray beam that hits a set of atoms, interacts with the electronic shell and is subsequently released. The propagation direction is given by the wave vector K, such that

$$|\mathrm{K}| = \frac{2\pi}{\lambda} \qquad (2.4)$$

where λ is the wavelength of the incident radiation. A point in the space can be identified by a vector *r*, and it is useful to write the wave in this form:

$$\mathrm{Ae}^{\mathrm{i}(\mathrm{k}\cdot\mathrm{r}+\alpha)} \qquad (2.5)$$

where A is the amplitude and α the initial phase. We neglected the time evolution, because for the analysis of the effects of diffraction it is significant just the instant pattern. We assume that the scattering is elastic, so effects such as polarization and absorption are not critical, even if they involve corrections to the formulas for the spread intensity.

Geometry and variables in a scattering experiment

The key variable in a scattering experiment is the *Bragg wave vector*, defined as:

$$Q = K_i - K_s \qquad (2.6)$$

where K_i and K_s are respectively the incident and diffuse wavevectors of radiation in the middle.

In an scattering experiment in an isotropic medium containing heavy particles, we mainly treat with elastic and quasi-elastic scattering, for which the following relation holds:

$$\mathrm{Q} = \frac{4\pi}{\lambda} n \sin\left(\frac{\theta}{2}\right) \qquad (2.7)$$

which we call the Bragg wave vector.

θ is the scattering angle, and *n* is the index of refraction of the medium. For light in water *n* = 1.33, while for X-rays it is very close to unity. The Van Cittert and Zernike theorem, fundamental to the theory of scattering of waves from an extended object, relates the

density distribution of the object that spreads radiation in space r, to the diffuse intensity distribution in the space Q, in terms of Fourier transforms: the measure in the r-space, R, is reciprocally connected to the width of the intensity distribution in the Q-space. So, to get a detailed characterization of the shape of an object of size R, you must perform a measurement of scattering where Q varies by an order of magnitude smaller than Q_0 =2π/R, to an order of magnitude higher.

If, for example, R≈20 Å, we should use X-ray with λ=1-20 Å. A further consequence of the theorem quoted is the maximum value of the spatial resolution, which is given in terms of maximum wave number obtained in the measurement, Q_{max}, and is:

$$\Delta R = \frac{\pi}{Q_{mx}} \qquad (2.8)$$

This means that in a typical SAXS (Small Angle X-ray Scattering) experiment where Q ≤ 0.6 $Å^{-1}$ the maximum achievable spatial resolution is 5 Å, while for light scattering Q ≤ 0.003 $Å^{-1}$, so the maximum resolution is about 1000 Å. This does not mean that light scattering experiments cannot be performed on systems with sizes less than 1000, which indeed is a typical range of investigation of light scattering, but you cannot have a detailed description of the shape of the aggregates.

The wide and low angle scattering

To obtain information on the structure and size of the aggregates is necessary that the wavelength of the radiation is comparable with the measures of interest. With small-angle scattering, for dilute systems, where the distances between the particles are greater than their size, you can determine a distribution of aggregate measures. In the case of semi-dilute systems, the result of a small-angle scattering experiment is influenced by the structure of the particles and their spatial arrangement. Therefore, the distribution curve is the product of the aggregate scattering function (form factor P(q)) and the function of interaction between the various aggregates (structure factor S(q)). If the system is "dense", that is, the volume fraction of the solute is of the same order of magnitude as that of the solvent, it is more useful a crystallographic analysis. A colloidal aggregate is big about from 20 Å to 10000 Å. With WAXS (Wide Angle X-ray scattering) measures we access a range of distances of the order of some Å, corresponding to the distance between the lipid chains within the lamellar structure. The distribution of chains within the lipid bilayer is not random, but can be described by crystallographic models. At the

interface chains are regularly arranged at the vertices of a lattice. This order is propagated along the two-dimensional depth of the lipid layer, giving rise to an ordered phase. The Bragg peaks positions in the WAXS spectrum correspond to the typical distances of the system under consideration. From these it is possible to derive the geometry of the sample.

Contrast for scattering density

Given the high energy of photons X, the collision with the particles of the sample is generally elastic. When an X-ray beam hits an object, each electron becomes a source of secondary waves. All waves have the same intensity given by Thomson formula:

$$I = I_0 \frac{1}{a^2}\left(e^2 \diagup mc^2\right)^2 \frac{1+\cos^2 2\vartheta}{2} \qquad (2.9)$$

Where I_0 is the incident intensity, a the object's distance from the detector, e^2/mc^2=3.13 10^{-25} m, and the last term represents the polarization factor. The total diffused intensity is obtained by multiplying (3.09) for the squared scattering amplitude, that is:

$$I(q) = I_0 \frac{1}{a^2}\left(e^2 \diagup mc^2\right)^2 \frac{1+\cos^2 2\vartheta}{2} \left|F(q)\right|^2 \qquad (2.10)$$

The diffuse intensity is the amount actually get from a scattering experiment.

The scattering amplitude

The information about the shape, size and internal structure of a single particle are contained in F(Q), term which we call the scattering amplitude. In the case of disperse systems containing aggregates with a uniform scattering density, during the scattering the form factor on the single particle is generated by the difference between the scattering density of the aggregate, ρ_p, and the scattering density of the solvent ρ_h.
The form factor can be calculated as follows:

$$F(Q) = \int_V [\rho_p - \rho_h] \exp(iQr_j)^3 dr^3 \qquad (2.11)$$

where the integral is extended to the whole volume of the aggregate.

2.1.2. Experimental apparatus

The SAXS experiments presented in this thesis work have been performed at the instrument ID02 at the ESRF (European Synchrotron Radiation Facility) in Grenoble. The ESRF synchrotron is able to produce a thin and very intense beam of X-ray. In particular, ID02 is a line of small-angle diffusion, characterized by a high brightness. The beamline has a high flux of monochromatic photons with a low divergence, typically with dimensions of 80μm x 300μm at the sample level. The optics is optimized for experimental uses with a fixed wavelength of about 0.1 nm (12.4 keV). In figure 15 we see a scheme of the line.

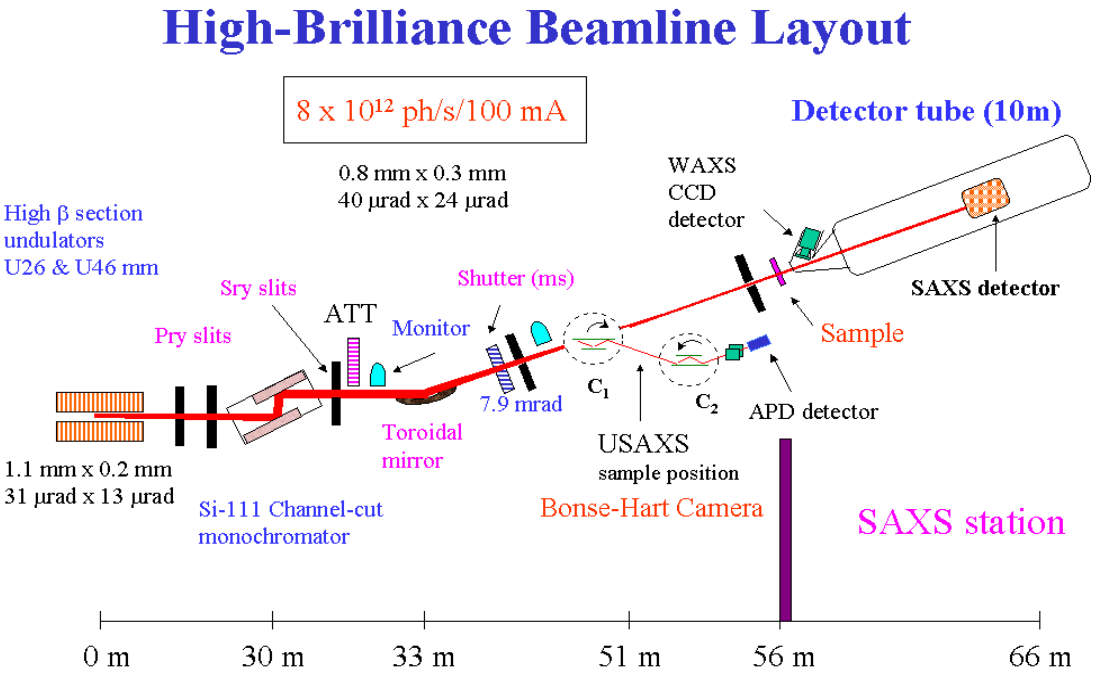

Figure 15: ID02 beamline scheme

X-Ray scattering measurements were performed at the high brillance ID02 beamline of ESRF in Grenoble, FR, where both spatial (beam dimension: 0.3mm*0.8mm), and time (exposure time: 0.1 sec) punctuality can be attained, without sample damage. The problem of temperature stability has been addressed in our laboratories in Milano, where a thermostat has been built *ad hoc*, suitable to be mounted on ID02 beamline. It consists of Peltier elements: the error in the stabilization of temperature inside the capillary is of the order of cK. The sample holder can keep up to six capillaries which can be irradiated in succession so that almost simultaneous measurements of multiple samples is assured, and there is equivalence of environmental conditions for all the samples.

In this kind of measurements the choice of the capillaries is very important, because they must be biocompatible, have a small volume, and transmit as much as possible. The optimal choice for biocompatibility would be glass, but glass capillaries, if too small, are very fragile and non-uniform in size, being pulled up. In addition, the glass capillaries transmit about 50% of the radiation. We used plastic capillaries developed in the laboratories of Milano and produced by ENKI, extruded to obtain thin and uniform thickness. The inner diameter was 2mm and the thickness 0.05mm and the X-ray transmission was 98%. The capillaries were filled with 30 µl of the various samples before being mounted on the sample holder.

To work with precision, especially during background subtraction, separate measurements were carried out in sequence on the empty capillaries, filled with pure water, and filled with the sample.

The measurements were made at fixed temperature, 30°C, over the melting transition of DMPC hydrophobic chains, and after the measure the sample containing capillaries were stored in oven at 30°C. For the SAXS measurements the sample position is fixed, while the detector can be moved automatically in a vacuum tube to a distance varying from 0.75 m and 10 m from the sample, so that a wide range of scattering wave vectors can be accessed: 0.1 nm-1 <q <3 nm-1, where $q = (4\pi / \lambda) \sin(\theta / 2)$, with λ the wavelength (~ 0.1 nm) and θ the scattering angle.

We performed our SAXS measurements at a sample-to-detector distance of 0.8 m to access the q range from 0.1 nm^{-1} to 4 nm^{-1}, corresponding to typical distances from 1.5 nm to about 60 nm.

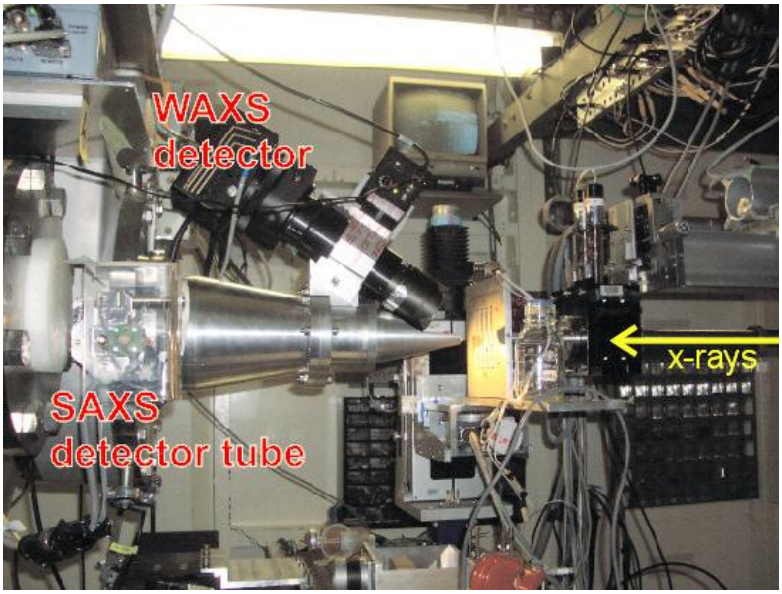

Figure 16: SAXS and WAXS detectors on the Id02 beamline at the ESRF of Grenoble

During a measure, the angular distribution of the scattered X-ray intensity is collected.

2.2 X-Rays and Neutrons Reflectivity

To study material at the molecular level, the diffusion of radiation is a well suited experimental technique. Diffraction provides access to volume properties of objects, while the reflectivity allows the study of surfaces and interfaces such as thin layers of polymers, surfactants films or monolayers at the air-liquid interface [Fradin et al. (2000), Sanyal et al. (2008)].

In this section we will recall the principles of neutron and X-ray reflectivity. We already discussed the X-rays/matter interaction, so we will focus on Neutrons in the following paragraph.

Neutrons-matter interaction

The neutron is one of the elementary constituents of the nucleus with the proton. It is an electrically neutral particle of spin 1/2, magnetic moment -1.913μN, whose mass is 1.008665 atomic mass units. The neutrons that are used for the study of condensed matter are called "thermal neutrons" (energy the order of 10 to 100 meV).

Neutrons can interact with matter via two types of interactions: the strong interaction and electromagnetic interactions. The dipolar interaction of the magnetic moment of the neutron with the magnetic moment of the kernel or unpaired electrons of atoms is an electromagnetic interaction. But as the magnetic moment of the nucleus is much lower than that of electrons, only the magnetic scattering due to the electrons is measured by

neutron scattering. This interaction is applied to the study of magnetic structures of solids. The strong interaction between neutrons and the nuclei of target atoms is governed by the Fermi pseudo-potential:

$$V_F(r) = \frac{2\pi\hbar^2}{M} b\delta(r) \qquad (2.12)$$

where *M* is the mass of a neutron and *b* the scattering length b of the target atom. Differently from the diffusion length of an atom for X-ray, the trend of *b* for neutrons does not depend monotonically from the atomic mass (see Figure 17 below) and can even be negative. Even two neighboring elements or two isotopes can have very different scattering lengths. This is the case of hydrogen and deuterium where b_H = -3.74 fm and b_D = 6.57 fm. Thanks to this difference, by selective deuteration we can easily cancel the contrast of a portion of a sample to observe dissemination of the other party (eg deuteration of aliphatic chains lipid to observe the distribution of heads [Fragneto et al. (2003)].

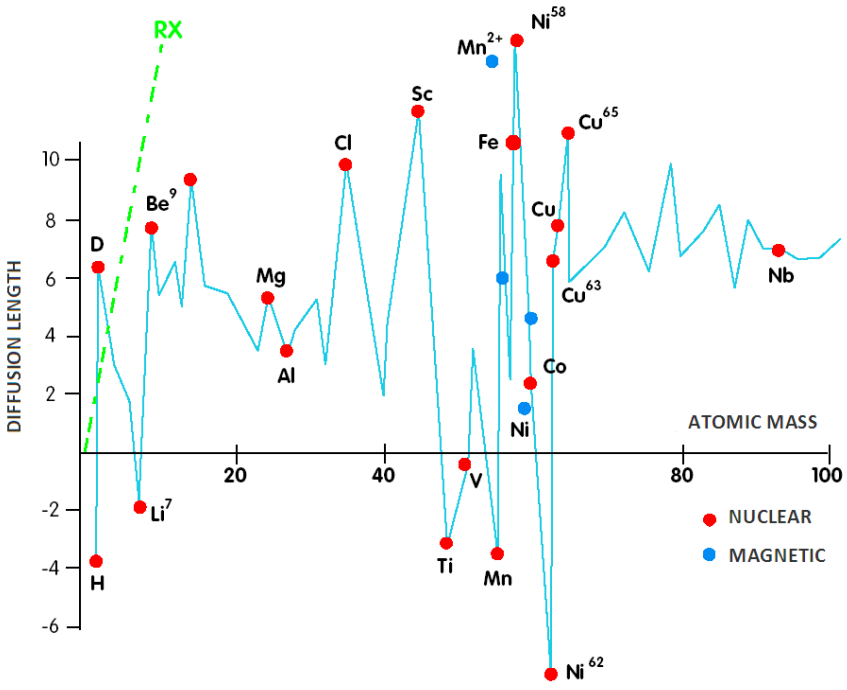

Figure 17: Atomic diffusion lengths of atoms as a function of the atomic mass.

We call ‘coherent diffusion length’ the mean value of the diffusion length <b>.

The fact that isotopes of the same chemical element have different lengths is the origin of the incoherent scattering. This type of diffusion is analogous to a diffuse scattering. It is responsible of a radiation background in neutrons experiments.

X-Rays versus Neutrons

Neutrons and X-rays are two analytical techniques for the study of condensed matter. Thanks to very different scattering lengths of hydrogen and deuterium, one can easily cancel the contrast of parts the sample when it is characterized by neutron scattering. But thermal neutrons have a low energy: they do not damage the samples but the data acquisition is very long (on D17 beamline at ILL, Grenoble, the flux is 9.6 neutrons per second per square centimeter). Synchrotrons beams are much more energetic, but ionizing radiation has to be associated with sample damage. The flow is such high (1014 photons per second per square centimeter at the ESRF, Grenoble) that allows to acquire a wide range of diffused wave vectors in a very short time.
This is why they are complementary techniques.

2.2.1 Neutrons reflectivity

Neutron scattering experiments were carried mainly on the D17 line of ILL (Institut Von Laue-Langevin) in Grenoble. D17 is a line dedicated to the reflectivity of surfaces and interfaces [Fragneto and Cubitt (2002)], which uses a "white" beam of neutrons, whose flux is 9.6×10^9 neutrons/(s*cm^2) and wavelengths between 2 and 20 Å.
Other measurements have been carried on the FIGARO beamline at ILL [Wacklin et al. (2010)] where the cell is oriented horizontally and kept in position while changing solvents and temperature. Measurements were performed at the air-water interface.
In a neutron reflectivity measurement R, the ratio between the intensities of the reflected and incoming beams, is collected, as a function of q, the momentum transfer perpendicular to the interface. Reflectivity is related to the scattering length density across the interface by the approximate relation:

$$R(q_z) \approx \frac{(16\pi^2)}{q_z^2} \left|\rho(q_z)\right|^2 \qquad (2.13)$$

which is the reflectivity in the Born approximation [17]. $\rho(q_z)$ is the Fourier transform of the scattering length profile $\rho(z)$ along the normal to the interface, giving information

about the composition of each layer and about its local structure. The scattering length density is given by:

$$\rho(z) = \sum_j b_j n_j = \sum_j b_j n_j \qquad (2.14)$$

where n_j is the number of nuclei per unit volume and b_j is the scattering length of nucleus *j*.

The method of analysis often used for specular reflection data involves the construction of a model of the interface that may be represented by a series of parallel layers of homogeneous material. Each layer is characterised by a Scattering Length Density (SLD) and a thickness, which are used to calculate a model reflectivity profile by means of the optical matrix method [Born and Wolfe (1989)]. The interfacial roughness between any two consecutive layers may also be included in the model by the Abeles method. The calculated profile is compared to the measured profile and the quality of the fit is assessed by using χ^2 in the least-squares method.

To limit the diffusion of the incident beam by water or heavy water we take advantage from the fact that silicon does not absorb neutrons, the beam comes from the substrate, placed vertically. The experimental setup is schematized in figure 18.

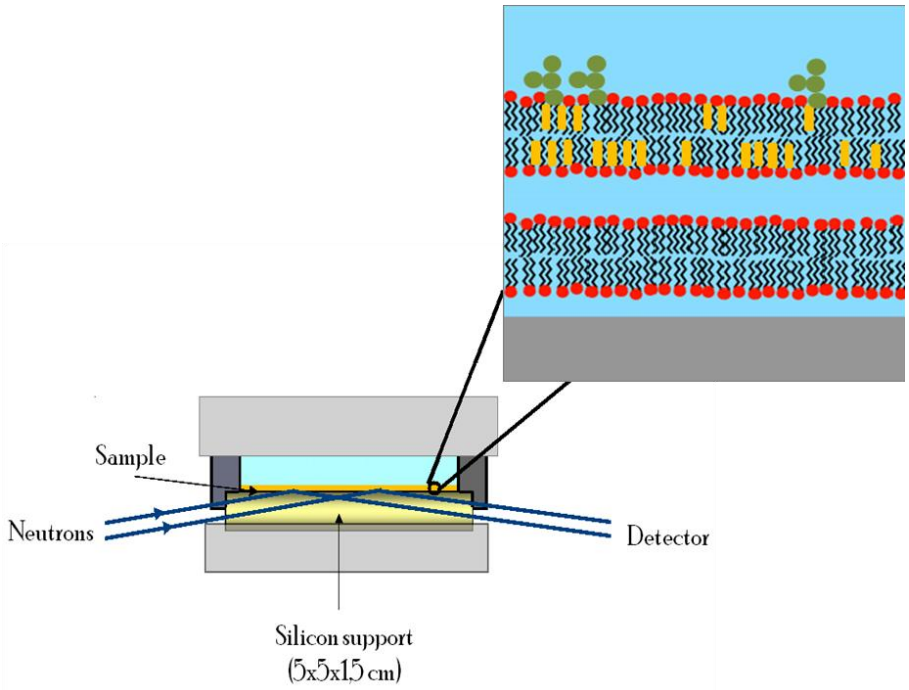

Figure 18: scheme of the cell used to perform neutron reflectivity experiments

The specular intensity depends on both the wavelength and the radiation angle of incidence. Two methods are possible to obtain a reflectivity curve: either we keep a fixed

wavelength and we vary the angle of incidence of the beam (monochromatic mode) or the beam maintains a fixed position and we change the wavelength of the beam during the acquisitions. This is the time-of-flight (TOF) mode.

On D17 both modes are available. The time of flight mode is well suited for kinetic studies because without changing the geometry, we can measure the reflected intensity of a decade if q in about one minute. This is the mode we have always used. In time-of-flight geometry, two discs called choppers are placed at the beginning of the line. They are pierced by a window and run at a fixed speed of 1000 turns / min. They are separated by a distance varying from 1 to 11 cm. The combination of rotation and distance between the choppers allows to select the energy (i.e. the wavelength) of the incident beam and absorb what is left. The wave vector transfer q_z is determined by the relation:

$$\frac{dT}{T}(q_z) = \frac{d}{D} + \frac{\phi}{2\pi}\frac{q_z}{q_{z,min}} \qquad (2.15)$$

where *d* is the distance between the choppers, φ the choppers opening, D the total distance to the detector, T is the time of flight of neutrons to detector, dT is the duration of a packet of neutrons, and finally $q_{z,\,min}$ the minimum vector transfer measurable for a given reflection angle. To measure a reflectivity curve from $q = 2 \times 10^7$ m^{-1} to $q = 3 \times 10^9$ m^{-1} we change the geometry of the experiment only twice. On D17 firstly we set the angle of incidence $\theta_{in} = 0.7°$ and $\varphi \approx 0°$, to keep the first part of the curve (up $I/I_0 = 10^{-3}$). Then we increase the neutron flux by increasing the opening angle of choppers up $\varphi = 3°$ (at the cost of reduced resolution of the experiment) and we choose $\theta_{in} = 3°$ for the final part of the curve, where $10^{-8} < I/I_0 < 10^{-3}$.

Compared to the sample surface illuminated by a synchrotron beam (few μm^2), the neutron beam illuminates a big area (10×70 mm^2) without damaging it. Therefore, even if the neutron flux is low, the acquisition of a reflectivity curve takes a reasonable time: 1.30 to 2 hours in our case. However, we choose to make some synchrotron experiments because the q_z range covered in specular reflectivity is smaller with neutrons (up to $q_z = 3 \times 10^9$ m^{-1}) than with synchrotron radiation (up to $q_z = 7 \times 10^9$ m^{-1} typically).

To reduce errors, each sample has been studied in different solvents. All of the membranes were, at some point, observed in three solvents, H_2O, D_2O and SMW (Silicon Matched Water, a mixture of H_2O and D_2O with the same SLD of Silicon, that is 7.06). Lipid mixtures have instead been deposited over three solvents: H_2O, D_2O and

Zero Match Water (a mixture of H_2O and D_2O with the same SLD of air, that is zero). Data were analyzed using the software Motofit [Nelson (2006)], allowing simultaneous fit of data sets referred to the same sample in different contrast conditions, using the SLDs reported in table 1.

Table 2. SLDs of used compounds

Material	**Neutron SLD (10^{-6}Å^{-2})[a]**
air	0
Si	2.07
SiO_2	3.41
H_2O	-0.56
D_2O	6.36
cholesterol	0.22
GM1 chains (gel phase)	-0.41
GM1 chains (fluid phase)	-0.33
GM1 heads	1.88
Lipid D-heads	5.70
Lipid D-chains (gel phase)	7.66
Lipid D-chains (fluid phase)	6.13
Lipid heads	1.74
Lipid chains (gel phase)	-0.41
Lipid chains (fluid phase)	-0.33

2.2.2. Need for synchrotron radiation

To perform diffuse scattering experiments the photon flux must be very important because the scattered intensity is proportional to the scattering volume. Studying an interface of a few nanometers the scattered intensity is very low, $I \approx 10^{-12}\ I_0$. This means that the detector receives one photon each ten billion of incident photons. In our experiments we have two major constraints, namely (i) keep reasonable acquisition time

(about 1 minute maximum) to avoid samples degradation, (ii) have a sufficient statistic (at least 1000 rounds) to be able to distinguish between background noise and diffusion through the interface. To satisfy all these constraints, we must have an incident photon flux at least 10^{13} photons / s which only a synchrotron can provide. For this reason we characterized our samples at the ESRF.

The principles of reflectivity are the same as for Neutrons, exception made for the contrast which is obviously different.

Table 3: properties of materials used

Material	**Neutrons SLD (10^{-6} Å^{-2})**	**X-rays SLD (10^{-6} Å^{-2})**
Lipid head	1.75	14.44
Lipid gel chains	-0.44	7.9
CH_3 groups of lipid chains	-0.44	4.77
cholesterol	0.22	9.58
Ganglioside head	2.23	14.83
H_2O	-0.56	9.38

2.2.3. Specular reflectivity calculation

We define refractive index of a mean as [De Bergevin (2009)]:

$$n = 1 - i\delta - i\beta \tag{2.16}$$

This index depends on the type of wave and also on its energy. But the definitions of δ and β are similar for neutrons and X-rays:

$$\delta_{\text{X-rays}} = \frac{\lambda^2 \rho_e r_e}{2\pi}$$
$$\delta_{\text{Neutrons}} = \frac{\lambda^2 \rho_d}{2\pi} \tag{2.17}$$

where λ is the wavelength of the incident wave, ρ_e the electron density, r_e the classical electron radius, ρ_d the neutron scattering length density, and:

$$\beta_{X-rays} = \frac{\lambda \mu_X}{4\pi}$$
$$\beta_{Neutrons} = \frac{\lambda \mu_N}{4\pi} \qquad (2.18)$$

with μ_X and μ_N absorption lengths of the material for X-rays and neutrons respectively.
For X-rays the refractive index is almost always less than 1, while with neutrons *n* can be more or less than 1 because scattering length density can be positive or negative. But in any case the refractive index is close to 1 as δ and β are between 10^{-5} and 10^{-8}.
In optics, the critical angle is the angle limit below which a wave incoming from a medium of index n_1 is totally reflected at the interface with a medium of index n_2. Descartes' law gives the simple relationship:

$$\cos\vartheta_c = \frac{n_2}{n_1} \qquad (2.19)$$

In our X-ray experiments, we used a beam energy equal to 27 keV. The critical angle corresponding to the interface water / silicon is 0.04°.
The Born approximation is to neglect multiple scattering. This approximation is not valid when the scattering cross section is large, that is when the angle of incidence of the beam is close to the critical angle.
In the X-ray reflectivity experiments, the incident beam comes just above the critical angle and therefore we cannot use the Born approximation. We use a perturbation theory called Born approximation of the distorted-wave (DWBA). We take as reference plane the silicon / water interface, and we consider the phospholipid membranes as a perturbation. This approximation is justified by the fact that the electron density of lipids is very similar to that of water.

Fresnel reflectivity

To calculate the specular reflectivity of supported bilayers, let's calculate the reflectivity of the planar interface water / silicon of respective index n_1 and n_2. For this, consider a wave with wave vector k_{in} forming an angle θ_{in} with the interface. The transmitted part of the wave is characterized by the wave vector k_t and forms an angle θ_t with the interface

(figure 19). The reflected wave has k_{sc} wave vector and the angle of reflection is $\theta_{sc} = \theta_{in}$. In this case the coefficient of reflection [Gibaud (2009)] is:

$$r = \frac{n_1 \sin\vartheta_{in} - n_2 \sin\vartheta_t}{n_1 \sin\vartheta_{in} + n_2 \sin\vartheta_t} \tag{2.20}$$

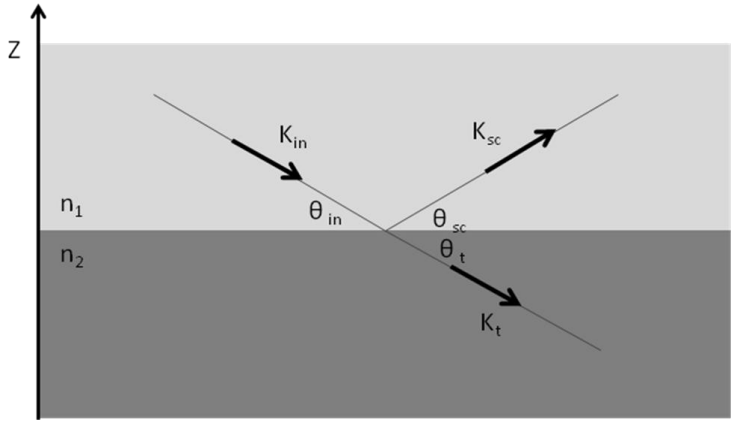

Figure 19. A wave coming from a medium with refractive index n_1 to one with index n_2 is partially scattered and partially transmitted.

Fresnel reflectivity is the squared modulus of the reflection coefficient. We obtain the following expression:

$$R_F = \left| \frac{k_{in,z} - k_{t,z}}{k_{in,z} + k_{t,z}} \right|^2 \tag{2.21}$$

Where $k_{in,z}$ and $k_{t,z}$ are the z components of the respective wave vectors on the z axis. Before the critical angle, the Fresnel reflectivity implies a 'plateau' corresponding to total reflection.

Specular total reflectivity

Knowing the Fresnel reflectivity, we can express the total reflectivity of the system as follows [Daillant and Alba (2000); Daillant et al. (2005)]:

$$R(q_z) = R_F(q_z) \left| 1 + iq_z \int \frac{\delta\rho(z)}{\rho_{Si} - \rho_{H_2O}} e^{iq_z z} dz \right|^2 \tag{2.22}$$

where q_z is the projection of the transferred wave vector on the z axis . ρ_{Si} ρ_{H2O} and are the electron densities of silicon and water respectively. $\delta\rho$ is the difference between the density of the real system and the state of reference (that is to say water in our experiments). This can be expressed in various ways and is the sum of the various layers we use to model the membrane under study.

We show as an example a X-rays reflectivity curve from a DPPC membrane in figure 20.

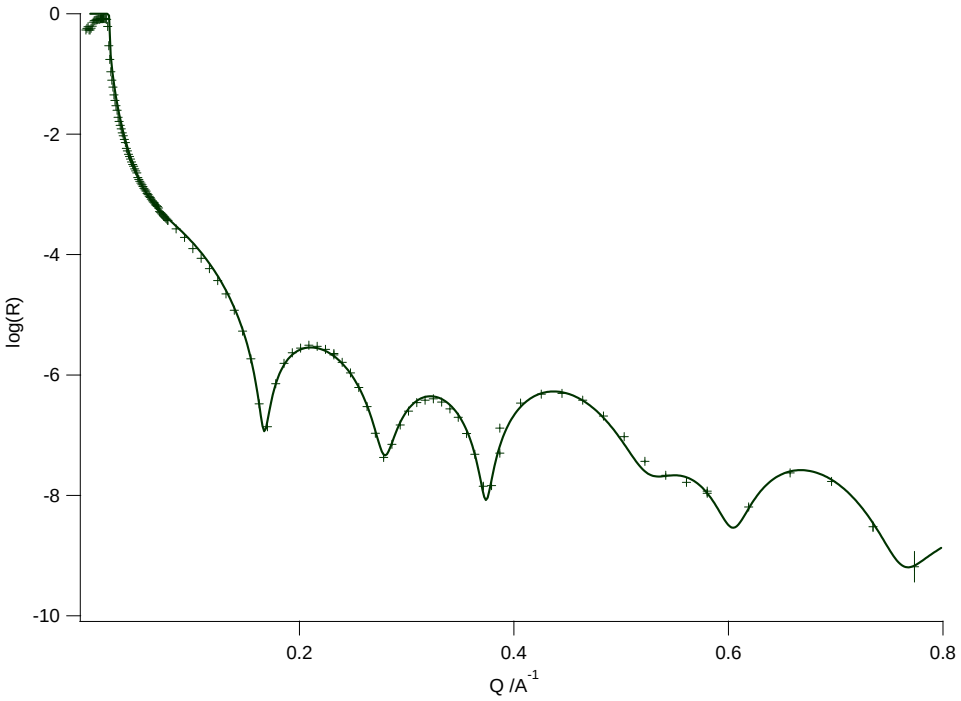

Figure 20: X-rays reflectivity from a DPPC membrane in water at 22°C.

The curve oscillates due to interference between waves reflected by the different interfaces of the sample. These oscillations are called Kiessig fringes. The fringes period depends on the smectic thickness, for example, a water layer deepening or an increase of the thickness of the membrane moves the first minimum to small q_z. In addition, the depth of the oscillations depends on the Scattering Length Density (SLD) profile and roughness. If the contrast of the heads of the membrane decreases, their SLD decreases and hence the oscillations are shallower. This applies even if the membrane is rougher because interference fringes are destroyed more quickly. Note that there is always a diffuse contribution in the specular direction because we are not performing an ideal experiment, so, for example, the instrument slots are not infinitely thin but have a finite width.

2.2.4. Data analysis

To analyze the data we used the dedicated software Motofit [Nelson (2006)].

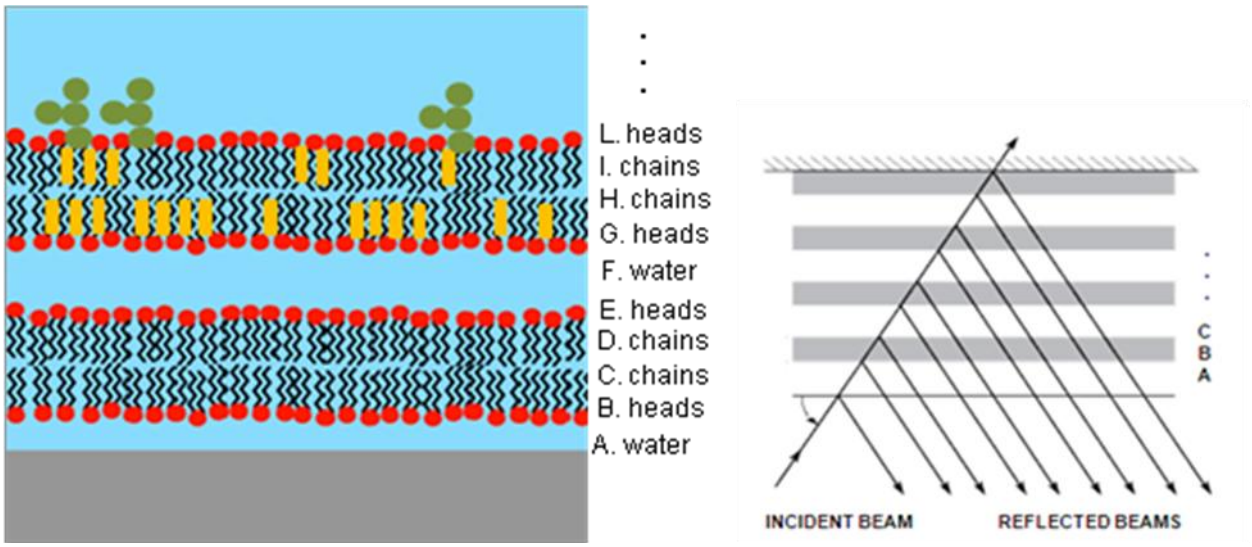

Figure 21: schematic representation of how we see the membranes, that is divided in layers each of them with a mean typical composition, schematized as a semi transparent mirror.

Motofit aids the fitting of specular X-ray and neutron reflectivity data. It works within the analysis package IGOR PRO (Wavemetrics, OR). The specular reflectivity is calculated as a function of the perpendicular momentum transfer, Q_z.

$$Q_z = \frac{4\pi}{\lambda}\sin\vartheta \qquad (2.23)$$

(Specular reflectivity (R) is defined as the ratio of reflected intensity over incident intensity, where the angle of reflection θ is equal to the angle of incidence.)

In particular, it is an easy way to analyse multiple-contrast Neutron Reflectivity and X-ray Reflectivity data. This is achieved through a simple GUI, and genetic optimisation for fitting (Genetic Optimisation allows the use of initial guesses that are far from a final solution, which would otherwise trouble normal least squares fitting packages).

The reflectivity is calculated using the *Abeles* matrix method for stratified interface. The measured reflectivity depends on the variation in the scattering length density (SLD) profile, (ρ (z)) perpendicular to the interface. Although the scattering length density profile is normally a continuously varying function, the interfacial structure can often be well

approximated by a slab model in which layers of thickness (d_n), scattering length density (ρ_n) and roughness ($\sigma_{n,n+1}$) are sandwiched between the super- and sub-phases. One then uses a refinement procedure to minimise the differences between the theoretical and measured reflectivity curves, by changing the parameters that describe each layer. In this description the interface is split into *n* layers. Since the incident neutron beam is refracted by each of the layers the wave vector, *k*, in layer *n*, is given by:

$$k_n = \sqrt{k_0^2 - 4\pi(\rho_n - \rho_o)} \tag{2.24}$$

The Fresnel reflection coefficient between layer *n* and *n+1* is then given by 2.20 and 2.21:

$$k_{n,n+1} = \left| \frac{k_n - k_{n+1}}{k_n + k_{n+1}} \right| \tag{2.25}$$

Since the interface between each layer is unlikely to be perfectly smooth the roughness/diffuseness of each interface modifies the Fresnel coefficient:

$$k_{n,n+1} = \left| \frac{k_n - k_{n+1}}{k_n + k_{n+1}} \right| e^{-2k_n k_{n+1}\sigma_{n,n+1}^2} \tag{2.26}$$

and is accounted for by an error function, as described by Nevot and Croce.
A phase factor, β is introduced, which accounts for the thickness of each layer.

$$\beta = k_n d_n \tag{2.27}$$

A characteristic matrix, c_n is then calculated for each layer.

$$c_n = \begin{bmatrix} \exp(\beta_n) & r_n \exp(\beta_n) \\ r_n \exp(-\beta_n) & \exp(-\beta_n) \end{bmatrix} \tag{2.28}$$

The resultant matrix is defined as the product of these characteristic matrices, from which the reflectivity is calculated.

$$M = \prod_0^n c_n \tag{2.29}$$

$$R = \left| \frac{M_{00}}{M_{10}} \right|^2 \qquad (2.30)$$

Data are fitted by a genetic optimization with least squares. We are allowed to change the parameters required for the base model:

• number of layers : how many layers there are in the model (in our case each head, chains and water ware fitted as single layers).

• sld top : Scattering length density of the Superphase (the incident medium for the radiation).

• sldbase : Scattering length density of the subphase.

• bkg : This adds in a Q independent linear background to the fit. In our case is 10^{-13}.

• sigma_base : The roughness at the top of the subphase.

• thick : thickness of the each layer (in Angstrom).

• sld : scattering length density of each layer.

• solv : how much of the subphase (solvent) penetrates into each layer, expressed as a volume percentage.

• rough : the roughness at the top of the each layer (in Angstrom).

From the fit we have each minimized parameter, and the total SLD profile of the system.

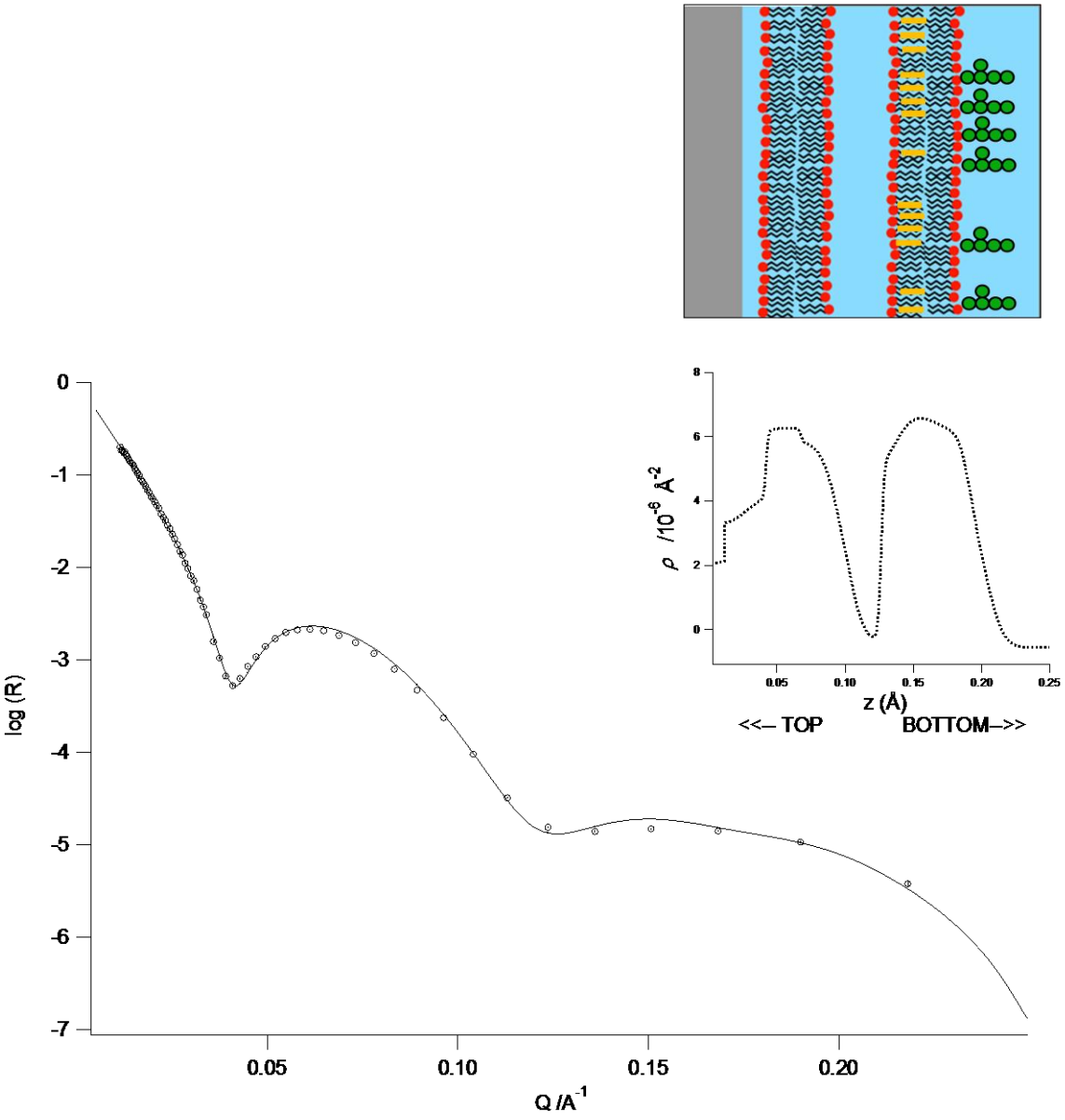

Figure 22: typical fit (line) of neutrons reflectivity data (in this case a double DSPC+DPPC membrane in h2O at 22°C). In the insert the SLD profile is shown.

The program allows also a contemporary fit of the same sample in up to four different solvents.

2.3. Samples preparation

2.3.1. Lipid vesicles

Lipids were from Avanti Polar Lipids Co., GM1 ganglioside was extracted and purified according to Tettamanti et al. [Tettamanti G, Bonali F, Marchesini S, Zambotti V (1973)]. DMPC vesicles were prepared according to the assessed extrusion protocol. DMPC is a phospholipid with two C_{14} hydrophobic chains and a phosphocholine as hydrophilic head. A manual extrusor from Avestin Inc. (LiposoFast) with a 0.5ml volume was used. About 2 mg of DMPC powder were weighted in a glass, ball-shaped container, dissolved in chloroform, and a film was depoposited over the balloon surface by evaporating the chloroform under continuous rotation. Chloroform evaporation was completed under vacuum for half an hour. Then the film was slowly wetted with a stream of humid nitrogen for half an hour, to avoid multilayer compact stack formation. Then, deionized water was added, to the final concentration [L.D. Mayer et al. (1986)]. The resulting solution was submitted to a freeze-and-thaw procedure (freeze in liquid nitrogen and melt in hot water) iterating the process 5 times, to detach eventual multilayer stacks. Then the sample was extruded 51 times trough twinned 800 Å polycarbonate filters, to let the lipid bilayer close up in monodisperse vesicles. Vesicles about 100 nm in diameter were obtained. After this procedure, the sample was stored over the chains gel-to-fluid transition temperature, to ensure for vesicles stability. In our case the final concentration of lipids in water was 4% bw, to have a good SAXS intensity.

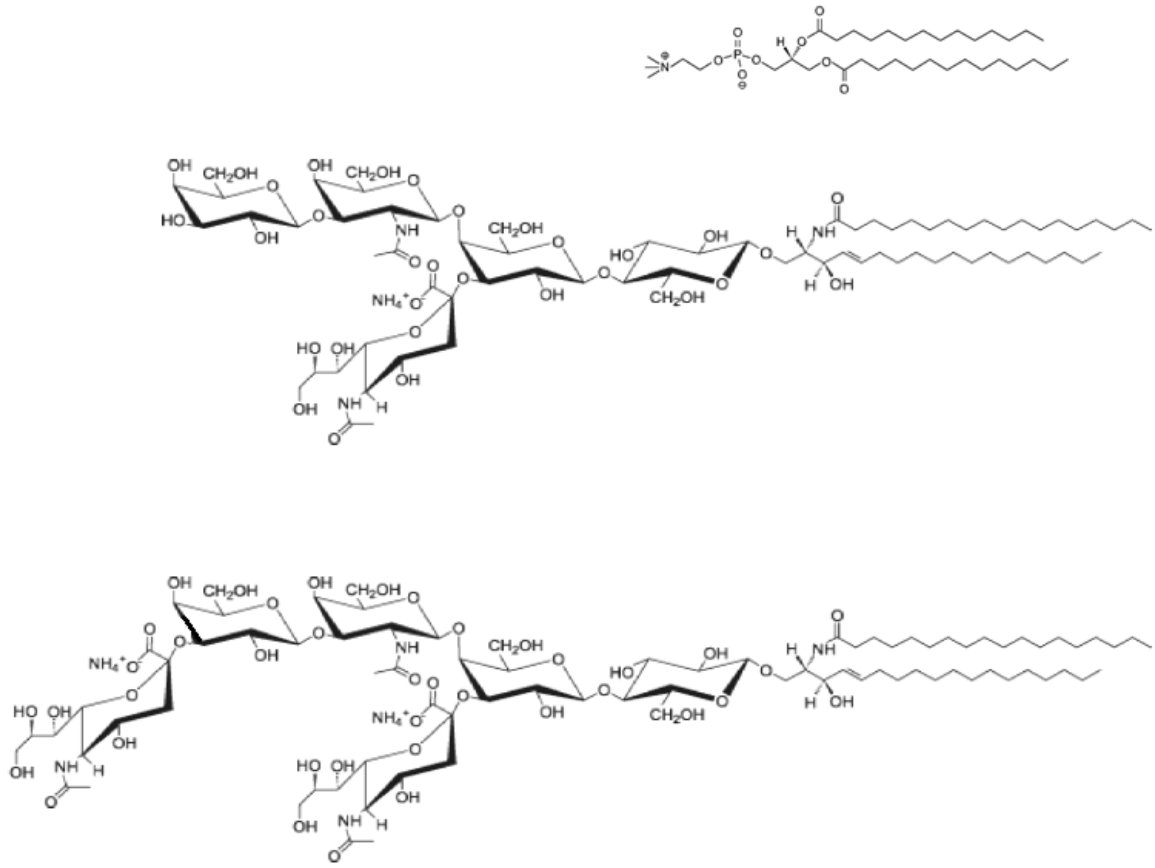

Figure 23: from top to bottom structures of DMPC, GM1 and GD1a

2.3.2. Ganglioside micelles

When dissolved in aqueous solution GM1 and GD1a gangliosides self-aggregate in micelles in a wide range of concentrations. We prepared micellar solutions by dissolving the dry powders in pure Milli-Q water to the desired final concentrations. For X-rays measurements we prepared three solutions: one of GM1, one of GD1a and a mixture 1:1 molar of the two gangliosides, to a final concentration of 4%. We also prepared a 1mg/mL GM1 solution (6.4×10^{-4} M), well above the cmc (2×10^{-8} M) [Corti M, Degiorgio V, Sonnino S, Ghidoni R (1982)], to be used for ganglioside incubation on a preformed floating membrane.

2.3.3. Langmuir-Blodgett and Langmuir-Schaefer techniques for supported membranes preparation

A Langmuir curve is obtained thanks to an apparatus (Langmuir trough) for the study of molecules at the water / air interface [Langmuir (1920), Blodgett (1935)]. It can also be used to study monolayers to be transferred onto substrates by the technique known as Langmuir-Blodgett. The principle of Langmuir curves is simple, it controls the area accessible to molecules deposited at the interface (via one or two side barriers) while measuring the surface tension γ of the molecular film.

Both H-lipids and fully deuterated lipids were used. Cholesterol was purchased from Sigma-Aldrich Co., d_{85}-DSPC, d_{75}-DPPC were from Avanti Polar Lipids Co., GM1 ganglioside was extracted and purified according to Tettamanti et al. [Tettamanti G, Bonali F, Marchesini S, Zambotti V (1973)]. According to a well assessed standard protocol [Blodgett K B, Langmuir I (1937)] [Fragneto G, Charitat T, Graner F, Mecke K, Perino-Gallice , Bellet-Amalric (2001)], cholesterol and phospholipids were independently dissolved in chloroform (99%) to a final concentration of 1mg/mL. GM1 ganglioside was dissolved in organic solvent, chloroform : methanol = 2:1, volume fractions. Mixed lipid systems were obtained by mixing appropriate amounts of single-lipid solutions. Lipids were then deposited on the surface of a Langmuir trough, equipped with a Wilhelmy plate for pressure sensing, filled with pure water, processed in a Milli-Q system (Millipore, Bedford, MA) to a resistivity of 18 MΩ•cm, and kept at T = 18°C (±0.5). What we measure is the difference between the surface tension of the pure water and that of the new surface. After spreading the solutions, organic solvents were let to evaporate completely for 15 minutes. Before deposition, monolayers were then compressed to a surface pressure of 40 mN/m, similar to the one in real systems [Charitat T, Bellet-Amalric E, Fragneto G, Graner F (1999)], while recording the corresponding pressure-area (π-A) isotherms. The maximum pressure is that corresponding to system collapse, by the formation of aggregates. The pressure-area curves, also called isotherms, are specific for each molecule. At 40mN/m all of the used monolayers are in the gel phase. They were then layer-by-layer deposited on a silicon substrate, as described in great detail in the following section. Asymmetric bilayers were realized by completely changing the monolayer in between different steps, and depositing a new one with the desired composition. Depositions were all realized in H_2O.

Figure 24:

Nima Langmuir trough

Floating bilayer buildup

Substrates were single crystals of silicon (5 x 5 x 1.5 cm^3) polished on one large face (111). The silicon blocks were cleaned before use in subsequent baths of chloroform, acetone, ethanol, water and treated with UV-Ozone for 30 min [Vid J R (1985)].

Double bilayer depositions were done in water coupling the Langmuir-Blodgett [Roberts G (1990)] and Langmuir-Schaefer Techniques [Tamm L K, McConnell H M (1985)], as follows. At the initial stage, the silicon block was immersed in water at 18°C in the Langmuir trough. The first layer solution was spread on the water surface and progressively compressed to 40 mN/m [Charitat T, Bellet-Amalric E, Fragneto G, Graner F (1999)]. The silicon block was then almost completely extracted and subsequently dipped again into water (speed 6 mm/min) across the monolayer, while keeping constant the pressure of the monolayer. Two facing monolayers were so adsorbed onto the block, constituting the adhering (supporting) bilayer. Then, the water surface was completely cleaned and a different solution was spread, with the composition desired for the inner side of the floating membrane. The third layer was then deposited by rising the block again, according to the same Langmuir technique. To prepare asymmetric floating bilayers, the surface of the trough was cleaned again and a solution with the composition desired for the outer side of the floating membrane was spread and compressed to 40 mN/m. The fourth closing monolayer was deposited by rotating the block by 90°, in the Langmuir Schaefer configuration, and lowering it carefully onto the surface. The block was then closed in a teflon holder and fixed by an aluminum thermostated cage. The

teflon holder is provided with a hole to allow for eventual addition of solutes directly in the few-millimeters-thick bulk water in contact with the deposition.

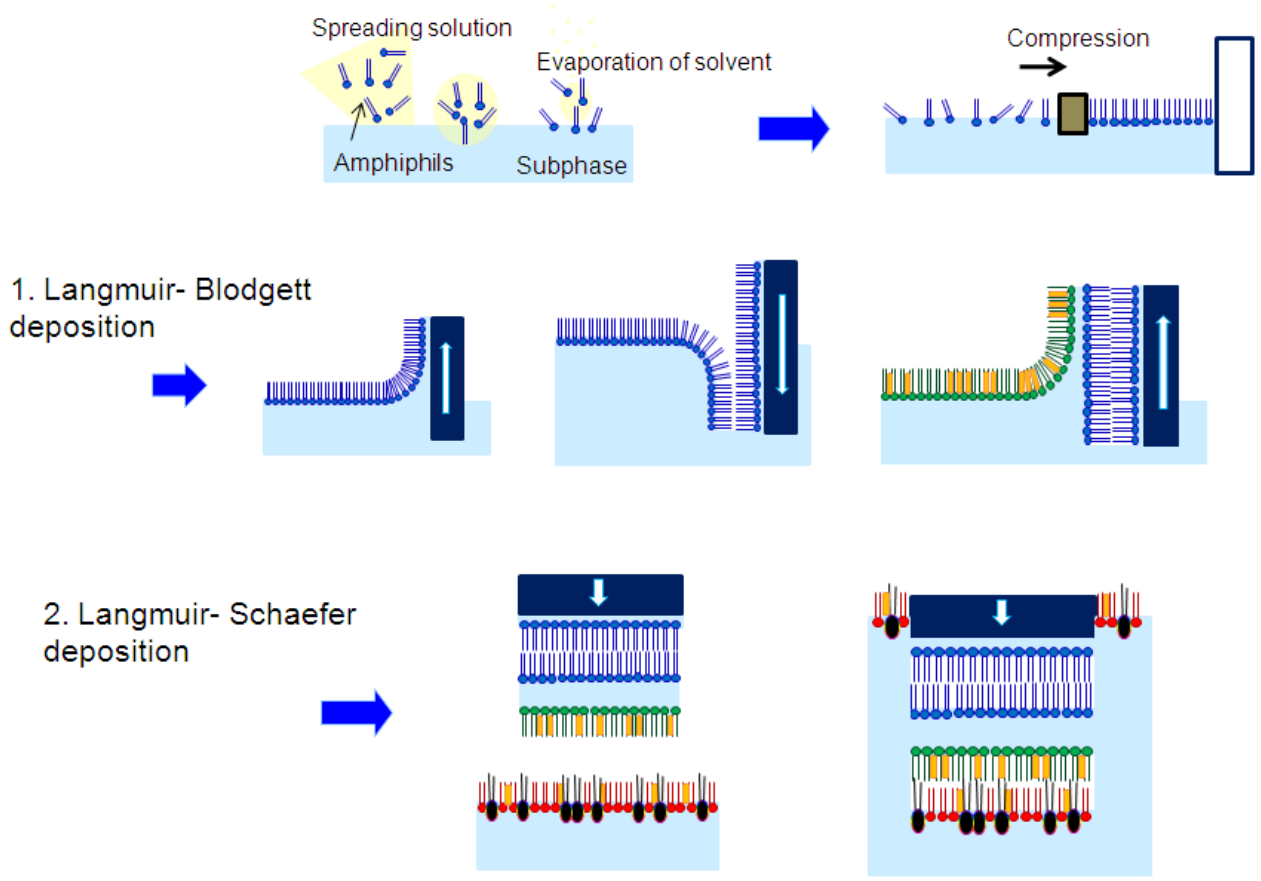

Figure 25: scheme of the Langmuir-Blodgett and Langmuir-Schaefer techniques

Regardless of our samples (bilayers or double), we transfer always the last monolayer by the Langmuir-Schaeffer technique. This method allows to deposit the sample directly in the cell sample holder (which is initially introduced into the wells of the Langmuir Trough), which prevents the multiplication of manipulations and the associated risks.

We underline that the 4-layers deposition procedure is long and laborious, taking itself about 3 hours. During this time, the in–progress sample is alternatively twice dipped into water or exposed to air for long times, necessary for monolayer removal and replacement, although in a protected and controlled environment. Nonetheless, the final system is impressively well done and stable, apart from sporadic events. An improvement of the technique is explained in the next chapter.

3. EXPERIMENTAL RESULTS

GEMs [Hakomori (1998)], Glycosphingolipids Enriched membrane Microdomains, are membrane microdomains mainly constituted by phospholipids with PC heads, glycolipids and cholesterol. GEMs are very important for cell functionality because they are suggested to act as membrane platforms through which cells recognize, and can give rise to many processes involving bigger molecules such as proteins. The structure of these domains as been widely suggested: they are thought to be enriched in cholesterol and glycolipids coupled, to assume an opposite disposition in the leaflets in the membrane, helping the formation of zones of positive and negative curvature, acting on the local fluidity of the membrane. We want to apply non-invasive techniques to the study of their structure and to the study of some interactions occurring at the surface of these domains.

We modelled the composition of GEMs using as matrix one phospholipid, mainly DPPC, cholesterol and gangliosides, in particular the disialo GD1a and the monosialo GM1.

Many complementary techniques could be used to investigate biomimetic membranes, each of them applying on a different model system. For example we can study the characteristics of biomembranes in solution, having information about the packing of the molecules forming micelles or vesicles; or we can study the structure of a single deposited biomimetic membranes, to have information about their transverse structure. We mainly used X-rays and neutrons scattering and reflectivity.

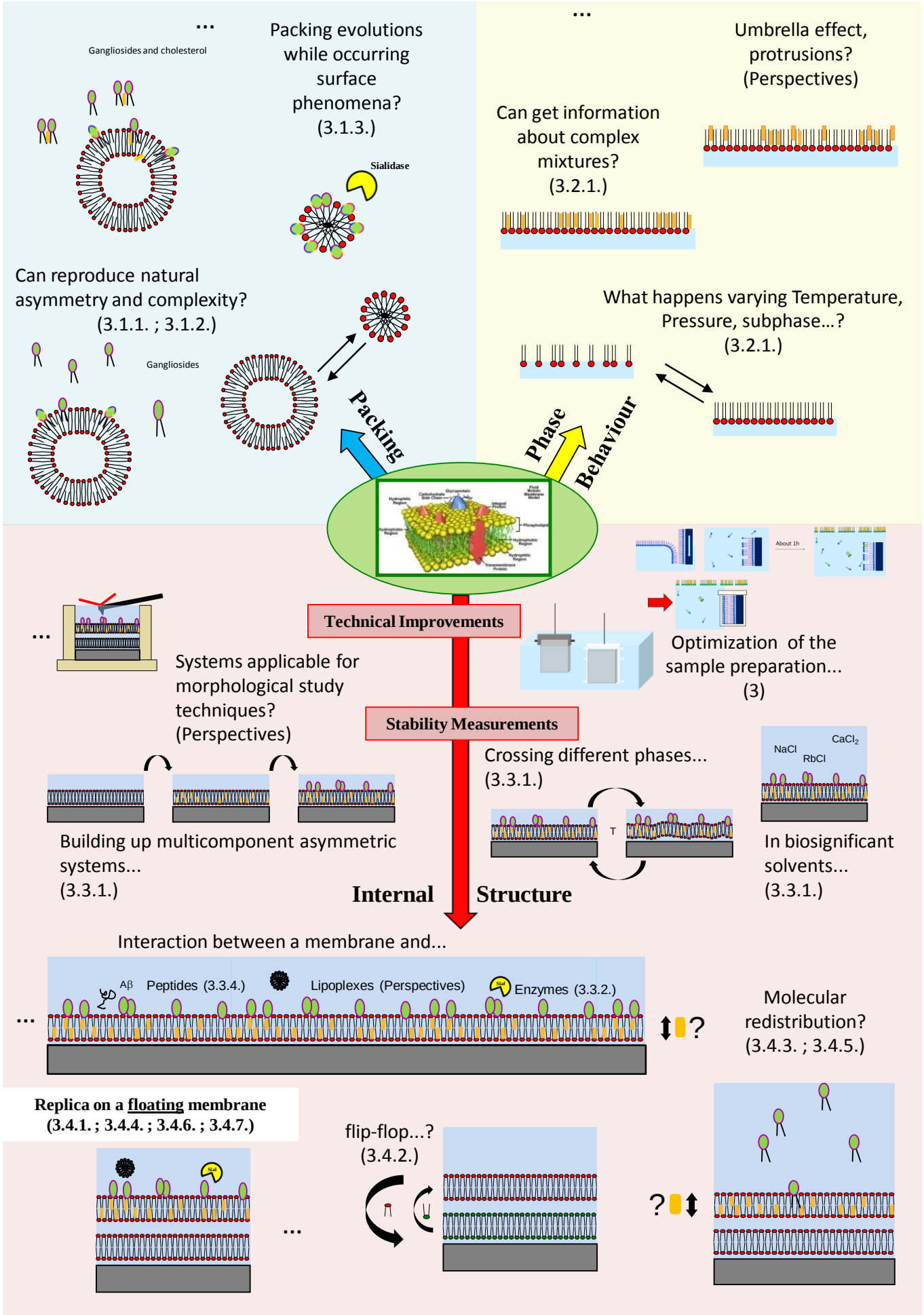

Figure 26: Schematic view of the main model systems studied.

The experimental scheme we followed can be resumed as explained below:

- We first studied the structure and interactions at the surface of various lipid micelles and vesicles in water solution by mean of X-rays scattering. We obtained information about the packing of mixed amphiphils while working an enzyme or mixing different aggregates of different molecules.
- We moved from ‘mean-value’ studies to ‘single system’ studies working on the behaviour of so-called Langmuir monolayers, by the study of their pressure-area diagrams and neutron reflectivity. We had information about the phase behaviour of lipid mixtures under various conditions.
- The characteristics of a single mimic membrane supported by a silicon block have been investigated, to get information about the main membranes structural characteristics and on the structural changes occurring as a consequence of interactions taking place at their surfaces, by mean of neutrons and X-rays reflectivity.
- Finally we investigated the structure of single complex mimic membranes free to fluctuate over a water layer, by mean of X-ray reflectivity and neutron reflectivity. Information have been obtained about structural dynamics occurring due to changes in the environment the membrane is inserted in.

COLLABORATIONS AND TECHNICAL IMPROVEMENTS

The investigation of the fine structural properties of complex biomembranes requests the use of non-average techniques and a sample construction highly controlled.

For this reason we decided to apply two potent advanced techniques to the study of membranes: the radiation reflectivity and the Langmuir-Blodgett / Langmuir-Schaefer techniques.

As explained in the previous chapter the Langmuir-Blodgett technique, coupled with the Langmuir-Schaefer one, allows to build up macroscopic (5 cm x 5 cm big) single complex membranes, with controlled composition in each leaflet, almost free to fluctuate in the solvent. Reflectivity of neutrons and X-rays are two complementary non- invasive techniques which allow the study of the internal structure of these systems.

Both techniques are not trivial and ask the use of very expensive instrumentation and of international facilities. For this reason we started an important collaboration with a French group driven by Giovanna Fragneto, working at the Institut Laue-Langevin (ILL) in Grenoble, France, where I spent part of my PhD. At ILL I could learn the Langmuir-Blodgett Langmuir-Schaefer technique and improve it, and I had the possibility to use big facilities to perform neutrons and X-rays reflectivity experiments.

In particular the Langmuir-Blodgett technique used for samples preparation is a long series of many delicate steps, some of which has been improved.

The first improvement we did is referred to the so called ‘dipper’, that is the holder used to dip the silicon block in and out from the water of the Langmuir trough while depositing layers. This was like a C made of a metal alloy, which could not obviously enter in contact with the pure water of the trough, with the consequence that just part of the silicon support could be immerged in water, about 4.5 cm, and great care had to be made during the depositions, especially during the deposition of the last layer with the Langmuir-Schaefer technique where it was almost impossible to control it. Moreover the taking of metal on silicon is not good and the block was in danger of falling. We ideated a new Teflon sheath bearing mainly two big advantages to the sample preparation: first the sample is hold in a better way and now there is no risk of falling; second the support can now be completely immerged in water and the coverage of the silicon block by the membranes can reach 100%. This is very important because being the membrane very thin, to have a good signal we need a big area, and we should avoid the borders. The

possibility to deposit a 5x5 cm big membrane instead of a 5x4.5 cm enhances a lot the goodness of our signal.

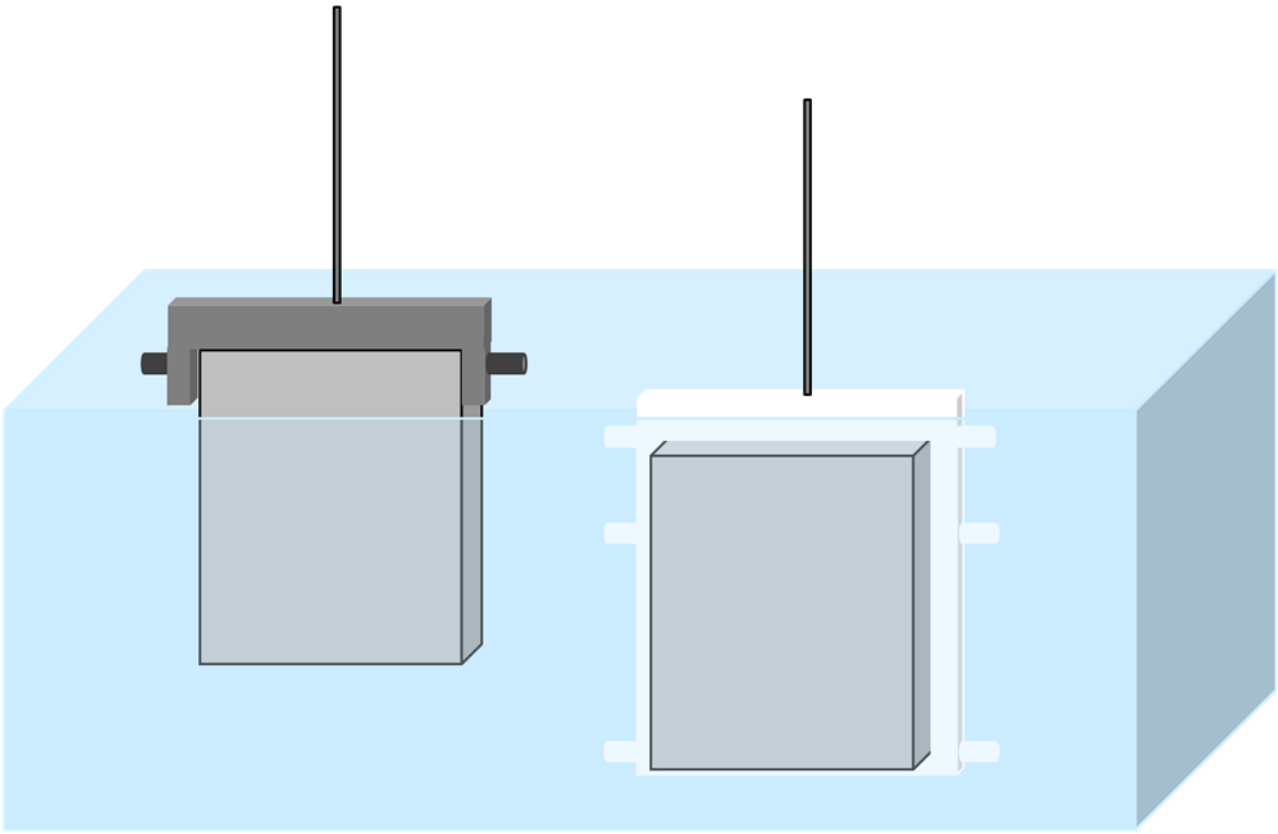

Figure 27: Thanks' to the new dipper designed we can obtain a full block immersion and, as a consequence, a 100% theoretical coverage.

When we deposit two subsequent membranes, between the deposition of the second and third layer, that is the external leaflet of the first membrane and the internal of the second one, the sample lies for a long time in water and at least one hour with a molecular layer deposited on the surface of the Langmuir trough. In this time frame monomer exchange can occur, spoiling the accuracy we used to have an exact composition in each layer. For this reason we built up a Teflon box to insulate the sample when in water. A schematic view of the box can be found in figure 28.

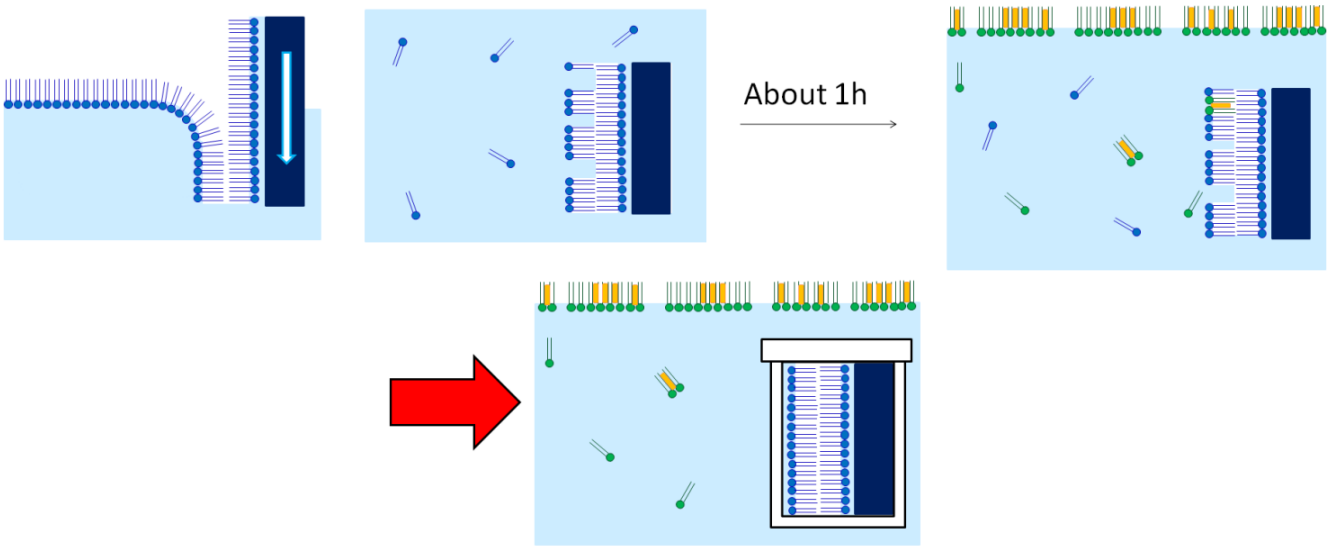

Figure 28: We ideate and constructed a Teflon box to avoid monomer exchange during the sample preparation by mean of Langmuir-Blodgett Langmuir-Schaefer technique

3.1. MICELLES AND VESICLES IN SOLUTION

We started our study from simple biosimilar systems, that is vesicles and micelles. They were chosen as they are extremely responsive to molecular packing changes.

We focused on asymmetry, an aspect found in natural membranes, where gangliosides reside only in the external layer. To recreate the asymmetry we started from phospholipid vesicles, where we let incubate different ganglioside micelles coming from the solution. Then we verified whether the presence of cholesterol modifies the incubation process and the final forming structures.

3.1.1. Incubation of gangliosides in phospholipid vesicles

We first studied the effects brought by the presence of a glycolipid to a phospholipid matrix. As lipid matrix we used the DMPC (Dimiristoylphosphatidylcholine), a 14 carbon hydrophobic chains phospholipid, and we let incubate in DMPC vesicles two gangliosides: the monosialic GM1 and the disialic GD1a, and a mixture of the two. We studied the structural changes brought by the gangliosides presence by Small Angle X-Ray Scattering (SAXS).

We prepared DMPC (see figure 29) vesicles according to the protocol described in the previous chapter to a final concentration of lipids in water of the 4%, in order to have a good SAXS intensity.

Micellar solutions were prepared by dissolving GM1, Gd1a (figure 29) and a mixture 1:1 molar of the two gangliosides in pure water and let to equilibrate for about 24 hours. The final concentration of each solution was 4%.

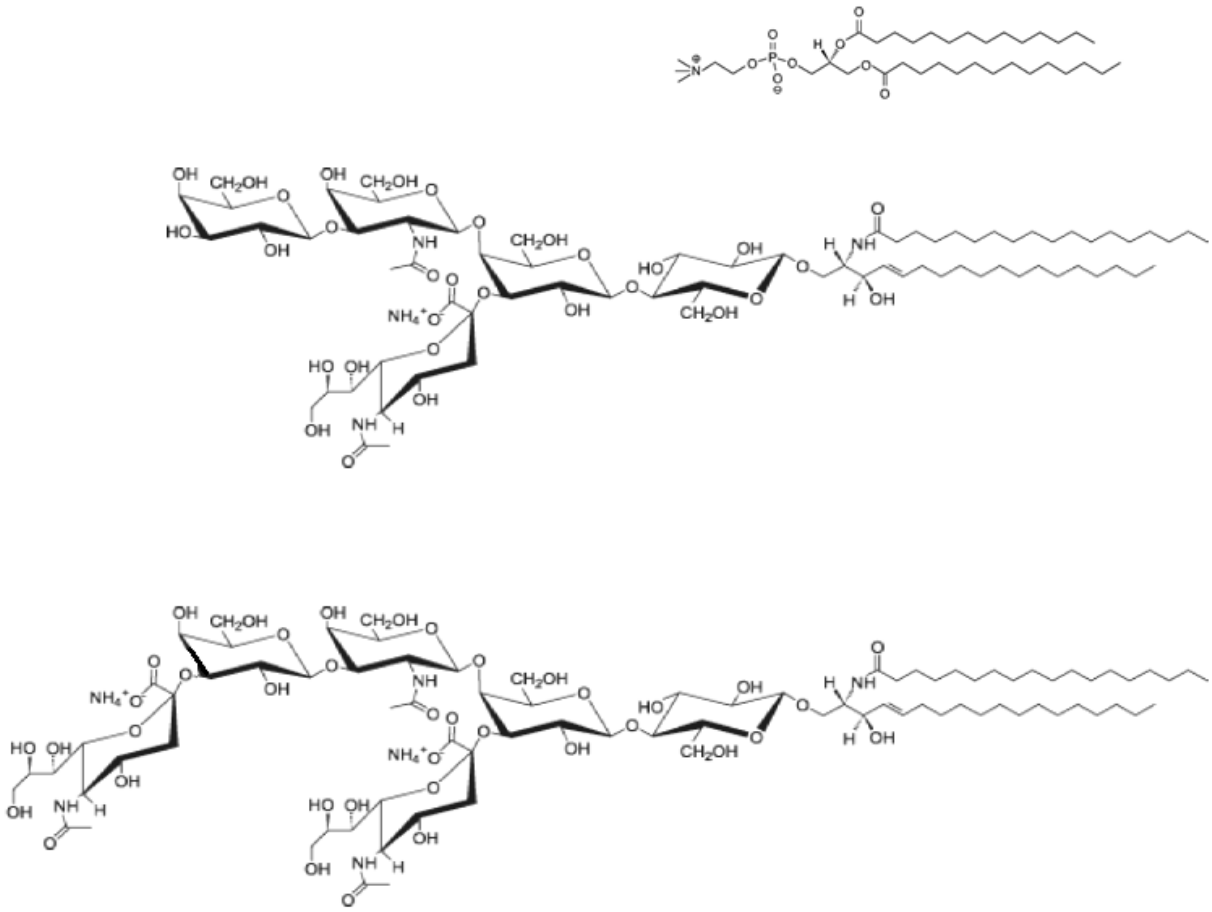

Figure 29: from top to bottom structures of DMPC, GM1 and GD1a

X-Ray scattering measurements were performed at the high brillance ID02 beamline of ESRF in Grenoble, FR. To work with precision, especially during background subtraction, separate measurements were carried out later on empty capillaries, a capillary with pure water, and a capillary with the sample in solution. Measurements were made at fixed temperature, 30°C, over the melting transition of DMPC hydrophobic chains and after the measure, the sample-containing capillaries were stored in oven at 30°C. During a measure, the angular distribution of the scattered X-ray intensity is recovered.

After measuring the empty capillary and a capillary filled with water for subtractions, we measured the starting points, that is the solutions of the DMPC vesicles and the micellar solutions of gangliosides. The corresponding spectra referred are shown in fig 30:

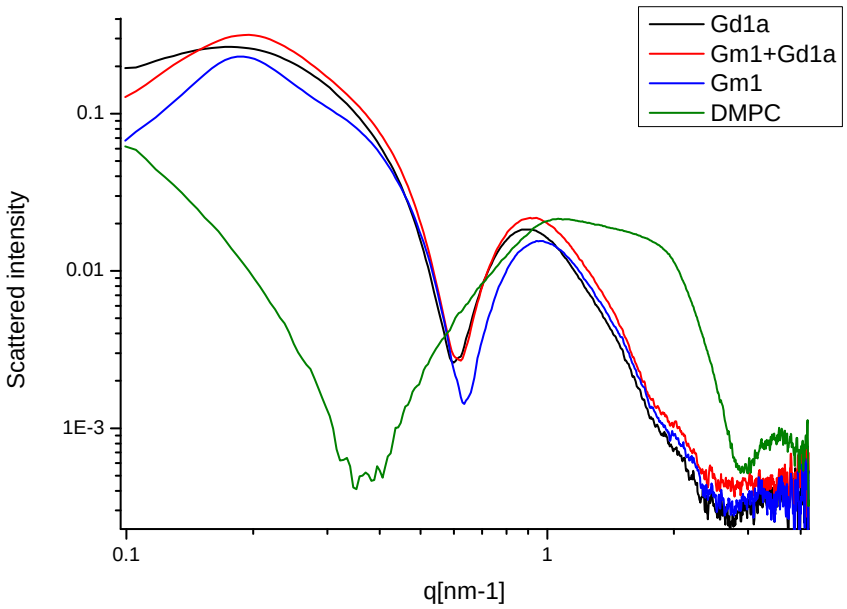

Figure 30: SAXS spectra referred to the DMPC vesicles solution, GD1a micellar solution, GM1 micellar solution, GD1a:GM1 1:1 molar micellar solution. The capillary and water contributes have been subtracted, T=30°C.

It is immediate to see that the typical spectral shapes referred to vesicles and micelles are very different. We are also sensible to different gangliosides, aggregating in different micelles (see the red, blue and black spectra in figure 30). Micellar solutions have been measured at the 0.4%, that is, the concentration they finally have in the mixed solution.

After measuring the starting points, we mixed the desired solutions and we measured their diffraction spectrum all along during 24 hours to follow the structural evolution of the DMPC vesicles while mixing with the different gangliosides micelles.

In figure 31 the time evolution of the three system is shown, from the black to the red spectrum.

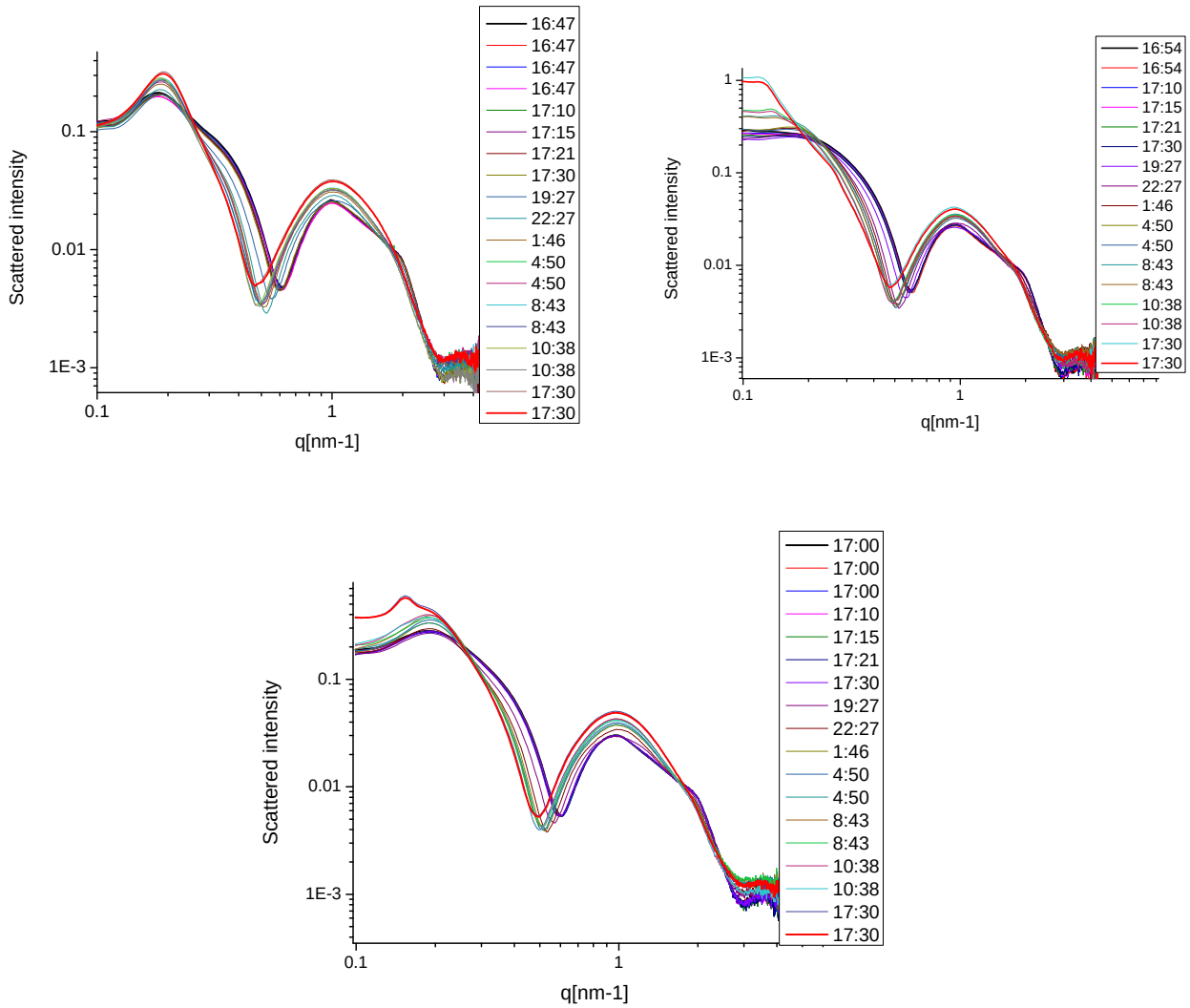

Figure 31: Time evolution of the spectra referred to the GM1 (up left box), GD1a (up right box) and their mixture (lower box) incubation in DMPC vesicles solutions. The starting point is black, the final red.

In the three cases under study the shape of the spectrum changes, suggesting that the system is evolving, that is vesicles and micelles are mixing (reasonably we can say that gangliosides enter the lipid vesicles).

DMPC vesicle+GM1 micelle

In figure 32 the spectra referred to the starting vesicles and micelles are shown: the GM1 micelle, the DMPC vesicle and the mixture of the two at 'time zero', that is when they had just been mixed. In figure 33 the time evolution of the system is shown. Since the contrast profile of the aggregates we are looking at is dramatically changing in time, the shape of the spectrum changes, the position and deepness of the minimum changes, a peak arises in the low q region (meaning that the new aggregates are interacting).

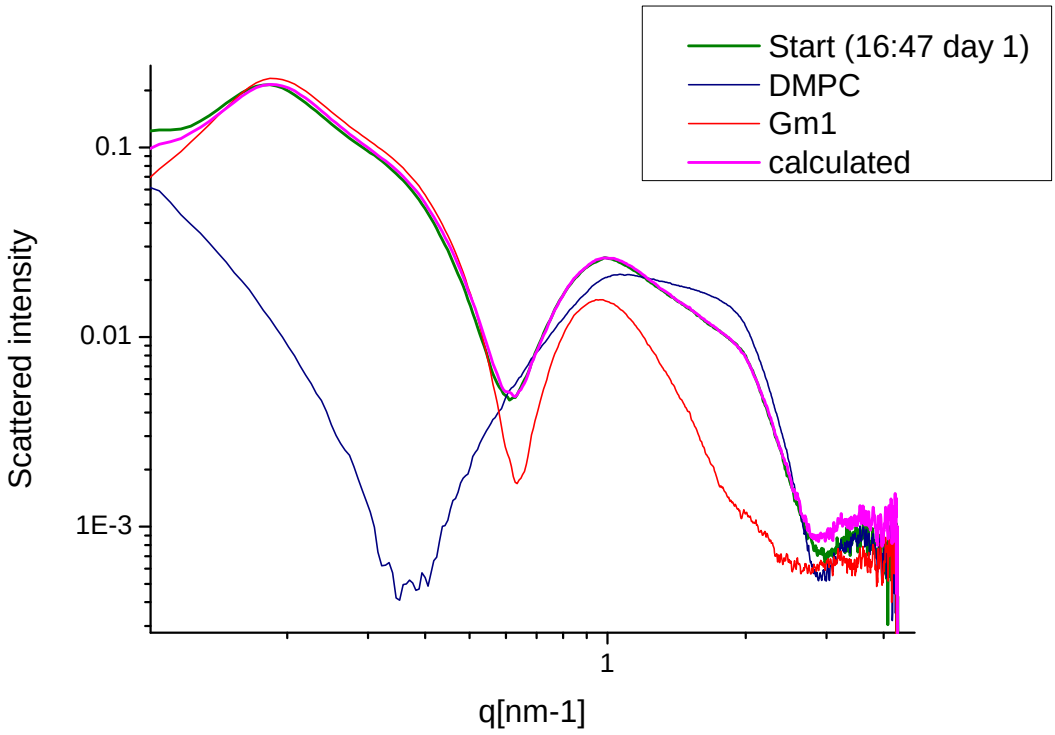

Figure 32: SAXS spectra of the GM1 micelle in red, the DMPC vesicle in blue, the experimental starting point of the mix in green and the algebraic sum of GM1 and DMPC spectra in pink.

As an example we show here that the spectrum referred to the mixed system measured at time zero, that is just after mixing, is the superposition of the spectra referred to micelles and vesicles. This means that the mixed system at time zero is a coexistence of the two (figure 32). Then the system evolves as shown in figure 33, because ganglioside micelles and lipid vesicles are mixing, giving rise to a new system.

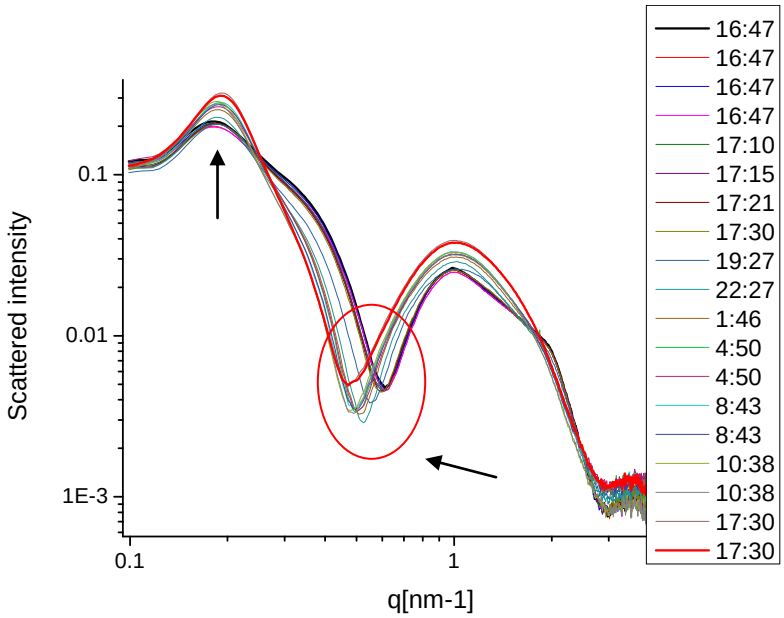

Figure 33: SAXS spectra referred to the evolution of the system DMPC vesicles mixed with GM1 ganglioside micelles.

As explained in the previous chapter the intensity plotted as a function of q is a sort of graphical distribution of probabilities. It talks about the typical distances and dimensions existing in the investigated system, balanced by the contrast of each molecule. The horizontal axis reports the scattered wavevector. A peak of intensity in a X-ray scattering spectrum means that the corresponding distances in the direct space are typical for the system, that is, there is something repeating after that distance with a good 'contrast factor', that is visible for X rays with respect to the other components. It could be an interparticle distance, a particle dimension or other. Low q values in the intensity spectrum correspond to long distances. The peak arising in the low q region is a so called 'structure peak', corresponding to interparticle distances. The rise of a structure peak means that an interparticle structure is forming, as expected if charged molecules (gangliosides) enter the vesicles that become charged and so interacting. We did not see the structure peak among micelles from the beginning because they are too dilute. Finally the whole shape of the spectrum is changing, not only because the particles shape is changing, but also because its contrast is changing. The intensity spectrum profile depend on shape, mass and contrast profile of the particles under study, and on the eventual structure forming among them.

As a first step to the study of the evolution of the system, we investigated the position of the minimum of intensity around q= 0.55 nm^{-1} as a function of time. Results are shown in figure 34:

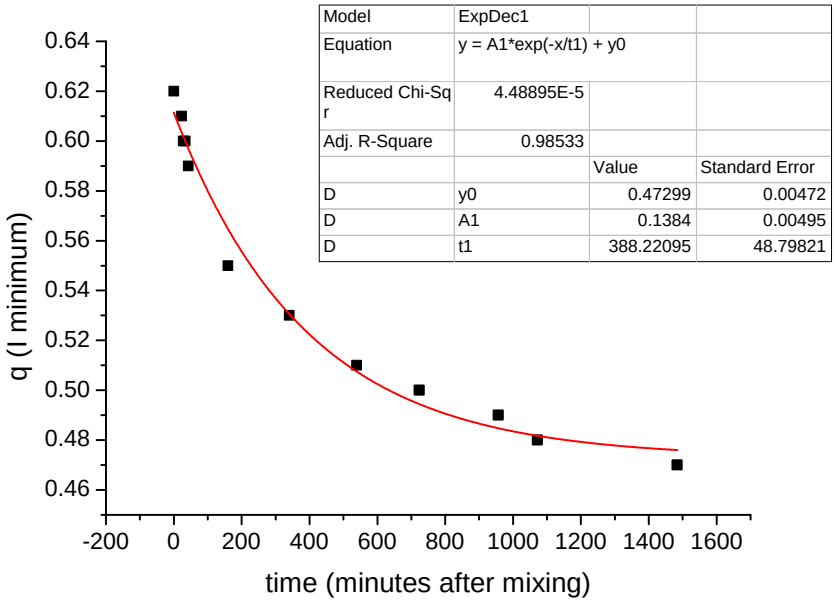

Figure 34: evolution of minimum of intensity position in time while mixing DMPC vesicles and GM1 ganglioside micelles.

The trend of the data is exponential, suggesting that the process starts faster, and then slows down, going towards zero. In fact when the solutions have just been mixed the mixing process is reasonably fast and goes towards zero when the systems are completely mixed, so the q position will change fast in the first minutes and will reach a definitive value which is that of the final vesicle. We fit the data referred to the q value evolution in time, with the following function:

$Y = yo + A*exp(-x/t)$

Results are reported in each graph and in the final table 4.

yo gives is the value towards which the system goes, even if no direct information can be obtained from that number, since to know how is the final product we should fit the whole intensity spectrum. *t* is the time after which we can consider the process completed. In fact *t* is the time at which the y value is reduced to 1/e = 0.37 times its initial value.

All the measurement have been performed at 30°C, in the fluid phase of DMPC, but as expected the presence of GM1 is changing the phase of the system and so its contrast profile, because contrast depends also on density.

DMPC vesicle+Gd1a micelle

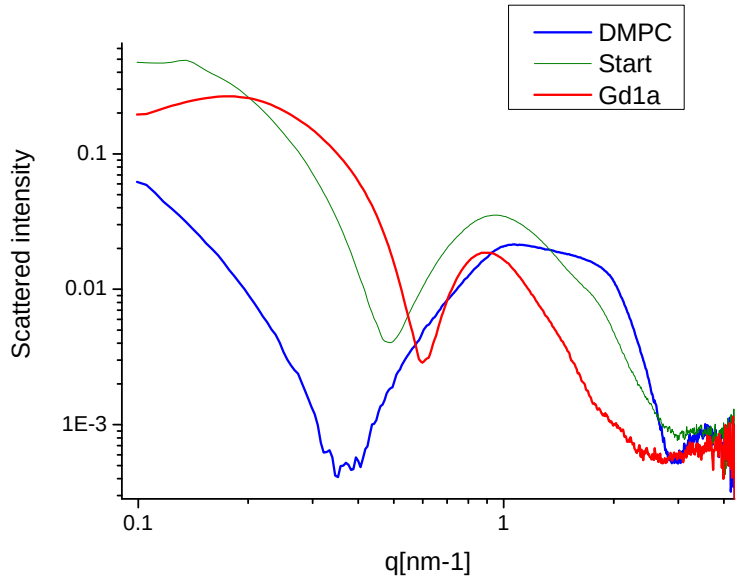

Figure 35: SAXS spectra of the Gd1a micelle, the DMPC vesicle and the experimental starting point of the mix, sum of the two.

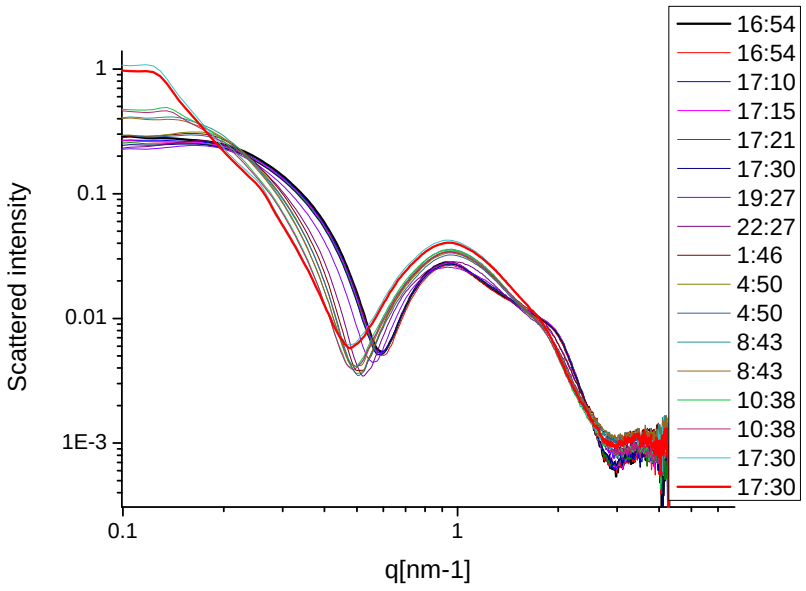

Figure 36: SAXS spectra referred to the evolution of the system DMPC vesicles mixed with Gd1a ganglioside micelles.

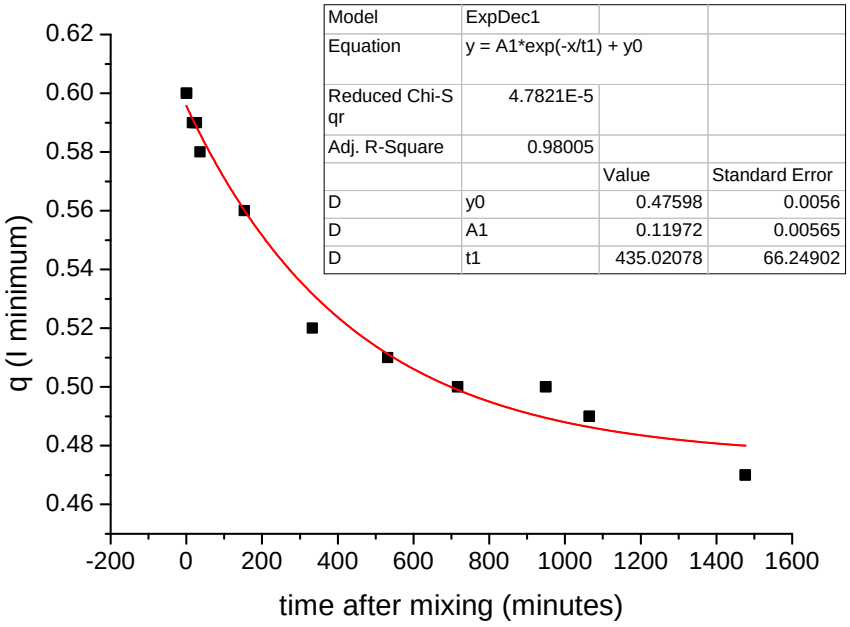

Figure 37: evolution of minimum of intensity position in time while mixing DMPC vesicles and Gd1a ganglioside micelles.

As before we performed all our measurement at 30°C, to be in the fluid phase of DMPC, but again as expected the presence of the ganglioside is changing the phase of the system.

DMPC vesicle+GM1 :Gd1a 1 :1 mol micelle

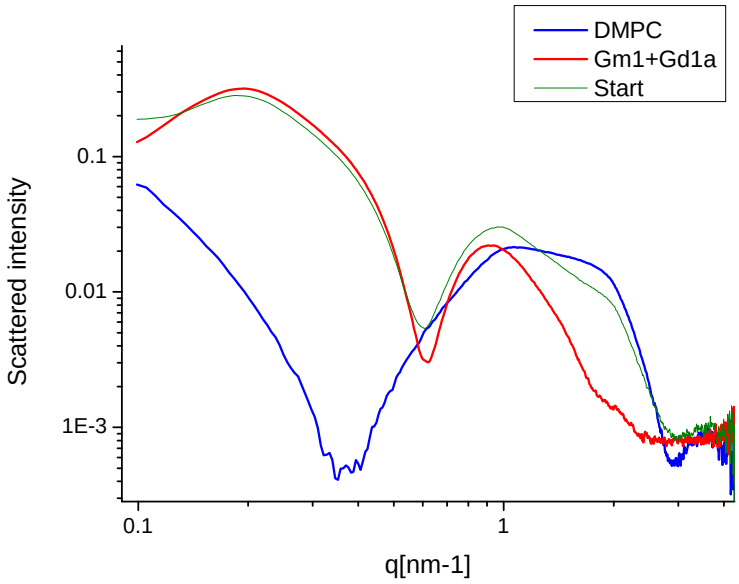

Figure 38: SAXS spectra of the GM1:Gd1a 1:1 mol micelle, the DMPC vesicle and the experimental starting point of the mix, sum of the two.

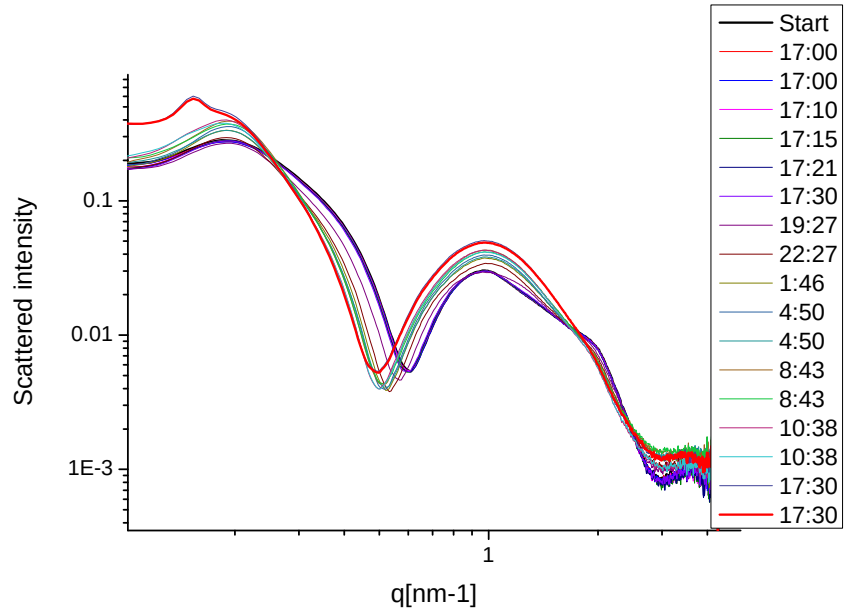

Figure 39: SAXS spectra referred to the evolution of the system DMPC vesicles mixed with GM1:Gd1a 1:1 mol gangliosides micelles.

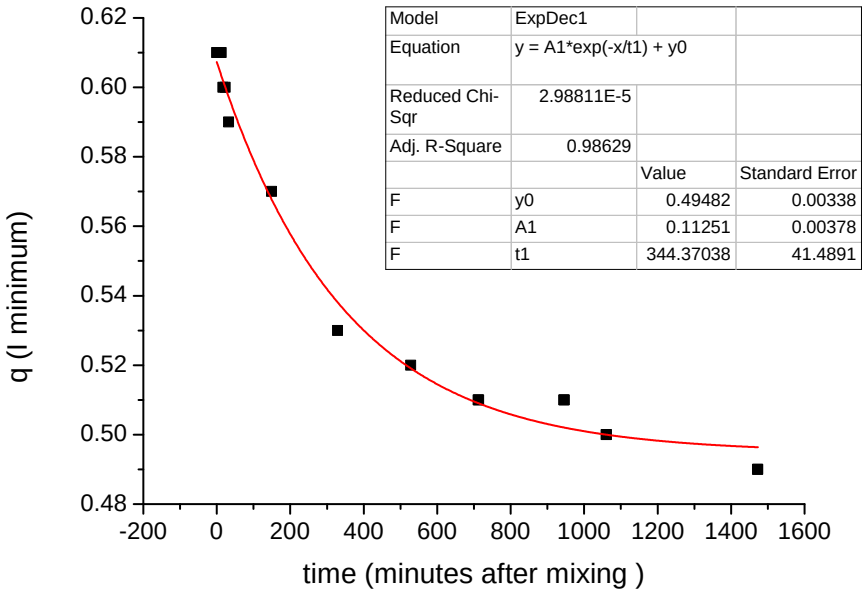

Figure 40: evolution of minimum of intensity position in time while mixing DMPC vesicles and a Gd1a:GM1 1:1 mol gangliosides micelles.

3.1.2. Incubation of gangliosides in phospholipids vesicles: cholesterol effect.

After seeing that systems in solution mix on ‘observable’ timescales, since our aim is the study of membrane microdomains enriched not only in glycolipids but also in cholesterol, and since cholesterol and gangliosides seem to form a couple, we now want to investigate what happens when cholesterol is present in these mixed system.

In particular, since cholesterol is highly hydrophobic, to participate to the mix, it has to be vehiculated by one of the two mixing systems: either the micelles, or the vesicles. We examined both cases during the mix of DMPC vesicles with GD1a or GM1 micelles. Moreover we divided every mix in two sub cases: DMPC:ganglioside:cholesterol 10:1:1 molar ratio or DMPC:ganglioside:cholesterol 10:0.5:0.5 molar ratio. We know the real situation to be DMPC:ganglioside:cholesterol 10:1:2.5 molar ratio, but experiments show that [Tomohiro Hayakawa and Mitsuhiro Hirai (2003)] GM1 and GD1a gangliosides micelles can stand a maximum cholesterol content to a total molar ratio 1:1.

We studied the following mixing solutions:

- DMPC 10mol + (chol 1mol + GM1 1mol)
- DMPC 10mol + (chol 0.5mol + GM1 0.5mol)
- (DMPC 10mol + chol 1 mol) +GM1 1mol
- (DMPC 10mol + chol 0.5 mol) +GM1 0.5mol
- DMPC 10mol + (chol 1mol + Gd1a 1mol)
- DMPC 10mol + (chol 0.5mol + Gd1a 0.5mol)
- (DMPC 10mol + chol 1 mol) +Gd1a 1mol
- (DMPC 10mol + chol 0.5 mol) +Gd1a 0.5mol

In figures 41, 42 and 43 the spectra referred to all the starting micelles and vesicles are represented, showing the effect of cholesterol on them.

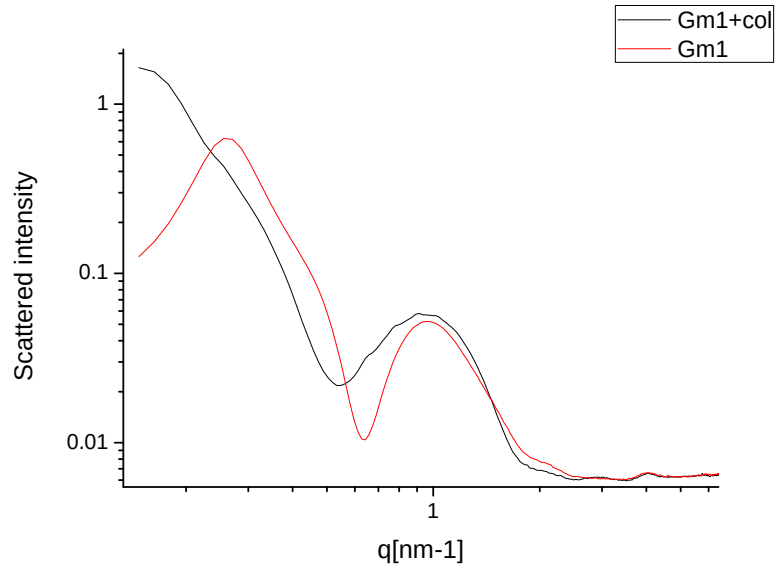

Figure 41: SAXS spectra of the GM1 micelle alone and with cholesterol in water. T=30°C.

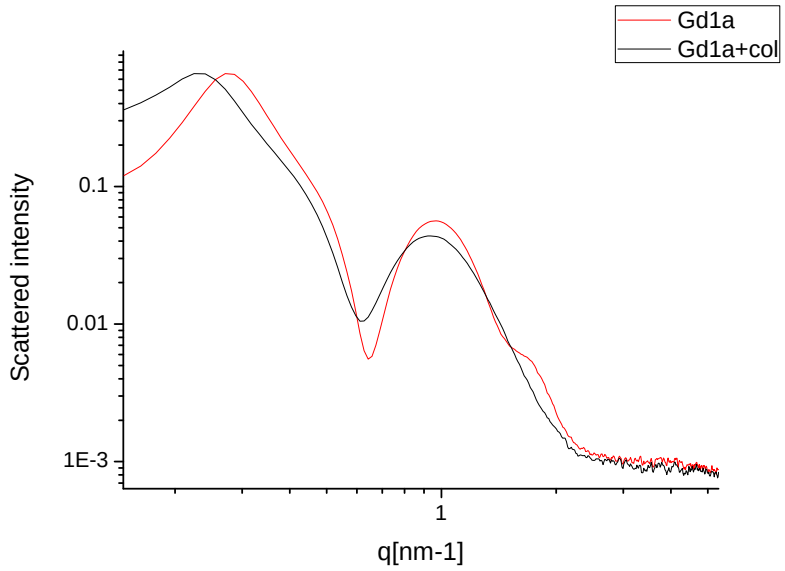

Figure 42: SAXS spectra of the Gd1a micelle alone and with cholesterol in water. T=30°C.

Cholesterol affects the structure of both micelles, modifying their shape and their structuring in the solvent.

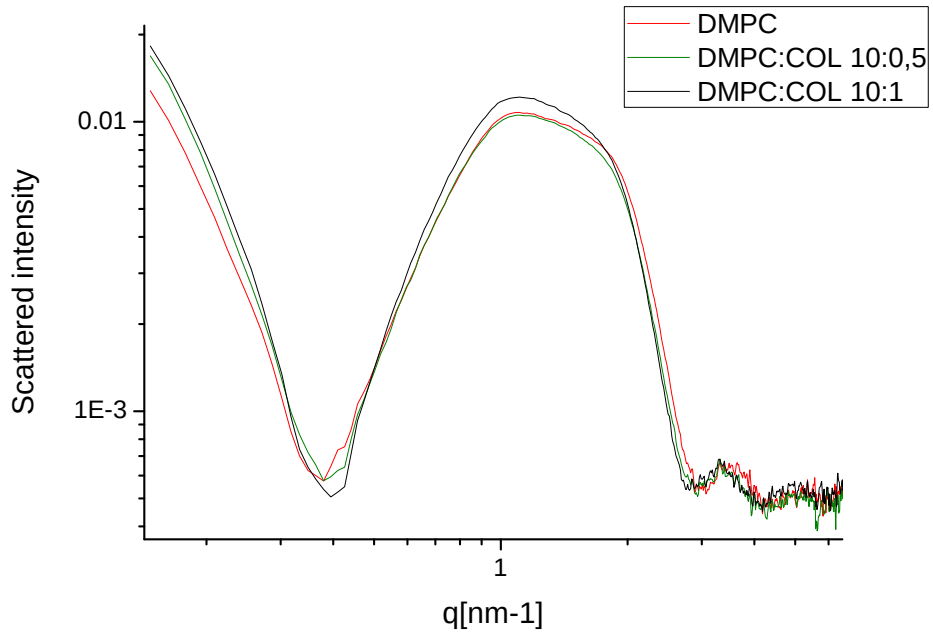

Figure 43: SAXS spectra of the DMPC vesicle alone and with different amounts of cholesterol in water. T=30°C.

DMPC 10mol + (chol 1mol + GM1 1mol)

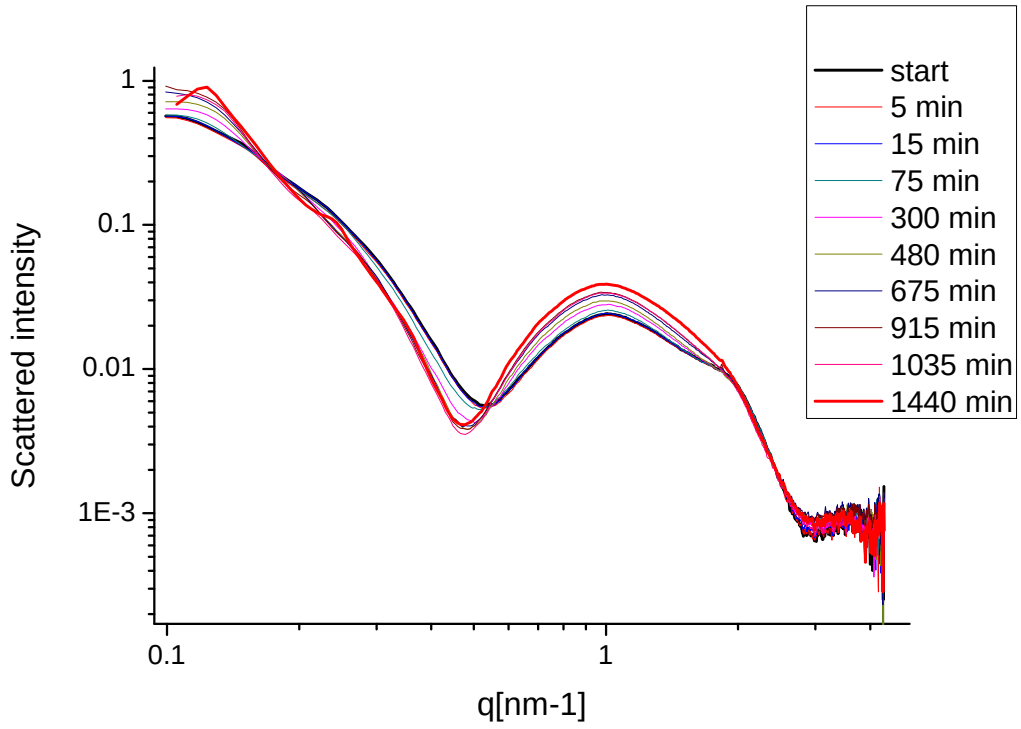

Figure 44: SAXS spectra referred to the evolution of the system DMPC vesicles mixed with GM1:cholesterol micelles. The molar ratio lipid:ganglioside:cholesterol is 10:1:1.

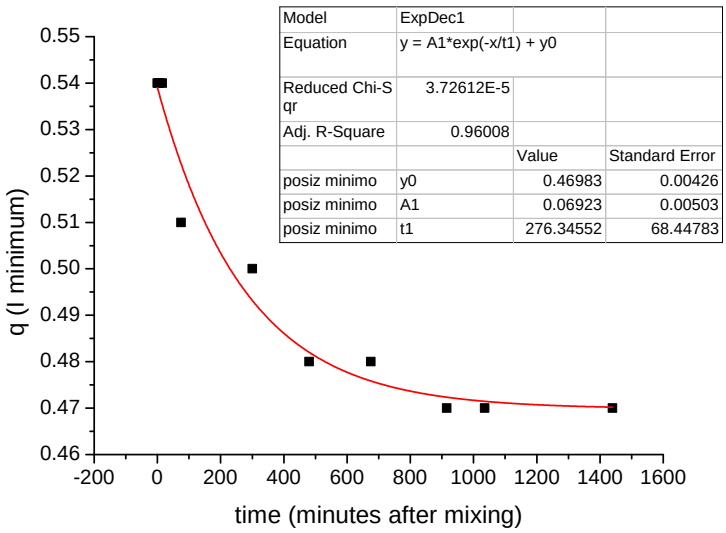

Figure 45: evolution of minimum of intensity position in time while mixing DMPC vesicles and GM1:cholesterol micelles. The total lipid:ganglioside:cholesterol molar ratio is 10:1:1.

At the end of the mixing, when the system is equilibrated, a structure peak arises in the spectrum, indicating that the system is ordering and the final vesicles, due to the presence of a charged ganglioside, interact and assume a structure, that is they keep at a preferred distance.

DMPC 10mol + (chol 0.5mol + GM1 0.5mol)

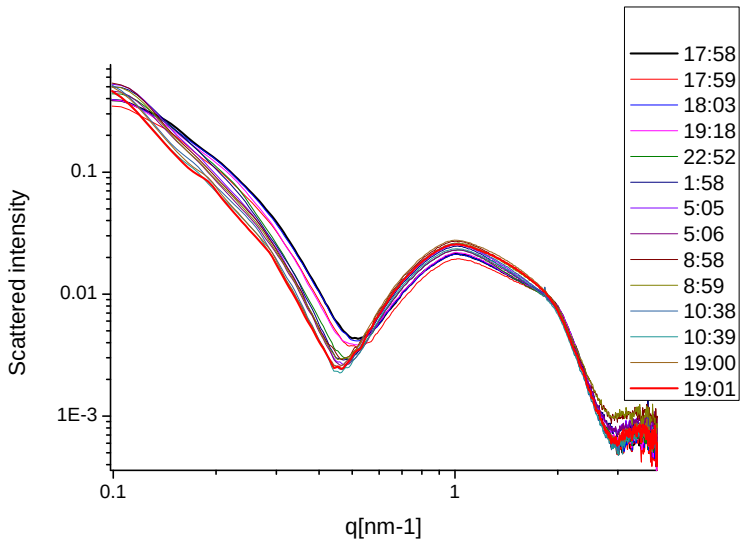

Figure 46: SAXS spectra referred to the evolution of the system DMPC vesicles mixed with GM1:cholesterol micelles. The molar ratio lipid:ganglioside:cholesterol is 10:0.5:0.5.

As expected, if compared to the sample with twice the ganglioside molar fraction, the appearing structure peak is broader.

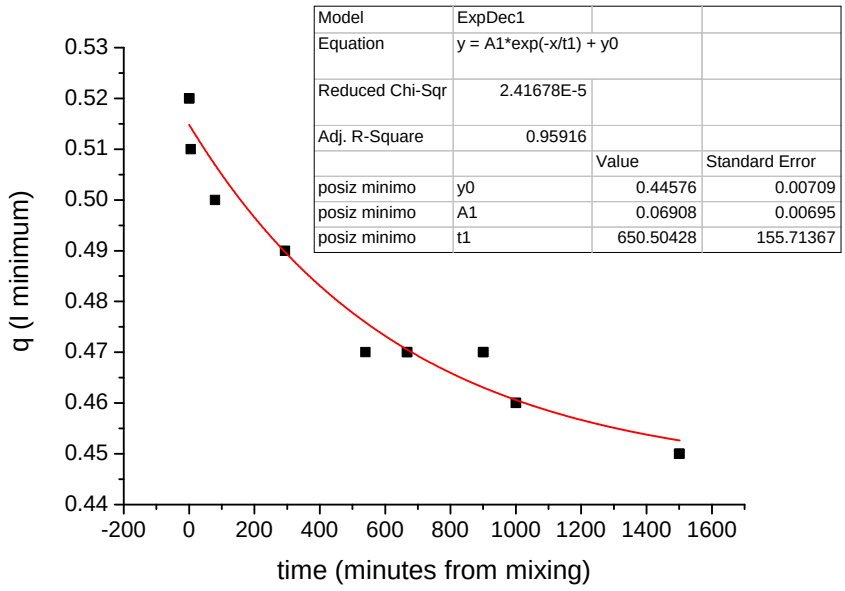

Figure 47: evolution of minimum of intensity position in time while mixing DMPC vesicles and GM1:cholesterol micelles. The total lipid:ganglioside:cholesterol molar ratio is 10:0.5:0.5.

(DMPC 10mol + chol 1 mol) +GM1 1mol

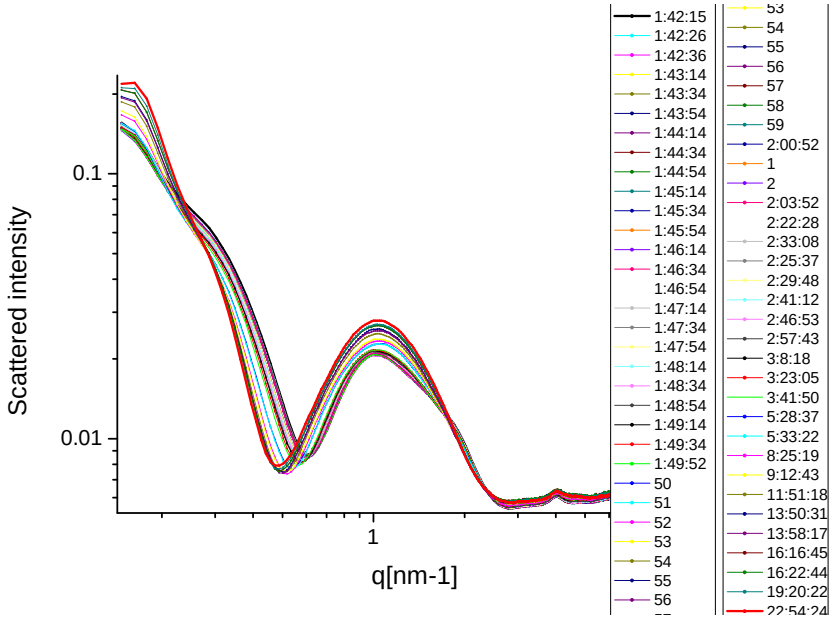

Figure 48: SAXS spectra referred to the evolution of the system DMPC:cholesterol 1:1 vesicles mixed with GM1 micelles. The molar ratio lipid:ganglioside:cholesterol is 10:1:1.

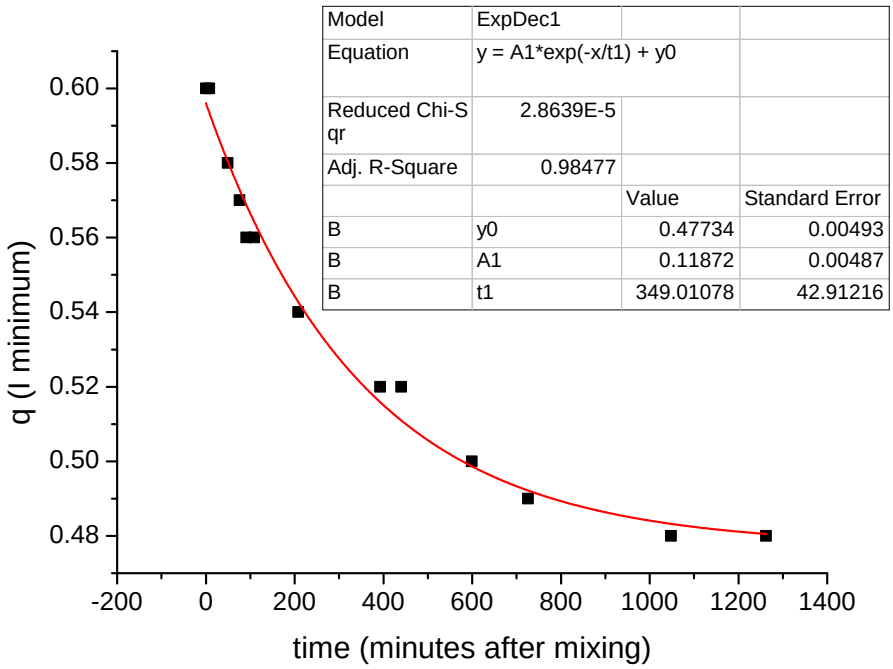

Figure 49: evolution of minimum of intensity position in time while mixing DMPC:cholesterol 10:1 vesicles and GM1 micelles. The total lipid:ganglioside:cholesterol molar ratio is 10:1:1.

(DMPC 10mol + chol 0.5 mol) +GM1 0.5mol

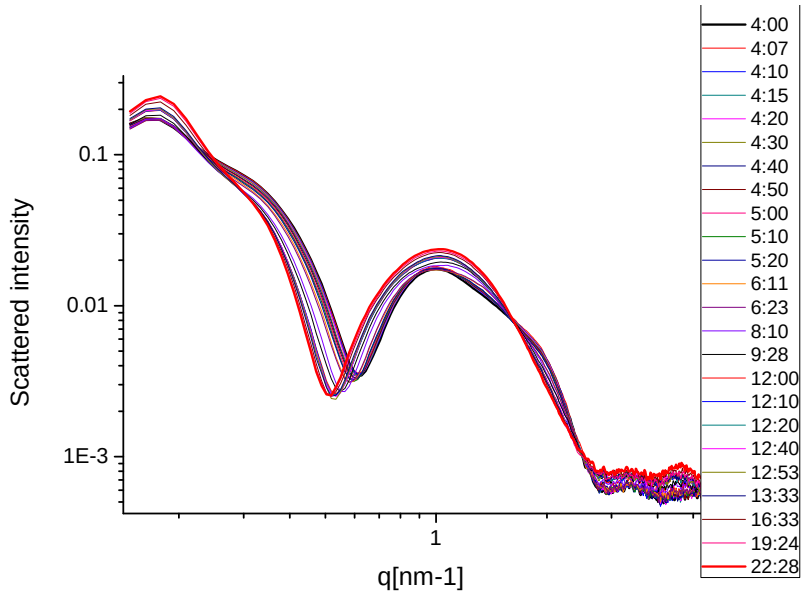

Figure 50: SAXS spectra referred to the evolution of the system DMPC:cholesterol 10:0.5 molar vesicles mixed with GM1 micelles. The molar ratio lipid:ganglioside:cholesterol is 10:0.5:0.5.

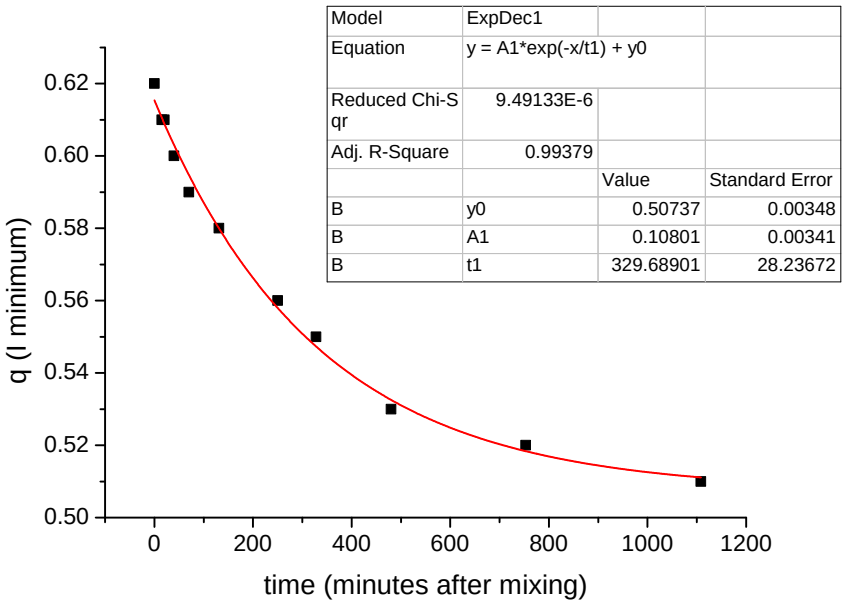

Figure 51: evolution of minimum of intensity position in time while mixing DMPC:cholesterol 10:0.5 vesicles and GM1 micelles. The total lipid:ganglioside:cholesterol molar ratio is 10:0.5:0.5.

DMPC 10mol + (chol 1mol + Gd1a 1mol)

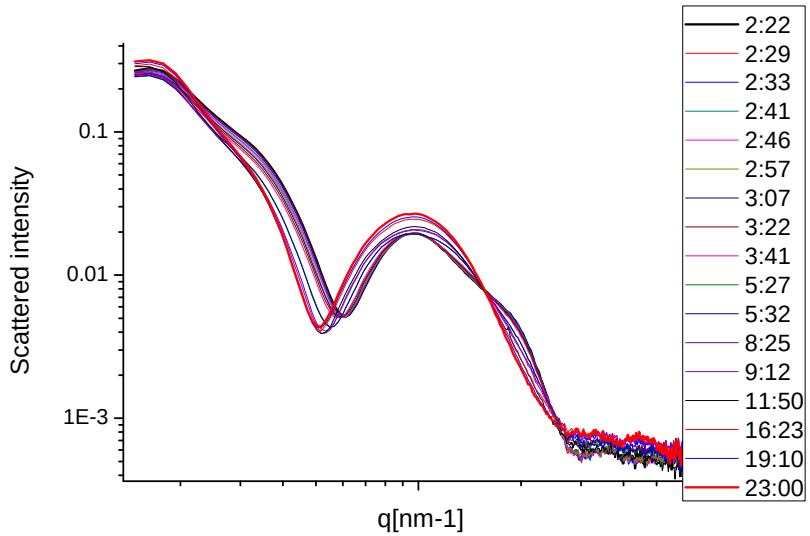

Figure 52: SAXS spectra referred to the evolution of the system DMPC vesicles mixed with GD1a:cholesterol micelles. The molar ratio lipid:ganglioside:cholesterol is 10:1:1.

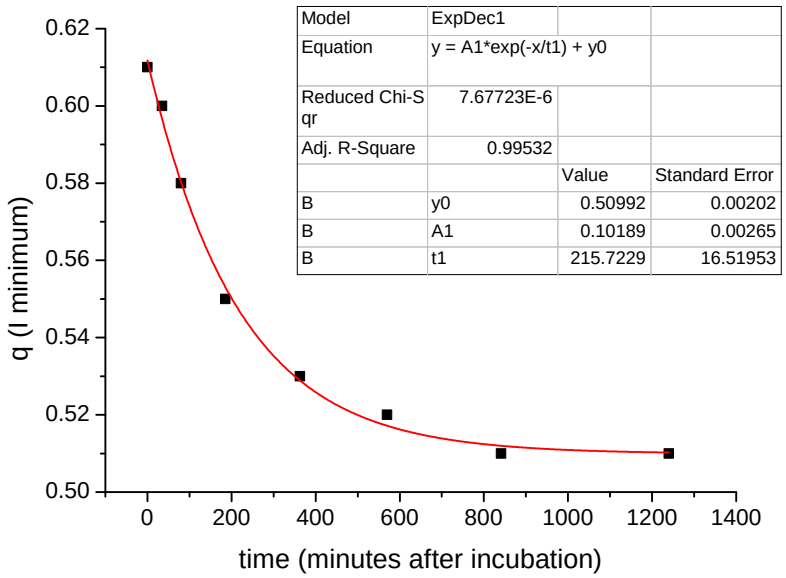

Figure 53: evolution of minimum of intensity position in time while mixing DMPC vesicles and GD1a: cholesterol 1:1 micelles. The total lipid:ganglioside:cholesterol molar ratio is 10:1:1.

DMPC 10mol + (chol 0.5mol + Gd1a 0.5mol)

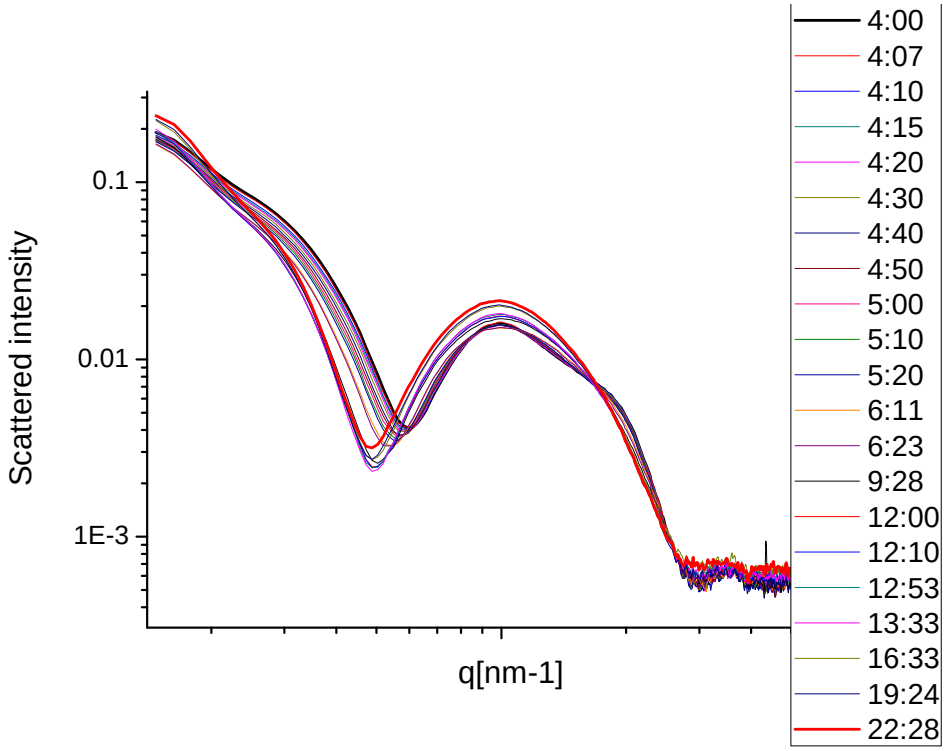

Figure 54: SAXS spectra referred to the evolution of the system DMPC vesicles mixed with GD1a:cholesterol micelles. The molar ratio lipid:ganglioside:cholesterol is 10:0.5:0.5.

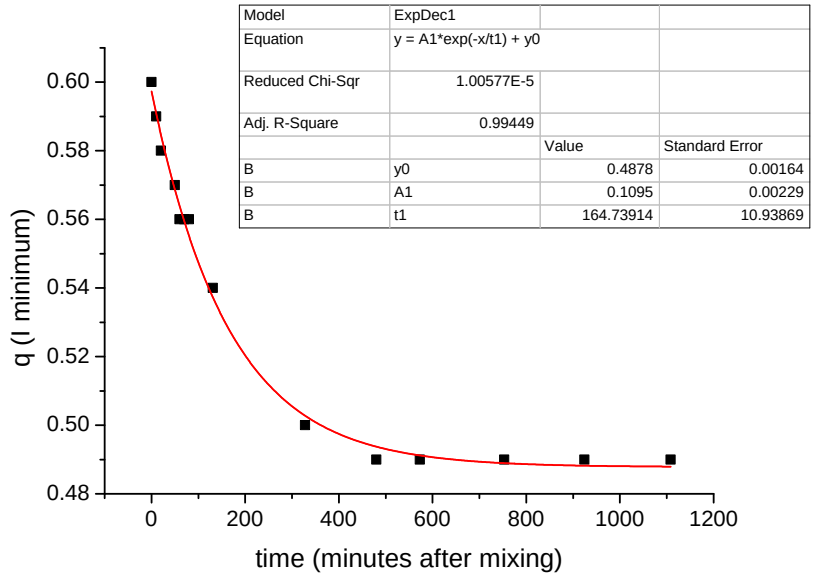

Figure 55: evolution of minimum of intensity position in time while mixing DMPC vesicles and GD1a: cholesterol 1:1 micelles. The total lipid:ganglioside:cholesterol molar ratio is 10:0.5:0.5.

(DMPC 10mol + chol 1 mol) +Gd1a 1mol

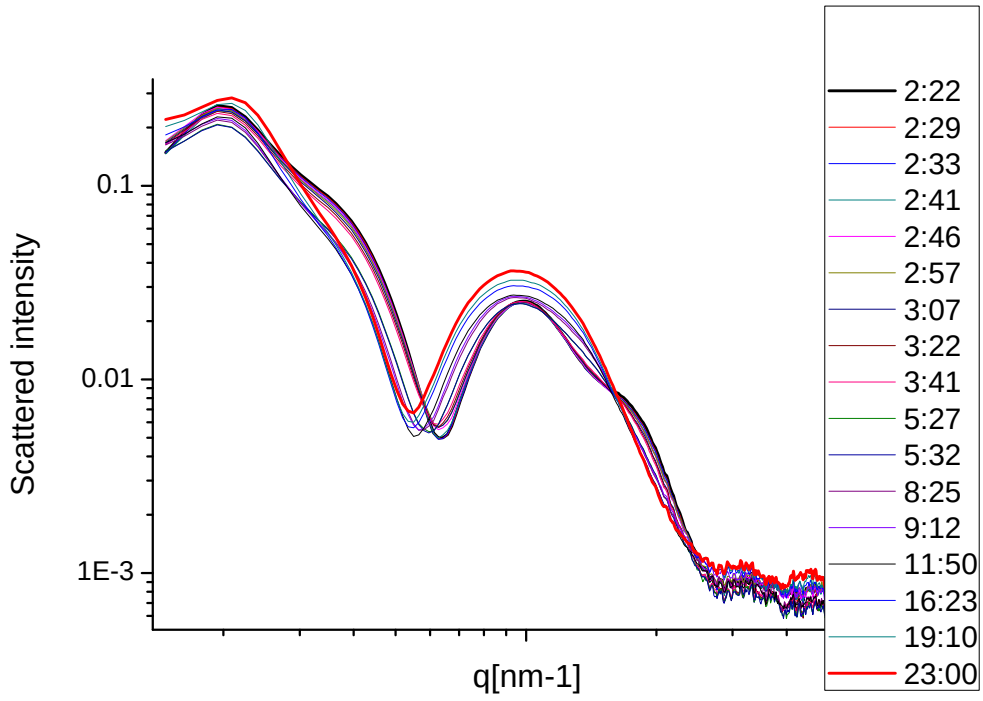

Figure 56: SAXS spectra referred to the evolution of the system DMPC:cholesterol 10:1 molar vesicles mixed with GD1a micelles. The molar ratio lipid:ganglioside:cholesterol is 10:1:1.

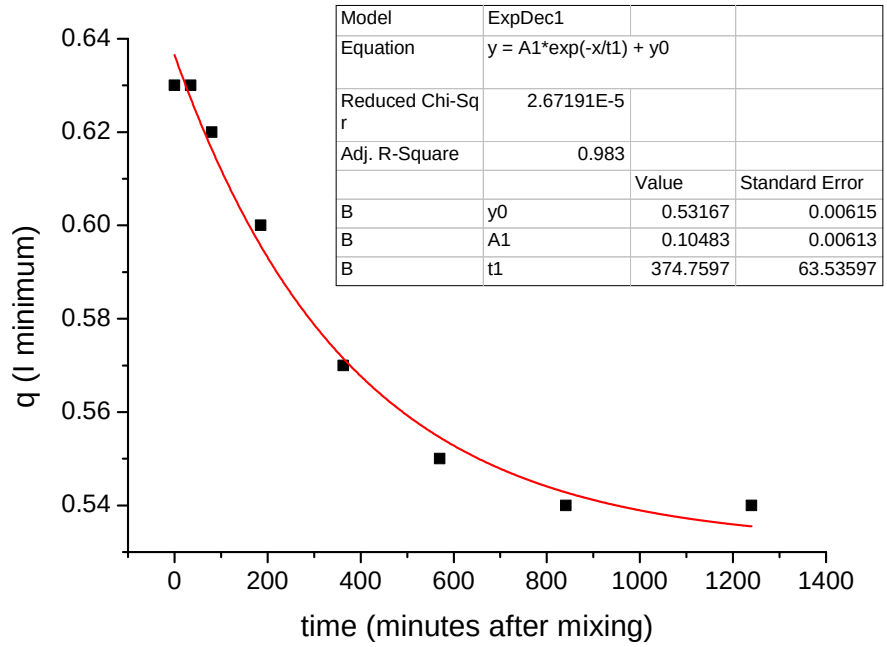

Figure 57: evolution of minimum of intensity position in time while mixing DMPC:cholesterol 10:1 molar vesicles and GD1a micelles. The total lipid:ganglioside:cholesterol molar ratio is 10:1:1.

(DMPC 10mol + chol 0.5 mol) +Gd1a 0.5mol

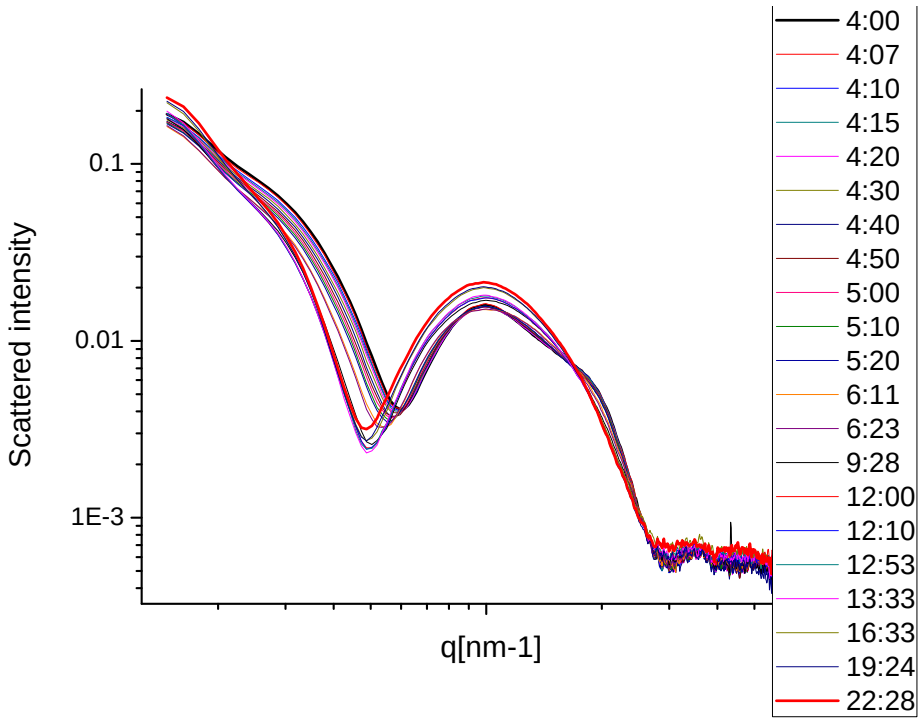

Figure 58: SAXS spectra referred to the evolution of the system DMPC:cholesterol 10:0.5 molar vesicles mixed with GD1a micelles. The molar ratio lipid:ganglioside:cholesterol is 10:0.5:0.5.

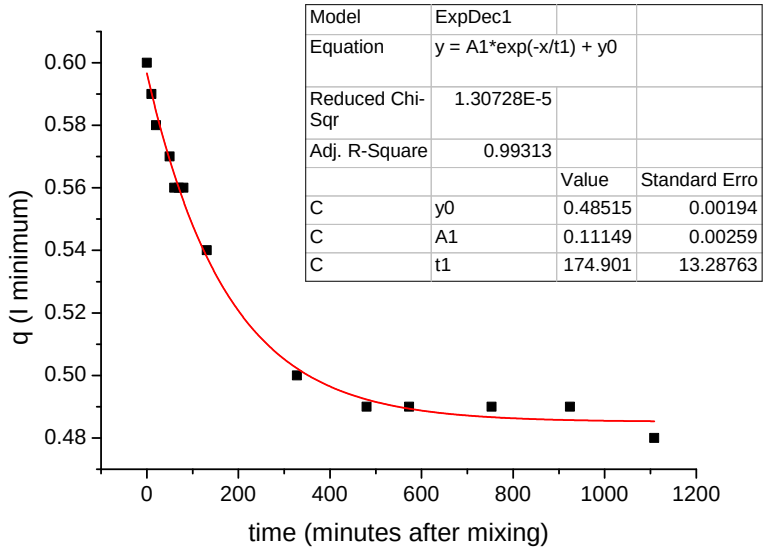

Figure 59: evolution of minimum of intensity position in time while mixing DMPC:cholesterol 10:0.5 molar vesicles and GD1a micelles. The total lipid:ganglioside:cholesterol molar ratio is 10:0.5:0.5.

Table 4: parameters obtained by the study of the SAXS spectra behaviour of the various mixing systems investigated.

Vesicle	Micelle	Typical decay time derived from fit (minutes)
DMPC 10 mol	GM1 1 mol	388
DMPC 10 mol	GD1a 1 mol	435
DMPC 10 mol	GM1:GD1a 1:1 mol	344
DMPC 10 mol	GM1:chol 1:1 mol	276
DMPC 10 mol	GM1:chol 0.5: 0.5 mol	650
DMPC:chol 10:1 mol	GM1 1 mol	350
DMPC:chol 10:0.5 mol	GM1 0.5 mol	330
DMPC 10 mol	Gd1a:chol 1:1 mol	216
DMPC 10 mol	Gd1a:chol 0.5: 0.5 mol	165
DMPC:chol 10:1 mol	Gd1a 1 mol	375
DMPC:chol 10:0.5 mol	Gd1a 0.5 mol	175

For what concerns the mixing in absence of cholesterol, while the typical mixing times of GM1 and GD1a micelles in DMPC are very similar, around 6 hours, the process takes longer in case of mixing DMPC and micelles of GM1:GD1a 1:1 molar.

In three components systems the resulting aggregates are different when the cholesterol is transported by the micelles or by the vesicles.

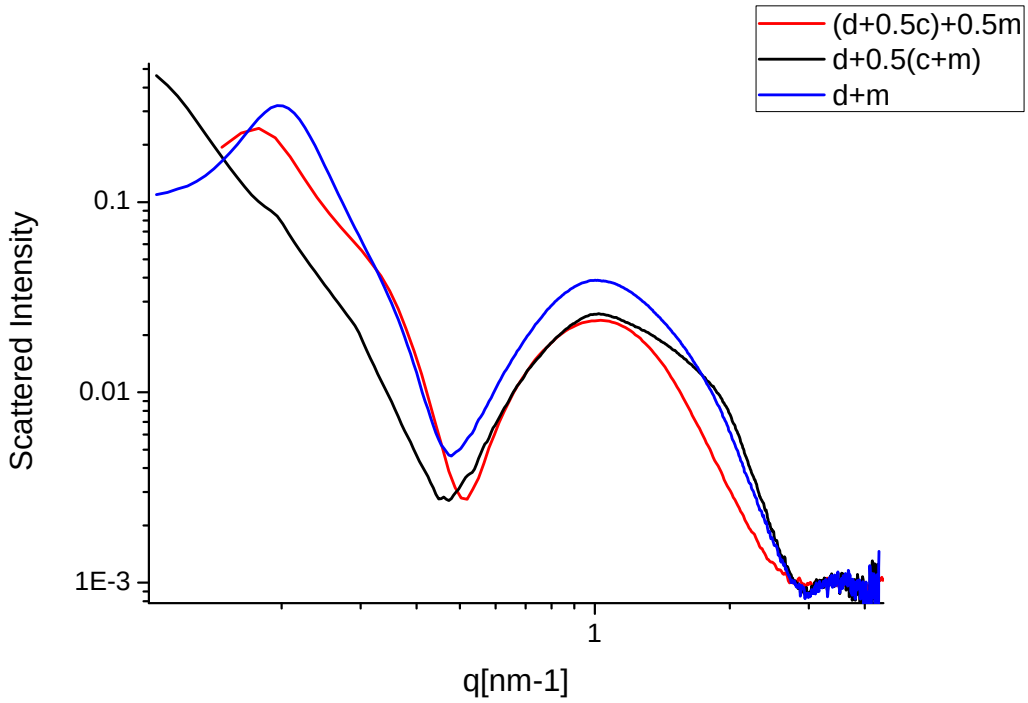

Figure 60: Final results of different mixed systems. In black DMPC+0.5(Chol +GM1), in red (DMPC+0.5Chol)+0.5GM1, in blue DMPC+GM1.

In figure 60 a comparison among the spectra referred to the final mixed systems DMPC+0.5(Cholesterol+GM1), (DMPC+0.5Cholesterol)+0.5GM1 and DMPC+GM1 is presented. It takes a very long time for DMPC 10 molar to mix with a micelle 0.5 molar of Cholesterol+GM1: 11 hours, and the final systems strongly depend on where the cholesterol is. If it was already in the vesicle, the process takes about 5.5 hours instead of 6.5 hours in absence of cholesterol (DMPC+GM1).

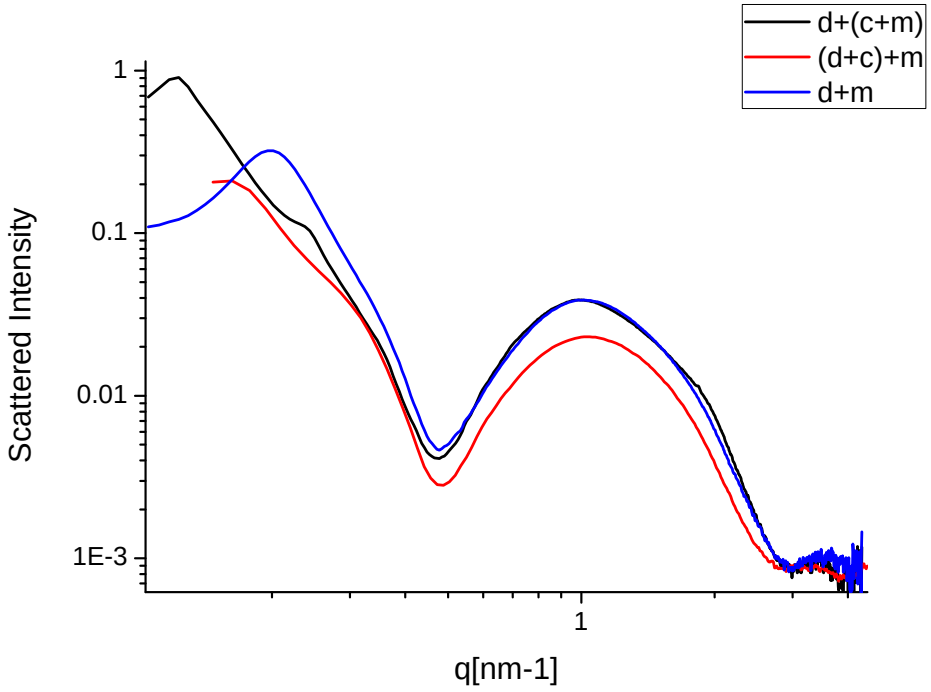

Figure 61: Final results of different mixed systems. In black DMPC+(Chol +GM1), in red (DMPC+Chol) +GM1, in blue DMPC+GM1.

In figure 61 we present the same case with twice the concentration of cholesterol and GM1 (lipid: chol:GM1 10:1:1 molar). The spectra referred to the mixing DMPC+(Cholesterol +GM1) and DMPC+GM1 are very similar at high q values, while different at low q values. In this case the mixing DMPC+(Chol +GM1) takes 4.5 hours, while when cholesterol is in the vesicle about 6 hours, as in absence of cholesterol.

So we can say that GM1 micelles incubate with the same typical times in DMPC vesicles and in DMPC+cholesterol vesicles.

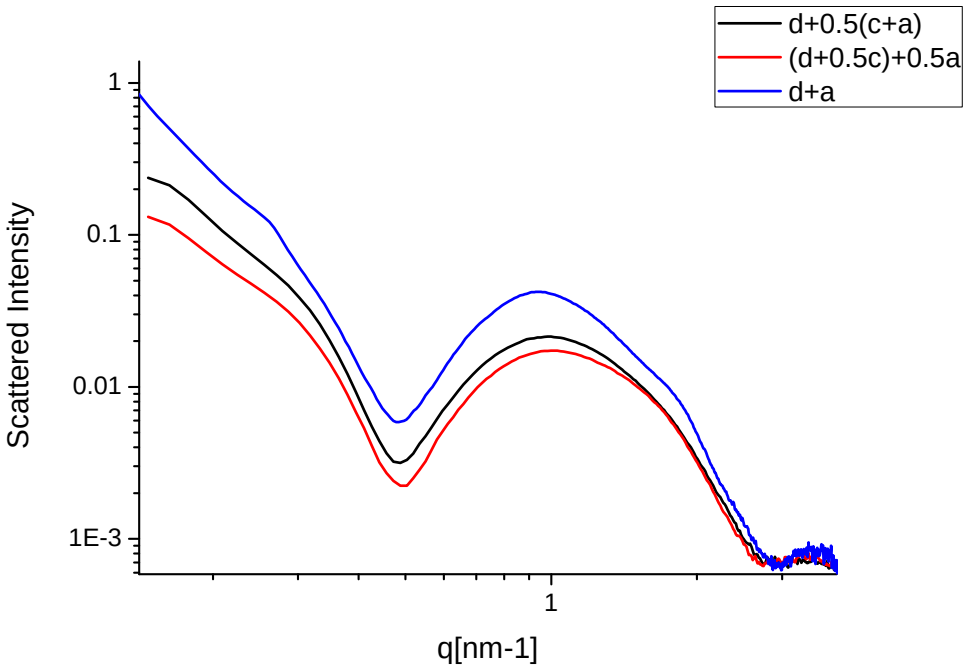

Figure 62: Final results of different mixed systems. In black DMPC+0.5(Chol +Gd1a), in red (DMPC+0.5Chol)+0.5Gd1a, in blue DMPC+GD1a.

A comparison between the mixing DMPC+ 0.5(Cholesterol+GD1a) and (DMPC+0.5Cholesterol)+ 0.5GD1a is shown in figure 62.

In this case, the time of the process is independent from where the cholesterol is, about 3 hours, and the resulting aggregates seem to be very similar. In the absence of cholesterol, the process takes longer: more than 7 hours.

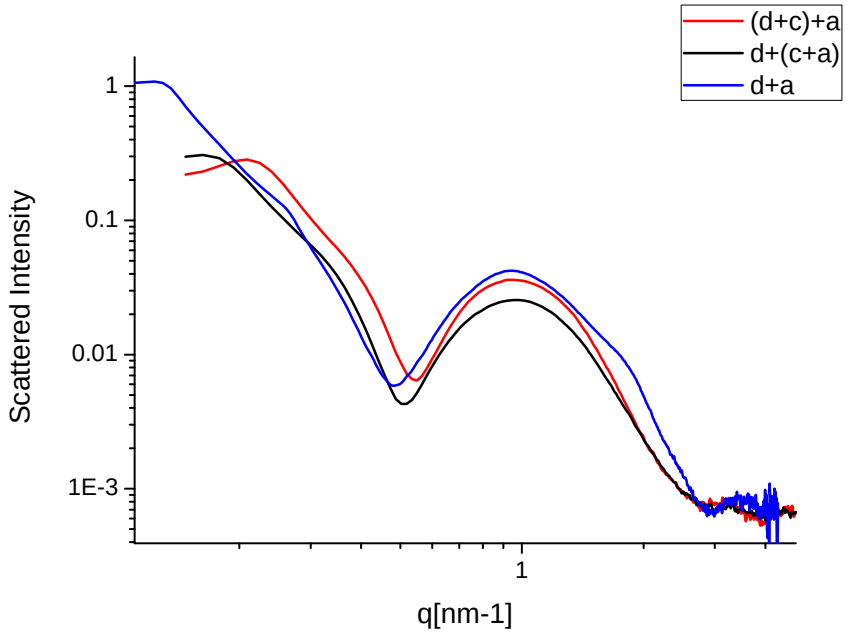

Figure 63: Final results of different mixed systems. In black DMPC+(Chol +Gd1a), in red (DMPC+Chol)+Gd1a, in blue DMPC+GD1a.

If we double the amount of GD1a and cholesterol with respect to the previous case, we note that the resulting systems are very different in the two cases (cholesterol in micelle or in vesicle), and in fact the processes require different times: the process is faster if cholesterol is in the micelle: 3.5 hours versus more than 6 hours. If it is in the vesicle, the typical time, over 6 hours, is more similar to that of mixing of pure DMPC vesicles with GD1a micelles in absence of cholesterol, which is over 7 hours.

In general we can say that cholesterol has been found to fasten the incubation process, in particular if originally embedded in the ganglioside micelles, exception made for the mixing DMPC10mol+ 0.5mol (Cholesterol+GM1).

3.1.3. Nanoscale structural response of ganglioside-containing aggregates to the interaction with sialidase

Elena Del Favero, Paola Brocca, Simona Motta, Valeria Rondelli, Sandro Sonnino and Laura Cantù

Department of Chemistry, Biochemistry and Biotechnologies for Medicine, University of Milano, Milano, Italy

Abstract It is well known that the curvature of ganglioside-containing nanoparticles strongly depends on their headgroup structure, as determined in aggregates with 'stationary' composition, that is, when the system finds its optimal structure at the moment of lipid dissolution in aqueous solution. In the present work, we directly followed the structural change in model aggregates, induced by on-line molecular modification of already-packed gangliosides, namely the one brought about by a sialidase, acting on the ganglioside GD1a and leading to the lower-curvature-aggregating GM1. We applied small-angle X-ray and neutron scattering techniques to follow the time evolution of the aggregate structure. We found that, while chemically undergoing the enzymatic action in both cases, the aggregated structure could be either very stable, in single component systems, or structurally responsive, in mixed model systems. Moreover, while in progress, the sialidase–ganglioside interaction seems to define a time lag where the system is structurally off the smooth route between the initial and the final states. We hypothesize that, in this time lag, the local structure could be very sensitive to the environment and eventually readdressed to a specific final structural fate.

J. Neurochem. (2011) 116, 833–839.

3.2. SINGLE SURFACE STUDIES

In the previous paragraph the results we obtained by studying the properties of model membranes in solution are shown. Many peculiar information can be obtained by X-rays scattering, about the aggregate shape (the form factor) and the structure assumed in solution (structure factor). In particular we studied the packing rearrangements due to external inputs. The information obtained with the scattering technique from a solution is obviously a 'mean' one, in the sense that we are investigating a huge number of membranes and the result of the measure is an average.

To investigate the internal structure of membranes, that is the disposition inside the leaflets of their components, the most suitable technique is reflectivity of X-rays and neutrons. In fact, the technique allows to study the internal structure of single membranes deposited over wide areas (in our case 5cmx5cm). These membranes are deposited layer by layer, allowing us to control its composition in an asymmetric way. In fact, another clue feature, very interesting and hard to reproduce in model systems, is asymmetry. Before talking about such systems we studied the properties of each layer we wanted to deposit by means of a Langmuir trough, to study the phase behavior of single component monolayers or mixed systems and to optimize the models used for our measurements.

3.2.1. Pressure-area diagrams

Pressure-area (π-A) isotherms were recorded on a Nima Langmuir-Blodgett trough, using a Wilhelmy plate for pressure sensing. All (π-A) experiments were carried out at 15°C (±0.5), below the melting temperature of the lipids used. Water for the subphase was processed in a Milli-Q system (Millipore, Bedford, MA), to a resistivity of 18 MΩ*cm. Each lipid solution was spread over the water subphase and chloroform was let to evaporate completely for 15min. All isotherms were recorded using a barrier speed of 25 cm^2/min.

Stability and reproducibility of Langmuir films were verified by performing various compression-expansion cycles on two different Nima Langmuir troughs.

We started by the study of the pressure-area behaviour of the gangliosides used for the experiments discussed in the previous sub-chapter, that is GD1a and GM1. Results are shown in figure 64. As a subphase, we used a NaCl 156 mM solution to avoid micelles formation and gangliosides entering in the water.

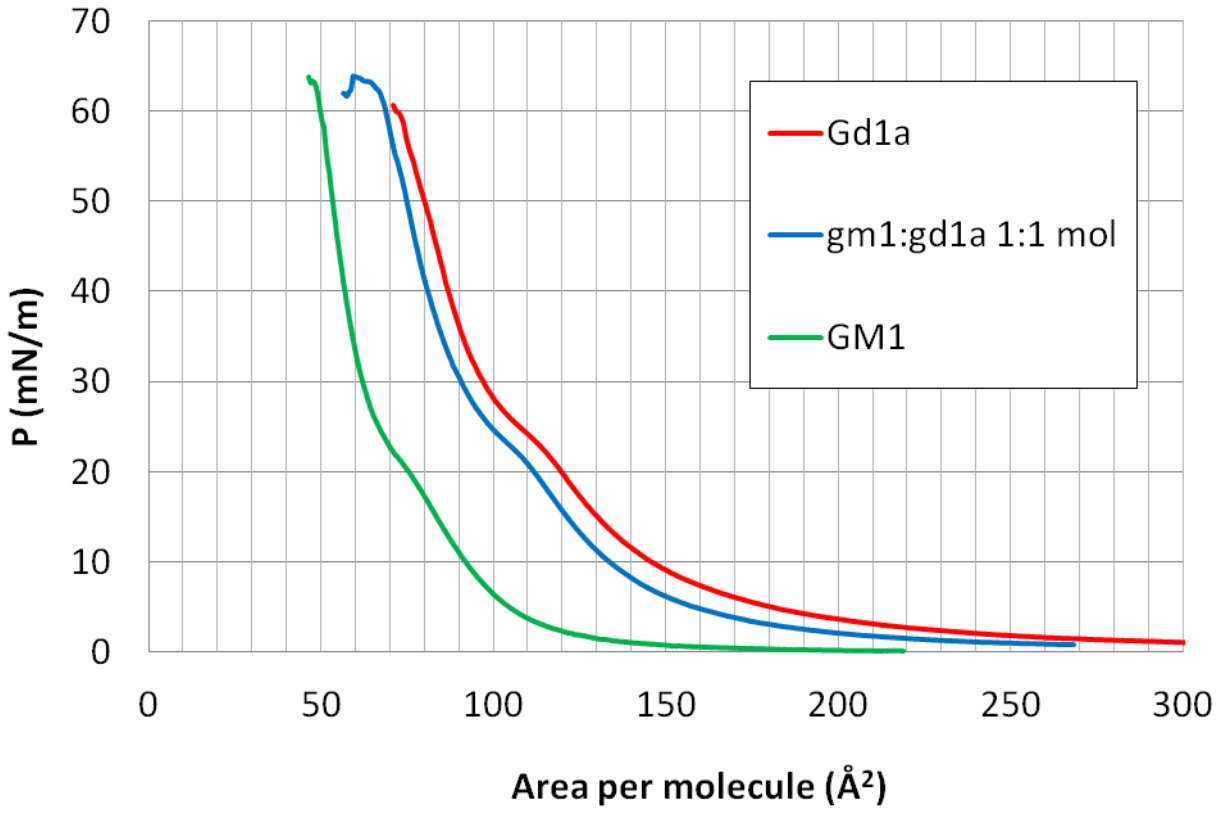

Figure 64: Pressure-area curves of the gangliosides used in our work. The subphase is water NaCl 156 mM, T=20°C.

It is immediate to see that the curves can be divided in three regions:

- At large areas per molecule, the pressure sensed by the Wilhelmy plate is very low, meaning that the molecules are not interacting. This is called 'gas phase'.
- While compressing the molecules start to feel the presence of the neighbors and the system enters the so-called 'liquid phase'.
- For pressures over 20 mN/m, the system is in gel phase: the molecules are tightly packed and small decreases of area result in correspond large increases of pressure.

From these phase diagrams, we have information about the mean molecular area of the surface under study in various phases. In particular we can extract the minimum molecular area, that is the minimal area below which the system collapses, in our case around 60-65 mN/m. According to our results, in NaCl 156 mM water solution and at 20°C, the molecular area of GD1a is 73 $Å^2$, that of GM1 is 50 $Å^2$ and that of their mixture

is 67 $Å^2$, as expected, intermediate value between those of the two separate components, but higher than the mean value, 61 Å.

This indicates that gangliosides from the same species pack according to steric rules that cannot be followed when mixing two gangliosides of different species. It could be that similar headgroups can rotate all in the same direction to minimize the occupied area, but this is not possible, or at least less successful, if neighbours don't belong to the same species.

Then we studied multicomponent systems to optimize the quality of the surfaces we intend to deposit on the silicon blocks to the study of single membrane systems. First we want to build up stable asymmetric floating cholesterol-containing bilayers with bio-similar composition. We verified the effect brought about by addition of cholesterol to d_{75}-DPPC, by recording the (π-A) curves of the mixed Langmuir monolayers at the air-water interface as a function of different molar ratios between d_{75}-DPPC and cholesterol, from the gas to gel phase and, particularly, to the 40 mN/m pressure required for deposition. The corresponding curves are reported in figure 65 and display the expected features, according to the existing literature. This guarantees the original integrity and compactness of the bilayer-forming monolayers. Moreover, the monolayers are stable in time and the pressure-area results are repeatable both after subsequent compression-expansion cycles and after monolayer re-spreading.

Progressive addition of cholesterol to d_{75}-DPPC results in progressively decreasing the occupied area per average molecule. For all the systems, at a given pressure, the measured area per molecule is lower than expected for ideal mixing. In fact, the effect of cholesterol is to rigidify and order the lipid chains, with a consequent reduction of the occupied area per average molecule at the air-water interface.

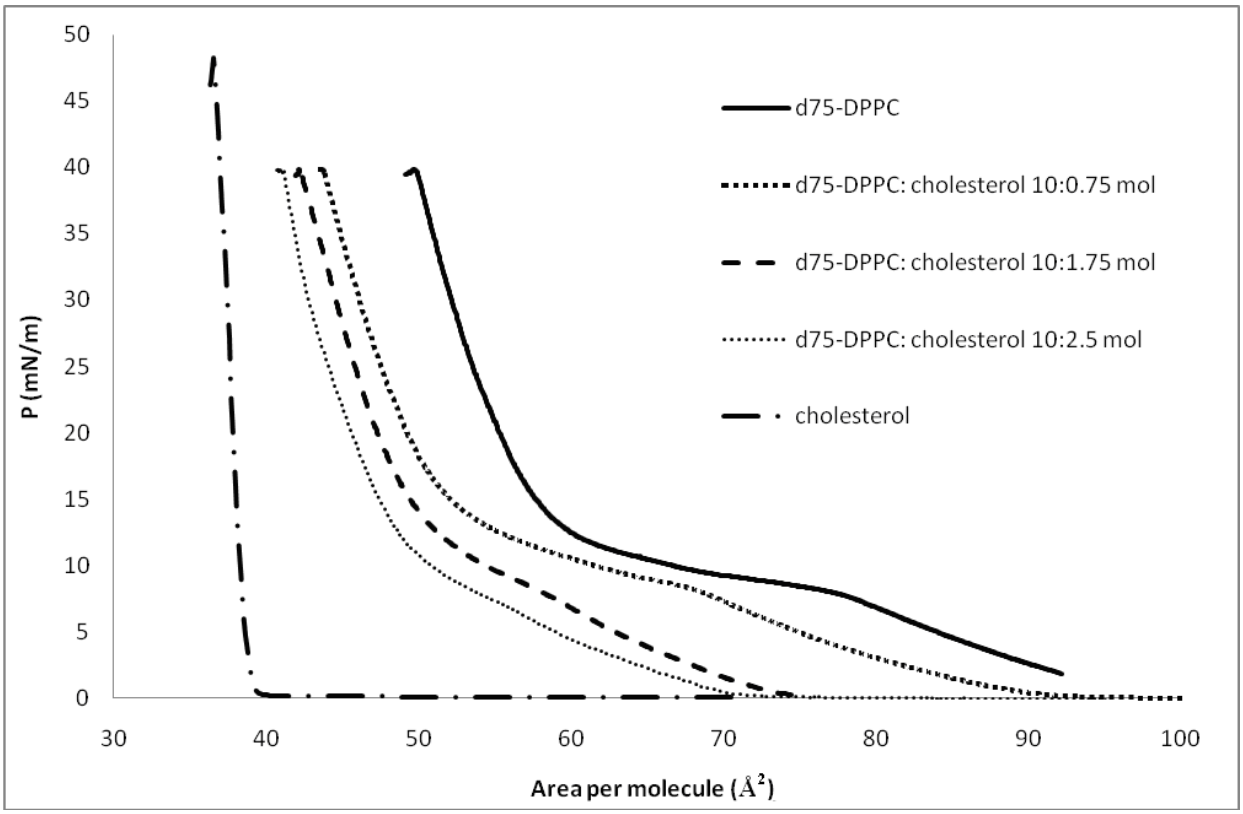

Figure 65: Pressure-area isotherms of various mixtures of d75-DPPC and cholesterol at 18°C. The subphase is water.

3.3. SUPPORTED BILAYERS

The study of the internal mechanisms of membranes requires the use of biologically significant single model systems and the possibility to investigate them with non-perturbative techniques. This can be obtained by coupling the Langmuir-Blodgett Langmuir-Schaefer technique with neutrons and X-rays reflectivity.

Langmuir-Blodgett (LB) Langmuir-Schaefer (LS) technique allows in fact to build up single or double hydrated model membranes deposited over large areas (in our case 5cm x 5cm) on silicon blocks. The technique has been widely explained in the previous chapter. We remember that coupling one LB and one LS depositions we can build up a single asymmetric membrane adherent to the silicon block, while coupling three subsequent LB and one LS depositions, we can build up two asymmetric membranes, the first supported by the silicon block, the second almost free to fluctuate in the solvent.

We started our studies applying reflectivity measurements to single deposited membranes. Neutrons and X-rays are complementary techniques because they interact differently with matter. Neutrons are heavy particles and they interact with atomic nuclei. X-rays are radiation, and interact with atomic electron clouds. The consequence is that the same membrane has different SLD profiles for neutrons and X-rays.

Table 5: Properties of materials used

Molecule	**Neutrons SLD (10^{-6} Å^{-2})**	**X-rays SLD (10^{-6} Å^{-2})**
Lipid heads	1.75	14.44
Lipid gel chains	-0.44	7.9
CH_3 groups of lipid chains	-0.44	4.77
cholesterol	0.22	9.58
Ganglioside heads	2.23	14.83
H_2O	-0.56	9.38

In table 5 the SLD values we used to treat x-rays and neutron scattering data, are reported.

Unfortunately, as we can observe, cholesterol and water have very similar SLD for X-rays. For this reason we have to use neutrons reflectivity to study the cholesterol transverse disposition inside the membrane, while the whole structure of the membrane can be studied by mean of X-rays reflectivity. Moreover the X-rays reflectivity spectrum as a wider q range. On the other hand neutrons are very sensible to isotopes, so for neutrons Hydrogen and Deuterium are very different. This is very important because we can enhance or minimize the visibility of various components of the membrane by playing with selective deuteration, not-perturbing the membrane properties. To check this, since with neutrons we used fully deuterated lipids to enhance the visibility of H-containing cholesterol and gangliosides inside the lipid matrix, we performed X-rays reflectivity measurements on a membrane of DPPC and one of d_{75}-DPPC to study eventual structural differences. Results show that no differences can be appreciated, as expected.

3.3.1. X-ray reflectivity from supported membranes: stability and main structural characteristics

We performed X-ray reflectivity measurements at the ID10B line of the ESRF Synchrotron in Grenoble and Neutron reflectivity measurements at the FIGARO and D17 beamline of ILL in Grenoble.

The measuring process has been explained in the previous chapter. Reflectivity data have been fitted by Motofit, with a 7 layers model: the silicon oxide, a water layer, a lipid heads layer, 2 lipid chains layers, a lipid heads layer. The characteristics of the silicon oxide have been determined by a starting measure of the silicon block (figure 66). In all the samples prepared a 1-2 Å thick water layer was found between the silicon oxide and the first deposited lipid heads.

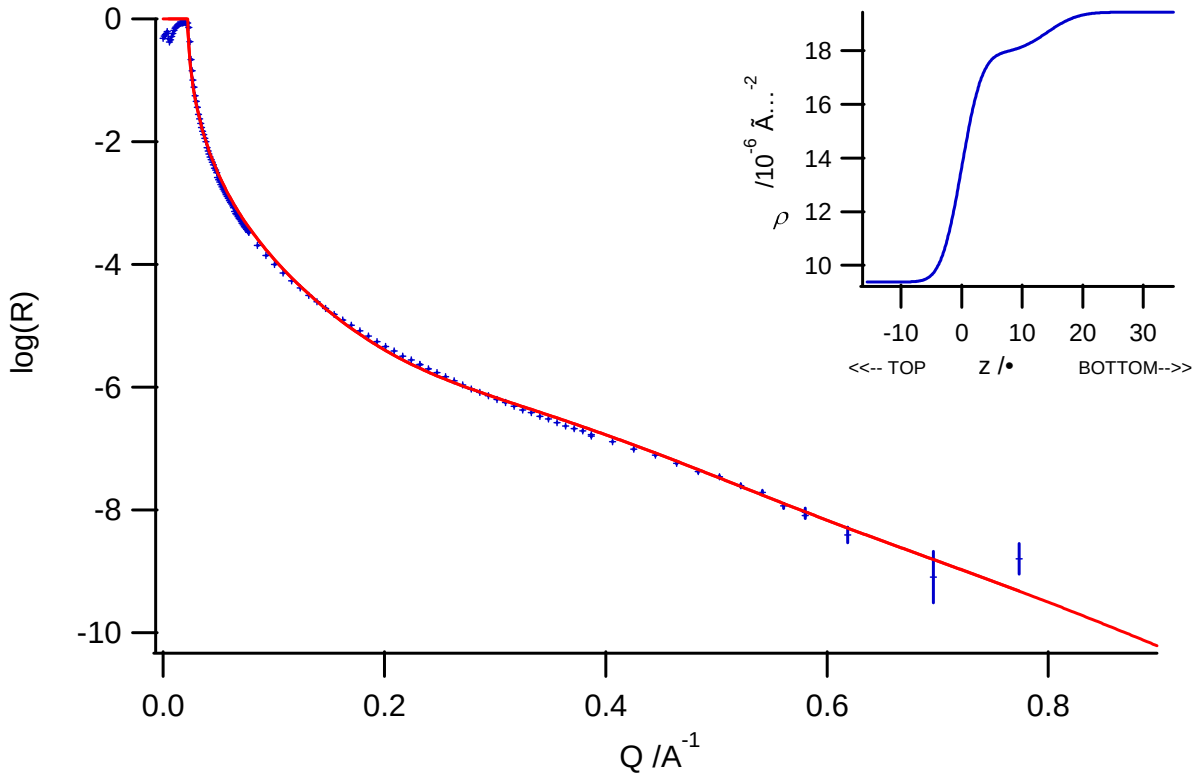

Figure 66: X-rays reflectivity spectrum from the silicon block. Dots are experimental points, red line is the fit. In the insert the SLD profile is shown.

We first studied the DPPC matrix at various temperatures heating the sample over the chains-melting transition temperature and cooling it back in the gel phase. The sample is stable. By the reconstruction of the contrast profile the known characteristics of a lipid membrane such as the variation of the thickness at various temperatures can be addressed.

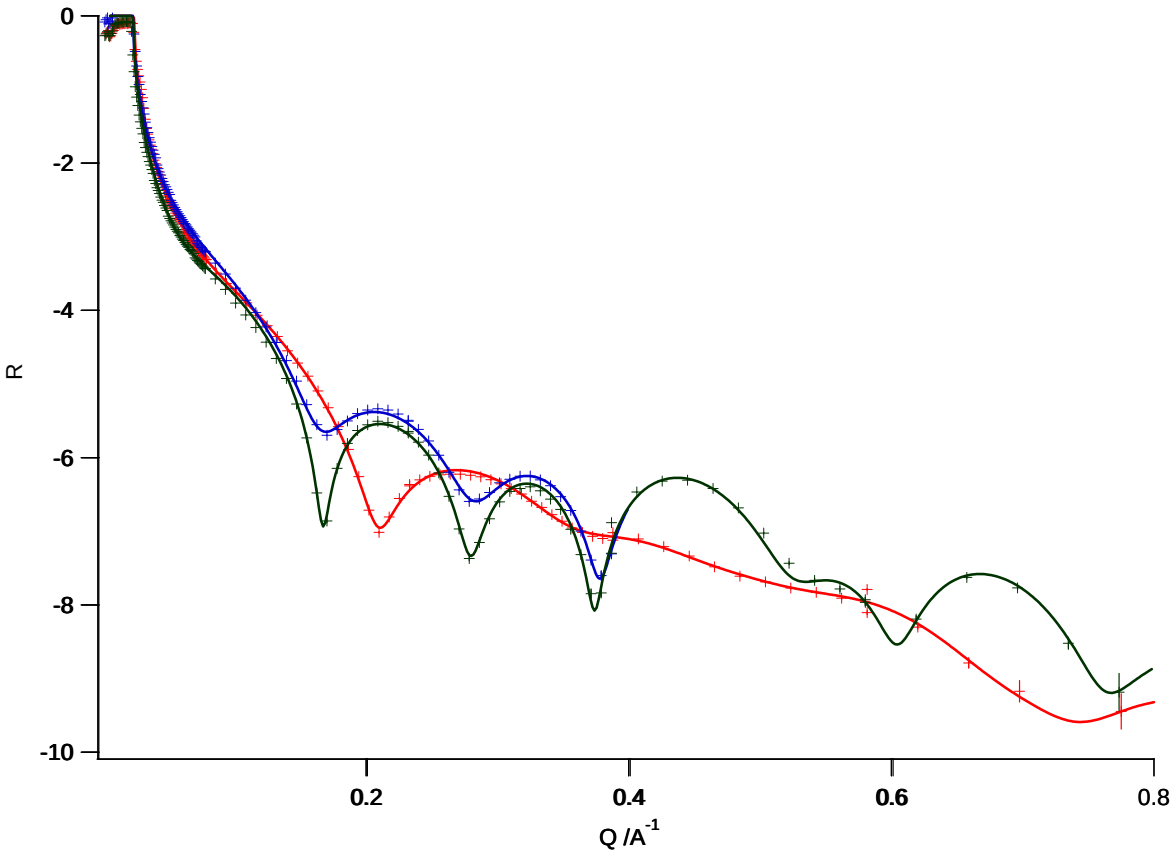

Figure 67: X-rays reflectivity spectra from a DPPC membrane in H_2O at various temperatures. Green: 22°C before annealing; red: 60°C; blue 22°C after annealing. Crosses refer to the experimental data, lines the fits.

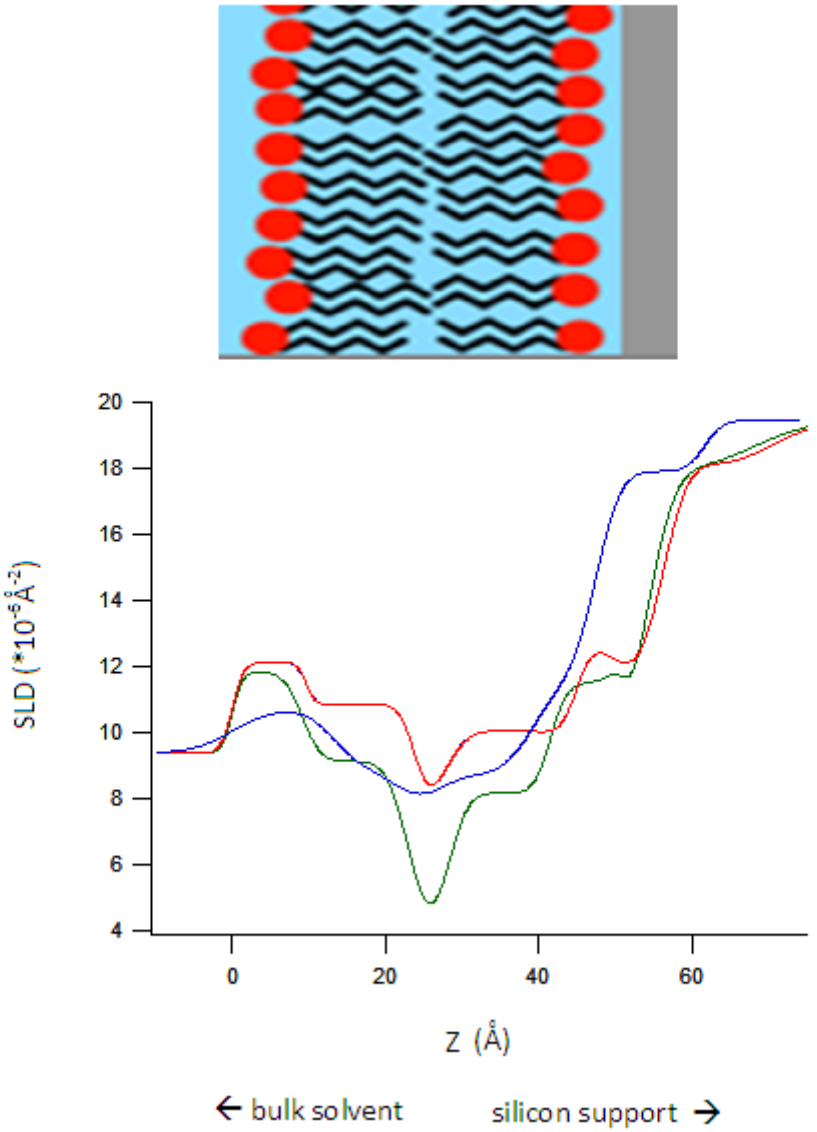

Figure 68: SLD profiles obtained by fitting the x-rays reflectivity data referred to the DPPC membrane at various temperatures. red 22°C; blue 60°C, green 22°C after annealing

Table 6: parameters obtained by fitting the x-rays reflectivity data referred to the DPPC sample.

	Thickness (±1Å)	**Solvent penetration (±2%volume)**	**Roughness (±2Å)**
DPPC 22°C	53	10%	~3
DPPC 60°C	47	10%	~3
DPPC 22°C back	51	10%	~2

Fit results, reported in table 8, show that the coverage of the silicon block is 90% (the parameter we obtain from the fit is the solvent penetration in the lipid chains, which in this

case is around 10%) and the roughness (between one layer and the subsequent, which in these systems is the same for all the layers) decreases annealing the system. Membrane thicknesses follow the expected trend: around 52 Å at 22°C, 47 Å in the fluid phase of the chains.

We performed the same measurements on a fully deuterated DPPC membrane to check its characteristics, since in neutrons reflectivity experiments we will use a deuterated lipid matrix. Comparing the spectra referred to DPPC and d_{75}-DPPC we observed that the fully deuterated DPPC membrane is 1 Å thicker than the DPPC one (54 Å versus 53 Å), but all the other characteristics are unchanged.

Once the stability and the structural properties of the lipid matrix have been verified, we investigated the structural changes brought by the presence of additional molecules, starting from cholesterol, being very abundant in real membranes. In real membrane GEMs, in fact, the molar proportion lipid:cholesterol is 11:2.5.

Different asymmetric cholesterol configurations have been tested: we first put 100% of the desired moles in the inner layer of the membrane, while in a second sample 70% of it has been deposited the inner layer of the membrane and 30% in the outer one. In presence of cholesterol the membrane thickens from 53 Å to 57 Å and is more compact (the solvent penetration is arount 5% instead of 10%), as expected. Moreover the spectra referred to different cholesterol dispositions are different also after annealing and differ from that of the pure DPPC (figure 69).

Fit results are summarized in table 9.

Table 7: parameters obtained fitting the X-rays reflectivity spectra of a pure DPPC membrane and membranes formed by DPPC and cholesterol.

	Thickness (±1Å)	**Solvent penetration (±2%volume)**	**Roughness (±2Å)**
DPPC 22°C	53	10%	~3
DPPC+CHOL(100/0) 22°C	57	5%	~2
DPPC+CHOL(70/30) 22°C	56	5%	~2

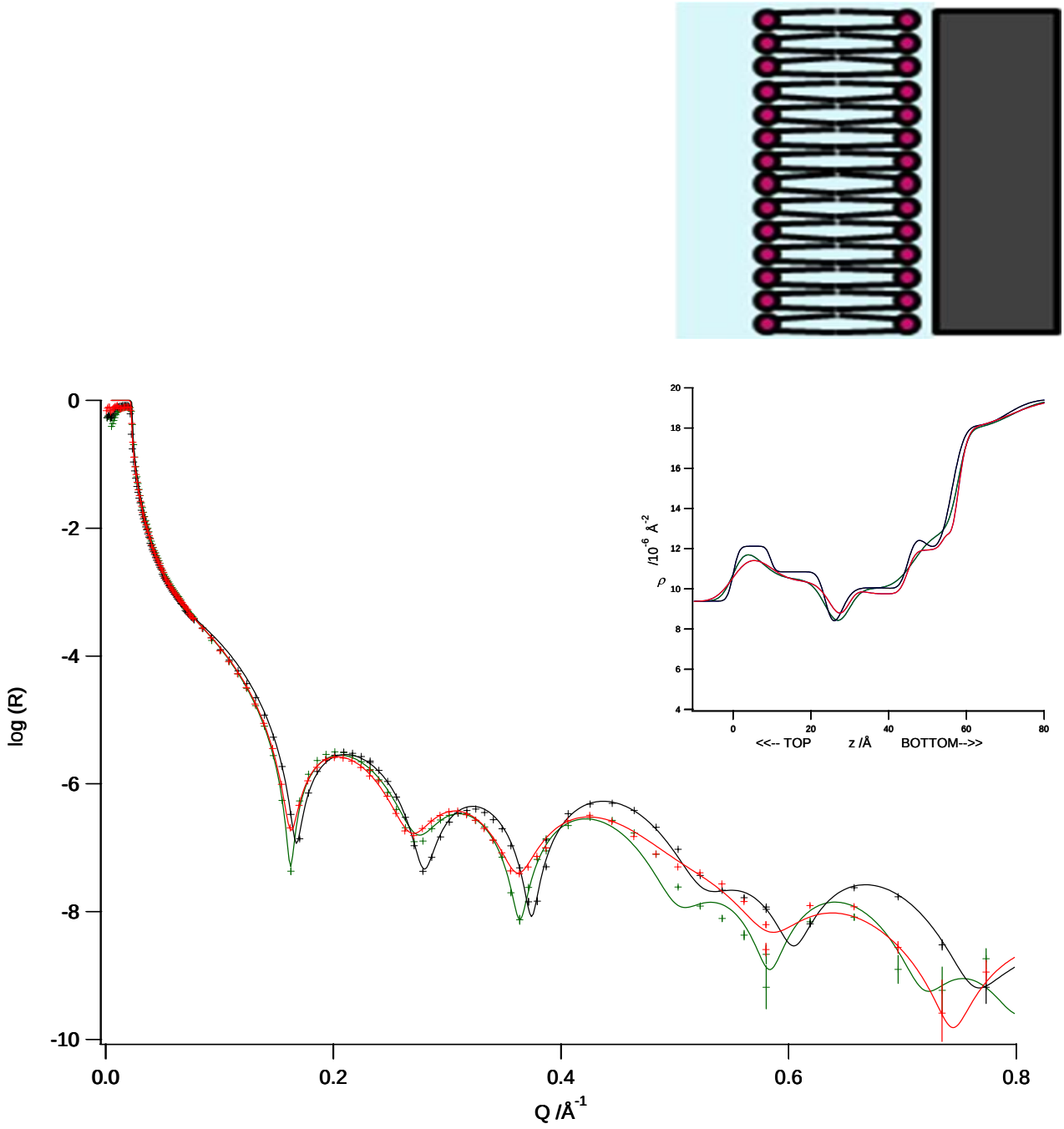

Figure 69: X-rays reflectivity from supported membranes at 22°C in water. Black spectrum refers to a pure DPPC membrane, the red to an asymmetric membrane of DPPC where the 70% of cholesterol is in the inner layer and the 30% in the outer, and green spectrum refers to an asymmetric membrane of DPPC where all the cholesterol have been deposited in the inner layer. Crosses are the experimental points, lines the fits.

This result is very important from the technical point of view because it means that different degrees of asymmetry can be created and kept, and we could in principle be sensible to the disposition of cholesterol throughout the membrane. Unfortunately with X-rays reflectivity measurements we are not sensible to cholesterol positioning.

The asymmetric disposition of cholesterol seems not to be affected by the standard protocol procedures such as annealing, but we will see in next section that cholesterol

asymmetry is disturbed by them in floating bilayers. The consequence is more evident in the case of floating membranes because they are nearly free to fluctuate in the solvent and not coupled to the silicon support, such as in the present case. The coupling with silicon could in fact affect the fluidity of the membrane and the mobility of molecules inside it.

Adding a glycolipid to the membrane, we truly complicate it, obviously from the structural point of view but also from the point of view of the molecular interactions, since glycolipids bear big charged polar heads, capable to deform the membrane. In figure 70 a comparison among the spectra referred to a pure DPPC DPPC membrane, a DPPC-cholesterol one and a DPPC-cholesterol-GD1a ganglioside membrane is shown.

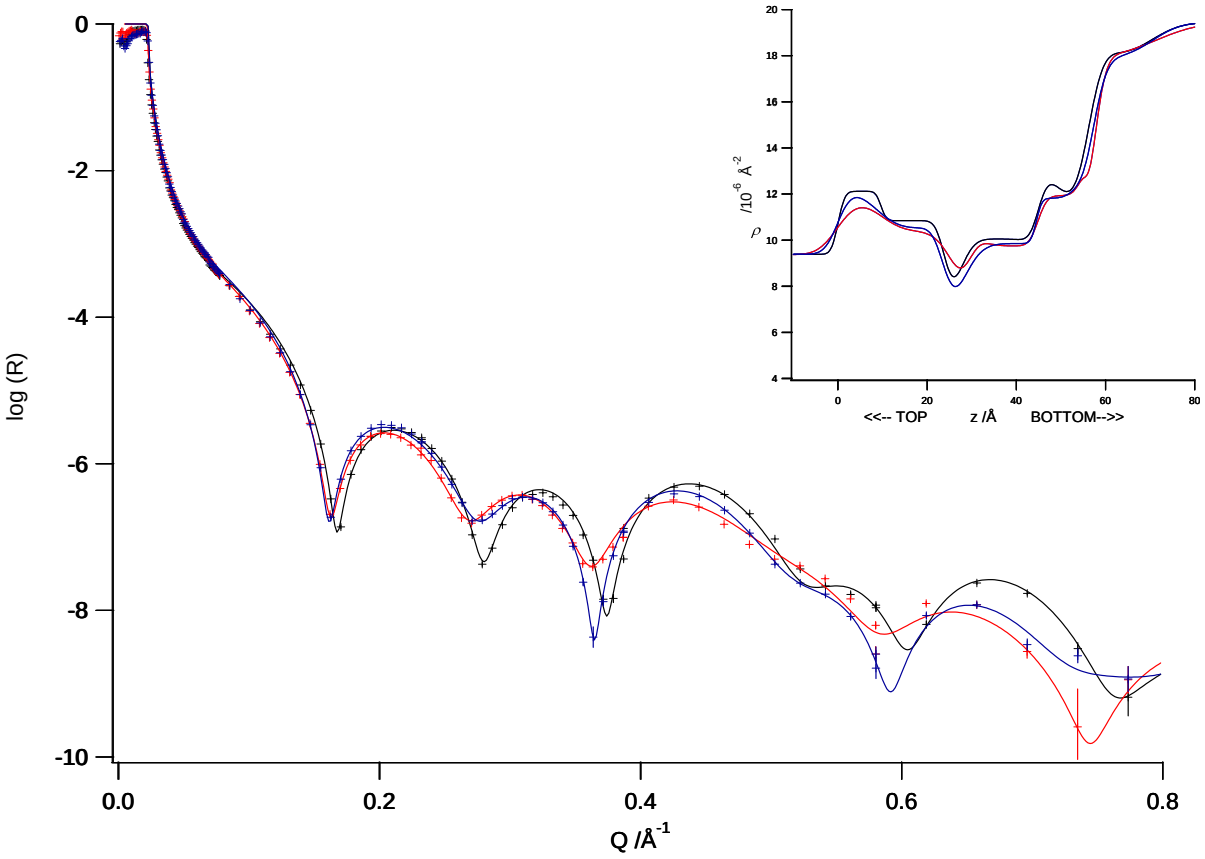

Figure 70: X-rays reflectivity from supported membranes at 22°C in water. Black spectrum refers to a pure DPPC membrane, the red to an asymmetric membrane of DPPC where the 70% of cholesterol is in the inner layer and the 30% in the outer, and blue spectrum refers to an asymmetric membrane composed by DPPC/cholesterol and GD1a ganglioside. Crosses are the experimental points, lines the fits. In the insert the correspondent contrast profiles obtained are shown.

Again different spectra correspond to different samples, meaning that we are sensible to the differences we want to study. All the membranes studied are stable in time and temperature.

The reconstructed contrast profiles referred to the GD1a-containing membrane at various temperatures crossing the chains gel-to-fluid phase transition (22°C, 60°C, 22°C back) tell us that the compactness of the membrane lowers increasing the temperature, but cooling back, it comes back to the initial values. In fact both roughness and solvent penetration increase increasing the temperature (roughness from 5 Å to 8 Å, solvent penetration from 5% to 10% in volume), and then come back to the initial values, suggesting that the membrane comes back to be stable, in the gel phase of the hydrophobic lipid chains. The situation we find in fluid phase is compatible with the fact that the membrane is more fluid, as expected, but not breaking, because it is a reversible situation. While the presence of cholesterol thickens the membrane, gangliosides do not. The results of the described studies are presented in figure 71.

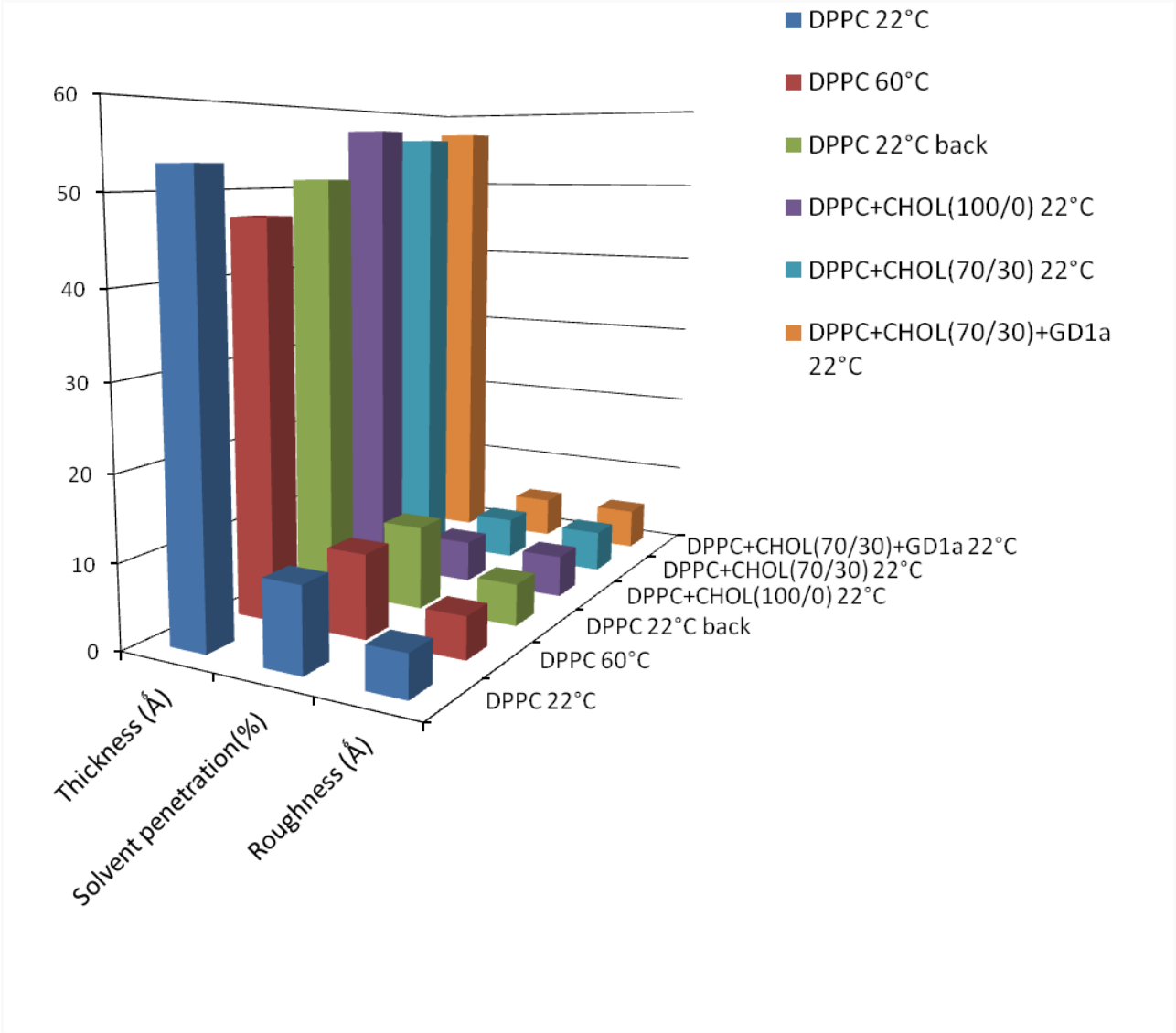

Figure 71: parameters obtained by the analysis of the experimental data obtained by X-rays reflectivity from the different samples studied.

By these measurements we studied the well known basic characteristics of model membranes and we tested the stability and accuracy of our model. We want now to study whether we are sensible to eventual structural changes arising from certain processes occurring at the surface of the membrane.

3.3.2. Structural effects brought by sialidase enzyme

In the previous section of this chapter we presented the results of an experiment carried on gangliosides-containing micelles, under the action of the enzyme sialidase, that removes the external sialic acid from the polar head of GD1a ganglioside.

We studied the effects brought by the presence of the same enzyme on model membranes composed by DPPC, cholesterol and gangliosides. In fact in true membranes, gangliosides belong to a metabolic pathway, and they are transformed into each other by the intervention of specific enzymes, while being already packed in an aggregate. We want to study whether from a flat membrane structural point of view is the same to be built up with the enzymatic-product-ganglioside, and to have its predecessor and gain the product by the enzymatic action.

To this scope we started our study by building up a model membrane containing GD1a ganglioside, we studied it and we let sialidase work on it, studying the resulting membrane. Then we studied the same membrane with GM1 instead of GD1a, because it is the ganglioside resulting from the sialidase action on GD1a. We let sialidase work also on this membrane to study any eventual activity even if not predicted. Finally we studied the same membrane with asialoGM1, which is a ganglioside similar to GM1 without its sialic acid (that is GD1a without both sialic acids).

The reference sample as been prepared as follows:

- 1^{st} layer of DPPC/Cholesterol 11/1.75 molar
- 2^{nd} layer of DPPC/Cholesterol/GD1a ganglioside 10/0.75/1 molar

The sample has been prepared to mimic the characteristics of GEMs, that is DPPC lipid matrix, asymmetric disposition of cholesterol in the two leaflets (70% in the inner leaflet of the membrane, 30% in the outer), ganglioside in the outer layer of the membrane, according to the predicted molar rations among components.
After measuring the reflectivity of the sample, we added salt to the solution it was immerged in. From figure 72 it is possible to see that the two spectra referred to the sample in water or in water NaCl solution 150 mM are different. In fact fitting the data we found that the sample in NaCl solution is thicker: 57Å versus the 55Å in water.

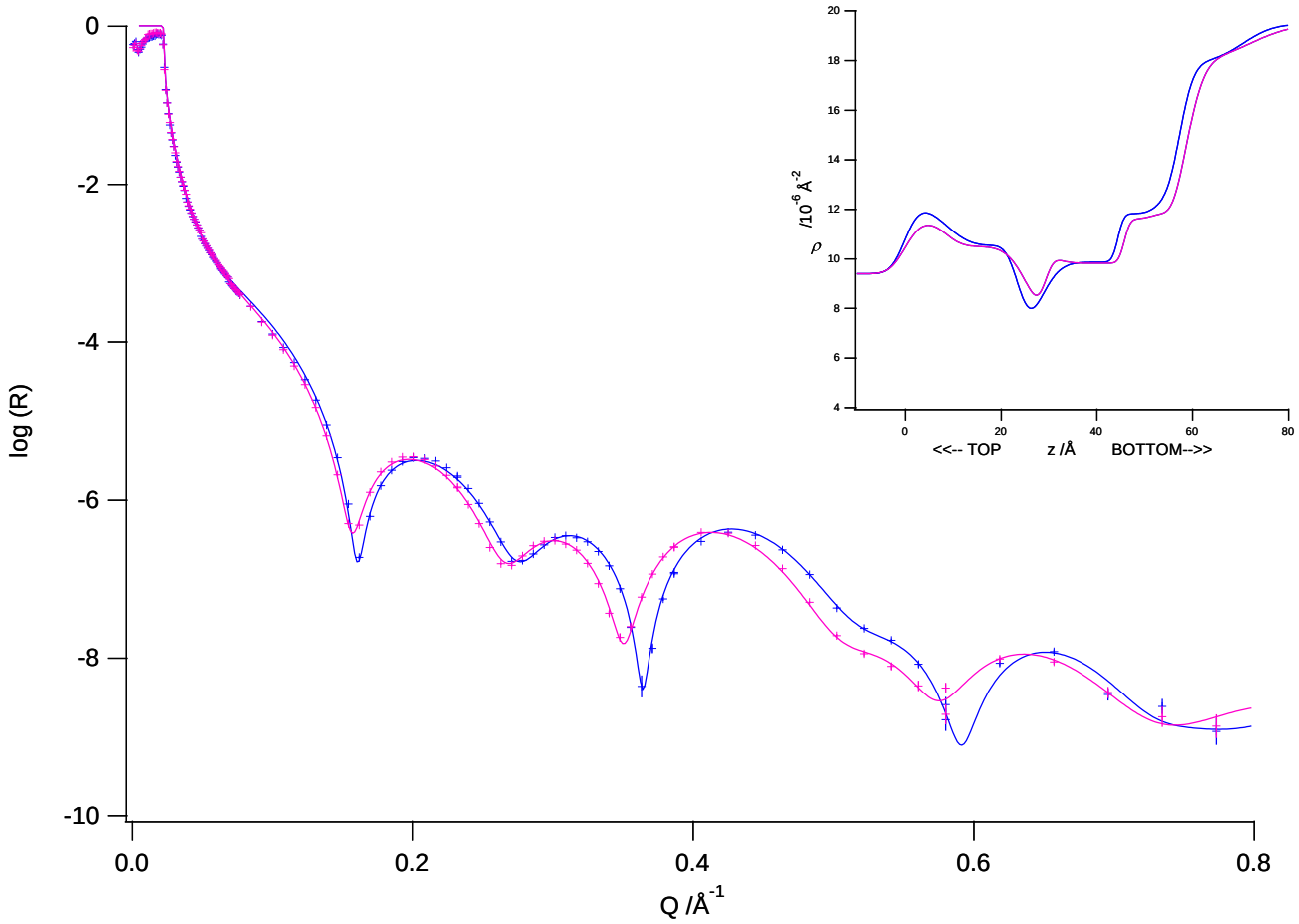

Figure 72: X-rays reflectivity from supported membranes at 22°C. Spectra refer to an asymmetric membrane composed by DPPC/cholesterol and GD1a ganglioside in pure water (blue) and in NaCl 156 mM solution (pink). Crosses are the experimental points, lines the fits. In the insert the correspondent contrast profiles obtained are shown.

The action of sialidase affects the structure of the membrane, as it is easy to see from the spectra in figure 73. As starting point we should use the sample in NaCl water subphase because the sialidase solution contains NaCl.

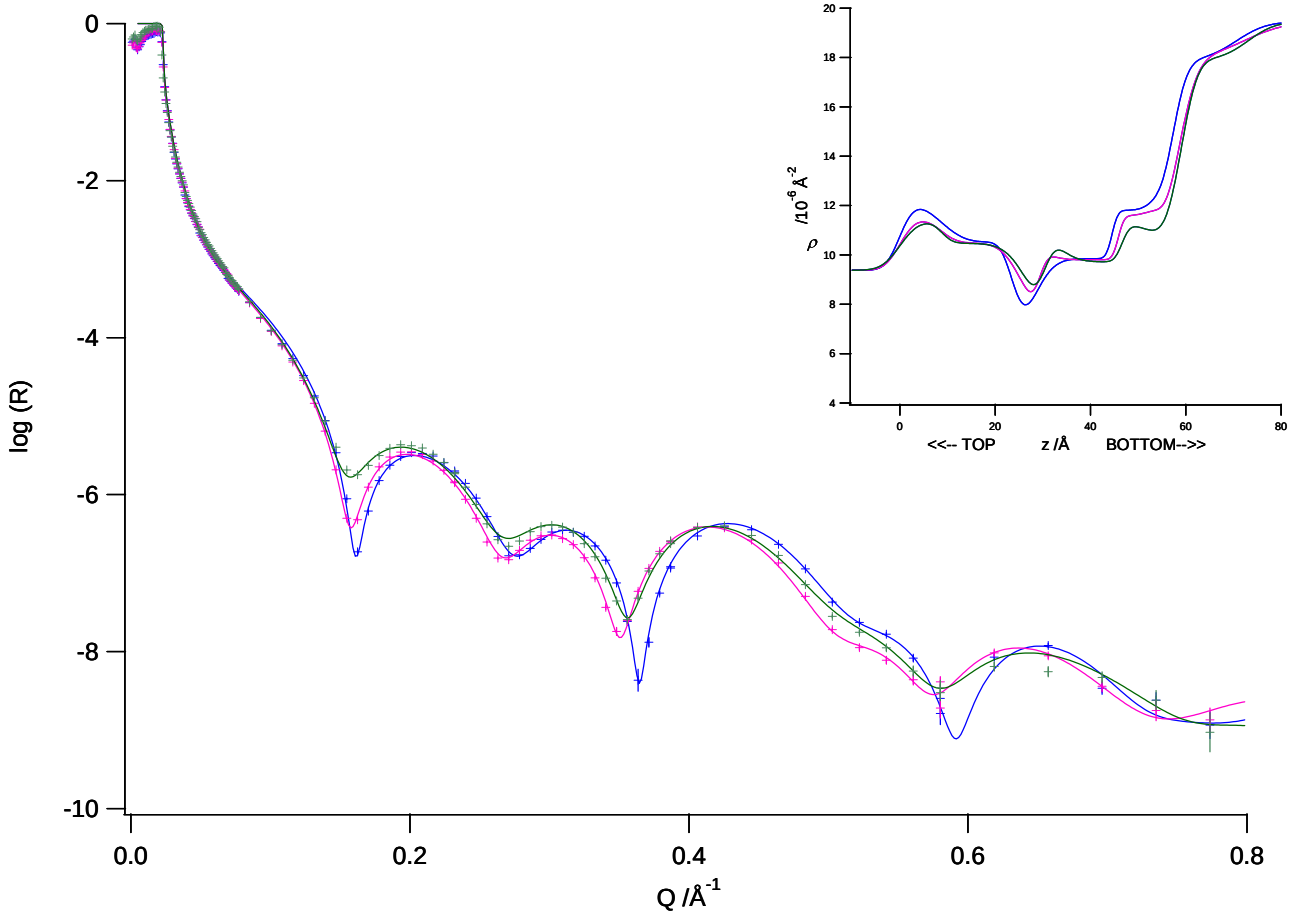

Figure 73: X-rays reflectivity from supported membranes at 22°C. Spectra refer to an asymmetric membrane composed by DPPC/cholesterol and GD1a ganglioside in pure water (blue) , in NaCl 156 mM solution (pink), and after the addiction of sialidase enzyme (green). Crosses are the experimental points, lines the fits. In the insert the correspondent contrast profiles obtained are shown.

The differences brought from the enzyme are more evident at high q.

As said before by X-rays reflectivity we are not very sensible to cholesterol disposition inside the lipid chains, so that the goal would be to use neutrons reflectivity. Unfortunately the q range accessible in a neutrons reflectivity experiment is from 0 to 0.25 $Å^{-1}$, while here the evident changes in the spectrum appear after q= 0.6 $Å^{-1}$.

We performed many subsequent measurements to the sample, but being the sample very delicate we damaged it. This is visible from the fact that the shape of the spectrum is unchanged but the minima of intensity are less pronounced.

We prepared this sample twice to check for reproducibility. Figure 74 shows that the spectra are almost superimposing and give us an idea of the error we can have on the measure. In fact all the differences we observed about different samples are bigger than these.

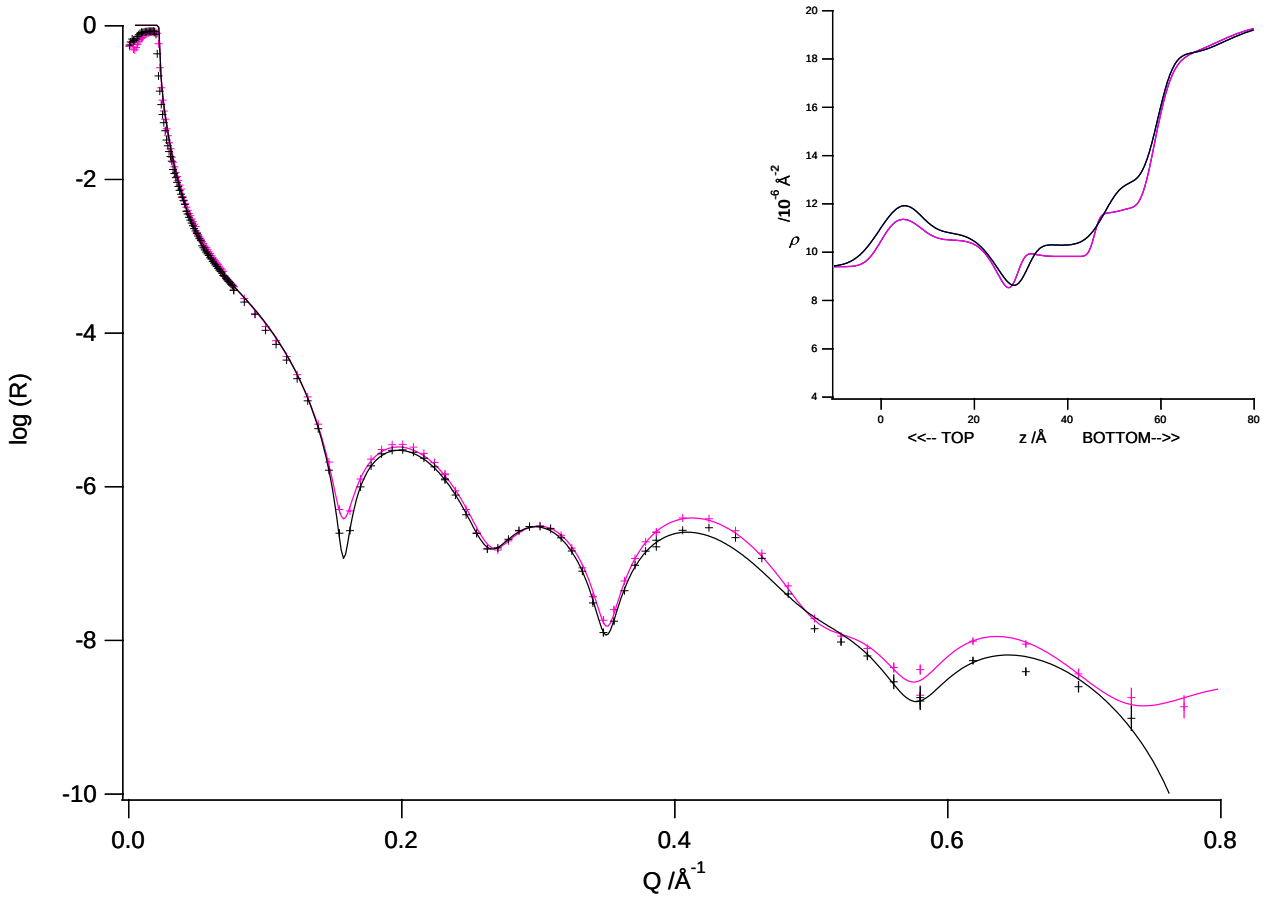

Figure 74: X-rays reflectivity from supported membranes at 22°C. Spectra refer to an asymmetric membrane composed by DPPC/cholesterol and GD1a ganglioside in pure water (blue) , in NaCl 156 mM solution (pink), and after the addiction of sialidase enzyme (green). Crosses are the experimental points, lines the fits. In the insert the correspondent contrast profiles obtained are shown.

To check if the product of the action of the enzyme on an existing membrane is the same of a membrane directly prepared with the product of the enzyme action, we prepared an asymmetric sample containing GM1 ganglioside instead of GD1a ganglioside, as follows:

- 1st layer of DPPC/Cholesterol 11/1.75 molar
- 2nd layer of DPPC/Cholesterol/GM1 ganglioside 10/0.75/1 molar

We prepared the sample directly in 156 mM NaCl water solution, to compare it to the product of the enzymatic action on the previous sample. Then we checked the activity of sialidase also on this sample.

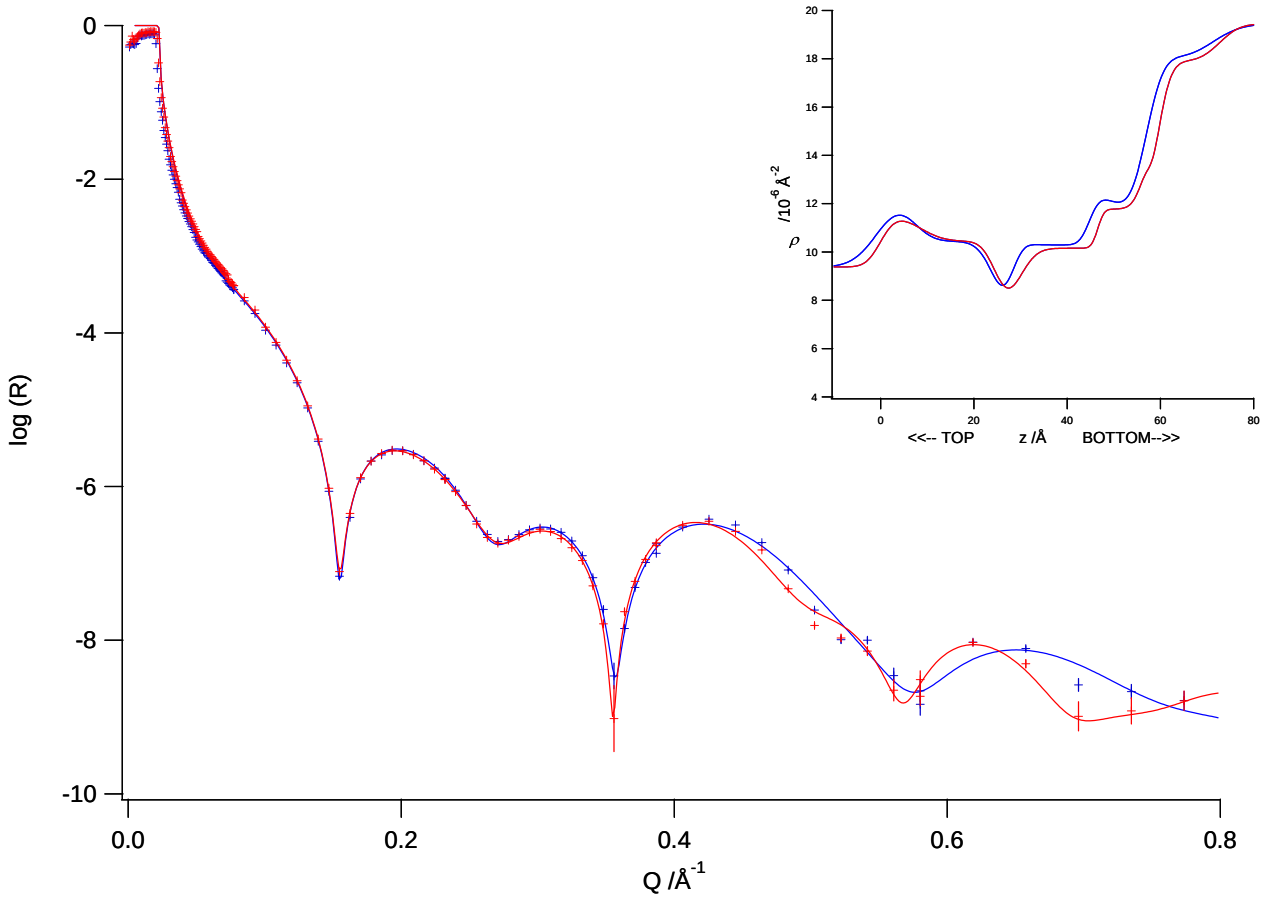

Figure 75: X-rays reflectivity from supported membranes at 22°C. Spectra refer to an asymmetric membrane composed by DPPC/cholesterol and GM1 ganglioside in NaCl 156 mM solution , before (blue) and after (red) the addiction of sialidase enzyme . Crosses are the experimental points, lines the fits. In the insert the correspondent contrast profiles obtained are shown.

First, we observed that the GD1a-containing sample after the action of sialidase is different from the GM1-containing sample before and after the action of the enzyme. In the high q region the spectra referred to the GM1-containing sample before and after the action of sialidase are different. This means that the enzyme works also on GM1 heads, even if not predicted.

We prepared a new sample with Asialo GM1 ganglioside, to check if the enzyme, instead of cutting one external sugar to GD1a, may cut both of them.

- 1st layer of DPPC/Cholesterol 11/1.75 molar
- 2nd layer of DPPC/Cholesterol/asialoGM1 ganglioside 10/0.75/1 molar

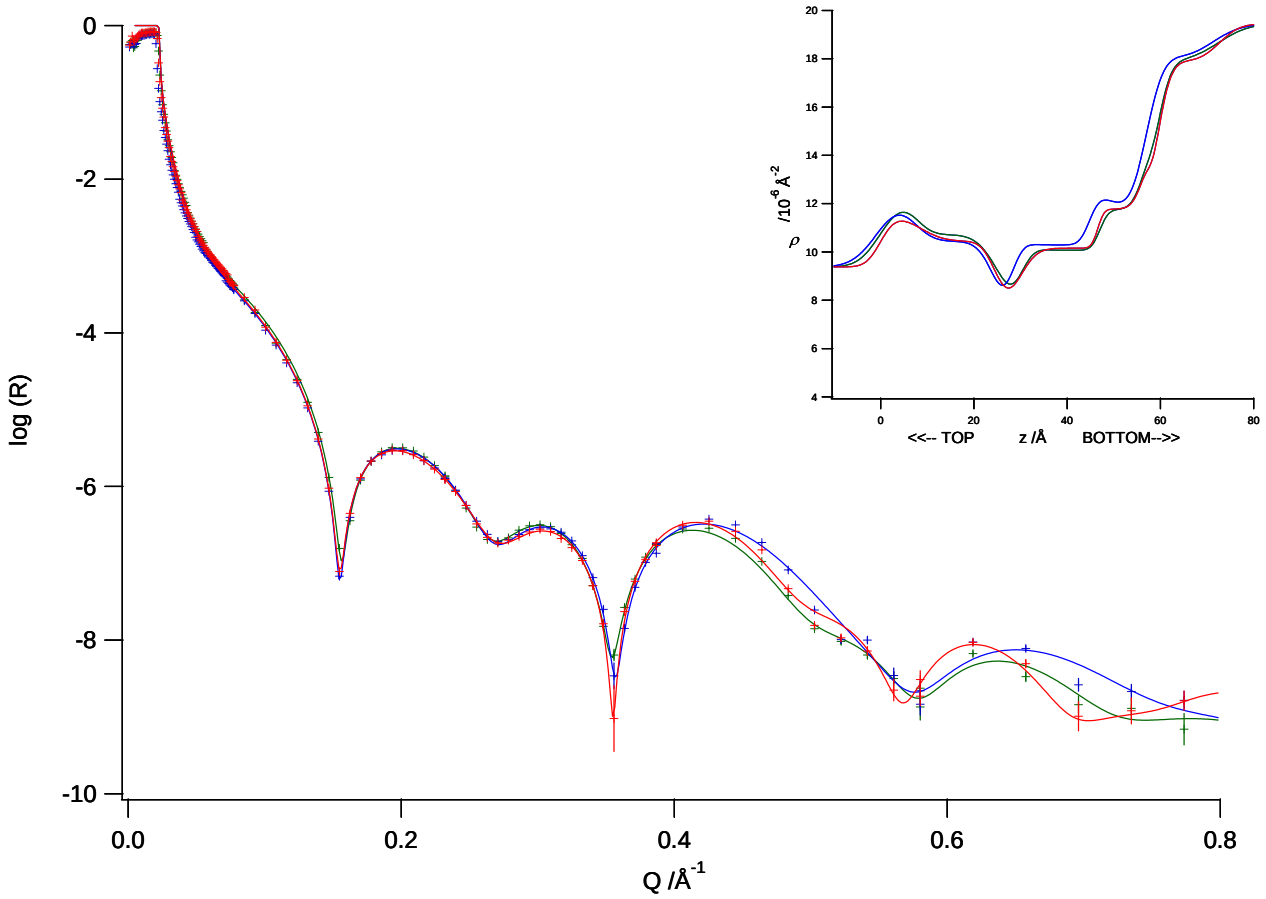

Figure 76: X-rays reflectivity from supported membranes at 22°C. Spectra refer to an asymmetric membrane composed by DPPC/cholesterol and GM1 ganglioside in NaCl 156 mM solution , before (blue) and after (red) the addiction of sialidase enzyme and to one composed by DPPC/cholesterol and Asialo GM1 ganglioside in NaCl 156 mM solution (green) . Crosses are the experimental points, lines the fits. In the insert the correspondent contrast profiles obtained are shown.

Each sample looks different from the others suggesting that probably gangliosides pack in some way which is different from one to the other, due to their different polar heads. Once they are packed, even if we change their steric hindrance, they reach new equilibrium situations, different from those they reach freely if packed from a disperse situation, that is when we compress them to build up the membranes in the Langmuir trough.

Table 8: parameters obtained by x-rays reflectivity measurements on different gangliosides containing membranes, to study the effect of sialidase enzyme.

	Thicknesses (± 1 Å)						
GD1a	**water**	**heads 1**	**chains 1**	**CH_3 group**	**chains 2**	**heads 2**	**total bilayer thickness (±1 Å)**
Sample in water	2	10	15	2	18	10	55
NaCl	3	9	17	3	17	10	56
Sialidase	2	10	16	2	20	9	57
GM1	**water**	**heads 1**	**chains 1**	**CH_3 group**	**chains 2**	**heads 2**	**total bilayer thickness (±1 Å)**
NaCl	1	11	17	3	19	7	56
Sialidase	1	11	18	3	17	9	58
Asialo GM1	**water**	**heads 1**	**chains 1**	**CH_3 group**	**chains 2**	**heads 2**	**total bilayer thickness (±1 Å)**
NaCl	1	11	17	4	18	8	58

Sialidase action results in an increase of the bilayers thickness both in GD1a and GM1 containing membranes. From the spectra comparison presented we see that big differences have been found among different samples, but by X-rays we are not sensible to the exact content of water and to the transverse position of cholesterol.

3.3.3. Comparison between X-ray and Neutron reflectivity applied to biomimetic supported membranes

To compare the results we obtained by X-rays reflectivity we adapted one of the membranes studied by X-rays reflectivity to the study by neutrons reflectivity. This means that to have a reasonable contrast profile we used fully deuterated phospholipids.

We built up a single asymmetric membrane containing cholesterol and GM1 ganglioside in a fully deuterated DSPC matrix. As lipid matrix we used DSPC instead of DPPC to enhance the quality of the deposition. The coverage we obtain in fact using deuterated lipids is lower than using hydrogenated lipids. and to enhance it we used a longer chains lipid (DSPC has 18 C in each hydrophobic chain, DPPC has 16). The first layer was

composed by d_{75}-DSPC: cholesterol in 11:1.75 molar concentration, and the second by d_{75}-DSPC: cholesterol:GM1 ganglioside in 10:0.75:1 molar concentration.

We measured the sample at 22°C, at 51°C and 22°C back in three different solvents: H2O, D2O, SMW (Silicon Matched Water, a mix of water and D2O with the same SLD of Silicon).

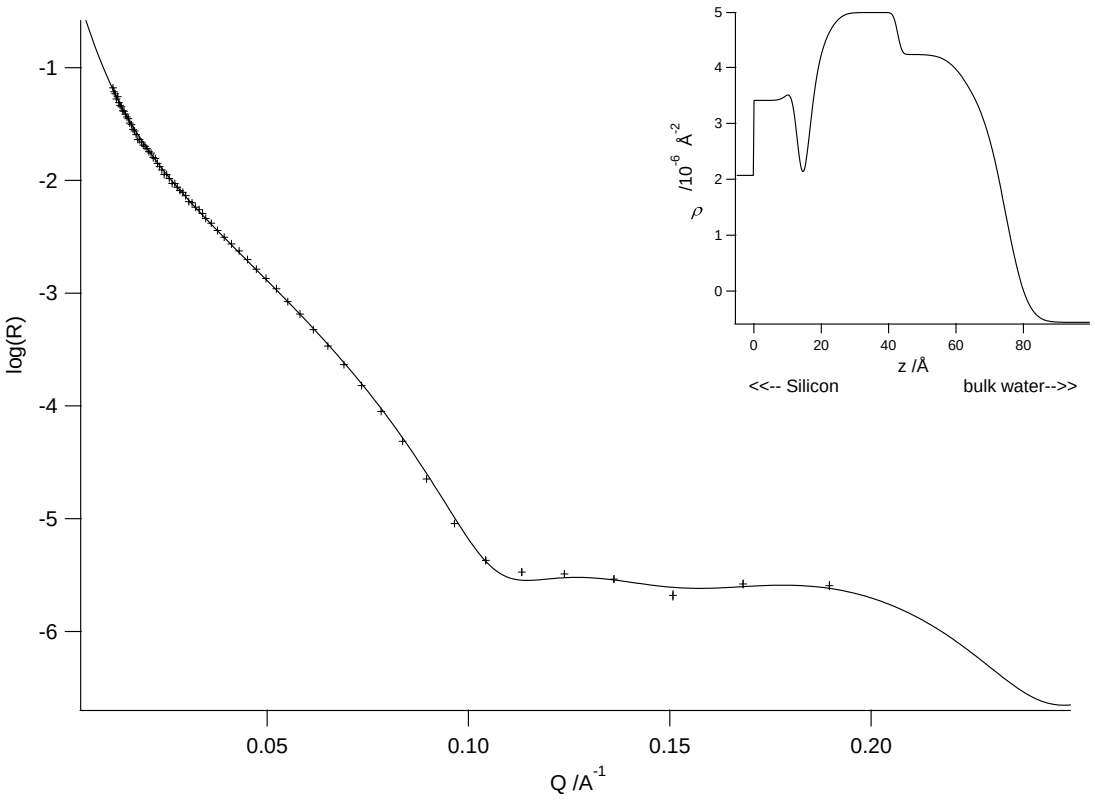

Figure 77: Neutron reflectivity (crosses) from the supported cholesterol and GM1-containig sample at 22°C after annealing. The subphase is water. In the insert the SLD profile is shown.

We did not go over the melting temperature of the mixture (the presence of GM1 and cholesterol further rises the chains-melting temperature of pure DSPC, which is 55°C) for technical reasons. The water volume in the cell is in fact small and we did not want to heat it too much. We fit the data with Motofit. Results are shown in table 4.

Table 9: parameters referred to the asymmetric DSPC-cholesterol-GM1 sample studied by neutron reflectivity.

	Thicknesses; roughness with respect to the previous layer (Å, Å)					SLDs ($*10^{-6}$ Å^{-2})				solvent penetration (% of volume)	
	Water (SiO2-heads)	heads 1	chains 1	chains 2	heads 2	SLD chains 1	%chol layer 1	SLD chains 2	%chol layer 2	chains 1	chains 2
22 °C	4; 6	7; 6	19; 6	22; 6	9; 6	7	74	6.7	26	10	22
51 °C	2; 1	6; 4	20; 1	23; 1	7; 1	5.55	68	5.21	32	3	13
22 °C after annealing	2; 1	7; 2	21; 1	20; 1	12; 1	6.73	63	6.4	37	24	31

The thicknesses, roughness and solvent penetration obtained are compatible with X-rays reflectivity results. Moreover in this case we are sensible to cholesterol disposition inside the membrane. No cholesterol redistribution occurs between the chains of the two leaflets of the membrane: the asymmetric disposition of cholesterol is reasonably kept. Moreover annealing the sample significantly reduces the roughness.

3.3.4 Interaction of Aβ peptide with a model membrane

The ability to draw ordered motifs on the surface of a hosting membrane is likely to constitute a major contribution of gangliosides to promoting morphological rearrangement of adhering macromolecules via structural templating. For example, this ability is at the basis of the gangliosides' role in the induction of amyloid fibril formation [Matsuzaki et al.(2010)] in Alzheimer's disease, i.e., the formation of those insoluble A β aggregates that are extracellularly deposited, forming the amyloid plaques. Gangliosides, highly enriched in neuronalplasma membranes, are responsible for specific interactions with A β that drive its conformational transition and A β fibrillogenesis. GM1-A β interaction and A β aggregation are favoured in a cholesterol-rich membrane environment [Mizuno et al. (1999); Kakio et al. (2001)]. On the other hand, a confocal microscopy and AFM study has shown that increasing the cholesterol content of GM1-containing microdomains reduces the ability of the amyloid-peptide to interact with the ganglioside and to affect the membrane [Cecchi et al. (2009)]. This further confirms that the GM1-cholesterol pair contributes to domain superstructuring in a controlled interplay.

After the annealing we injected in the cell the 1-40 sequence peptide of the β-amyloid. The A β40 peptides (SLD $1.49*10^{-6}$Å^{-2}) are the predominant form found. We studied its interaction with the model membrane at room temperature. We injected a huge quantity

of peptide to reach a concentration of 80 µg/l (the SLD of the subphase we used to fit the data is $1.5*10^{-6}Å^{-2}$ instead of that of the water which is $-0.56*10^{-6}Å^{-2}$). We measured the system in these conditions after one hour, then we washed it first with water to remove the excess peptide, and, after a measure, with a 150mM NaCl water solution.

The Reflectivity spectra we obtained are shown in figure 78:

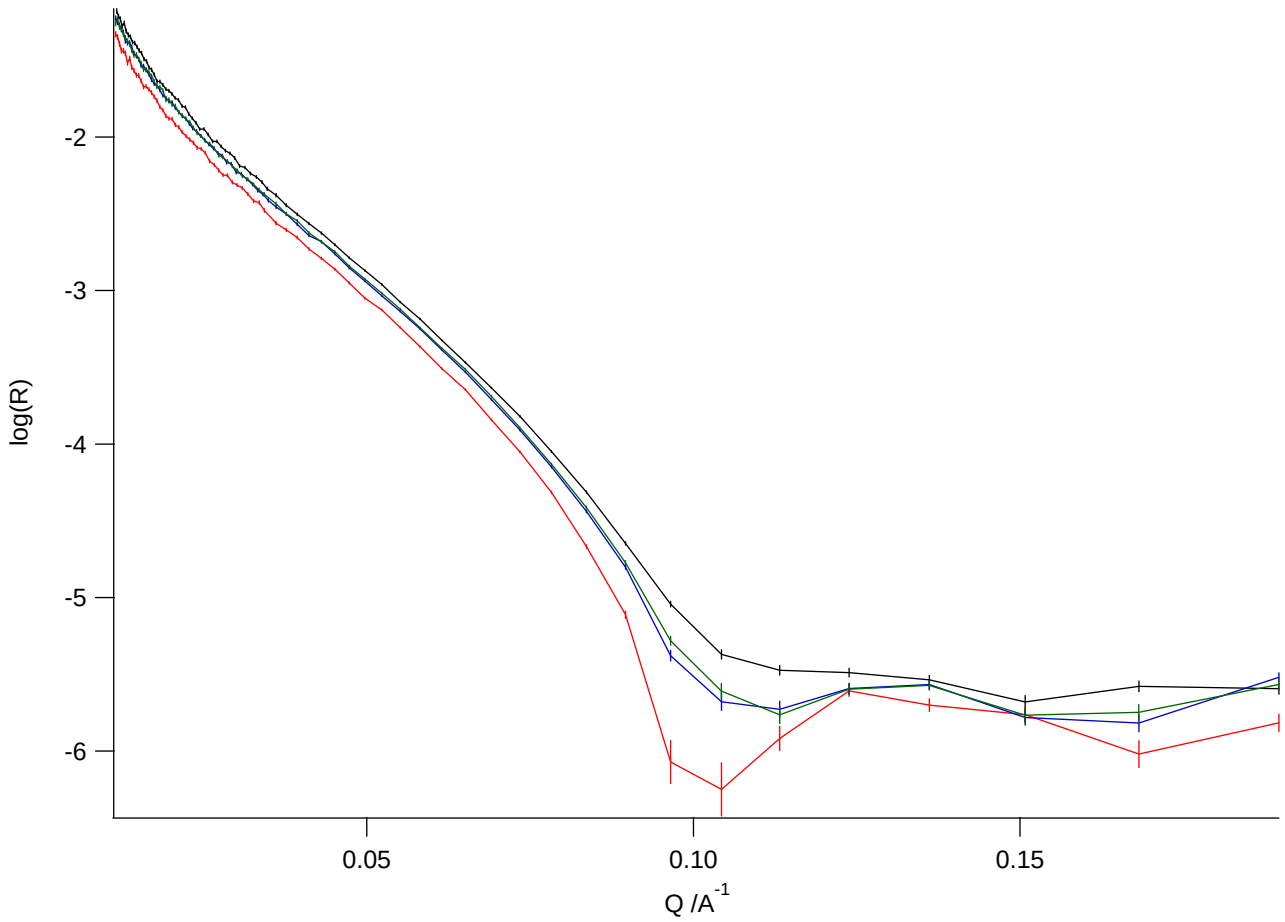

Figure78: Neutron reflectivity from the supported cholesterol and GM1-containig sample. The black spectrum refers to the sample at 22°C after annealing, the red refers to the sample after the injection of the peptide, the blue to the sample washed with water, the green to the sample washed again with water and NaCl.

Fitting the data with Motofit we obtained the parameters shown in table 10.

Table 10: parameters obtained by fitting the neutron reflectivity data referred to the interaction between the peptide and the adherent membrane.

	Thicknesses; roughness with the previous layer					**SLDs**				**solvent penetration**	
	Water (SiO2-heads)	**heads 1**	**chains 1**	**chains 2**	**heads 2**	**SLD chains 1**	**%chol layer 1**	**SLD chains 2**	**%chol layer 2**	**chains 1**	**chains 2**
22 °C after annealing	2; 1	7; 2	21; 1	20; 1	12; 1	6.73	63	6.4	37	24	31
22°C +WTL	2; 1	7; 3	21; 3	20; 1	15; 10	6.73	63	6.4	37	24	31
Washed with H2O	2; 2	7; 3	21; 3	20; 1	13; 10	6.73	63	6.4	37	27	34
Washed with H2O-NaCl	2; 2	7; 3	21; 3	20; 1	11; 10	6.73	63	6.4	37	27	34

By washing, that is by slowly changing the solvent hydrating the sample, the thickness and SLD of the external layer change and the solvent penetration increases in the whole membrane of about the 5%. This suggests us that the peptide deposits over the membrane, probably filling the empty space let by the ganglioside heads, as expected.

In figure 79 the SLD profiles of the membrane in its final phases is shown.

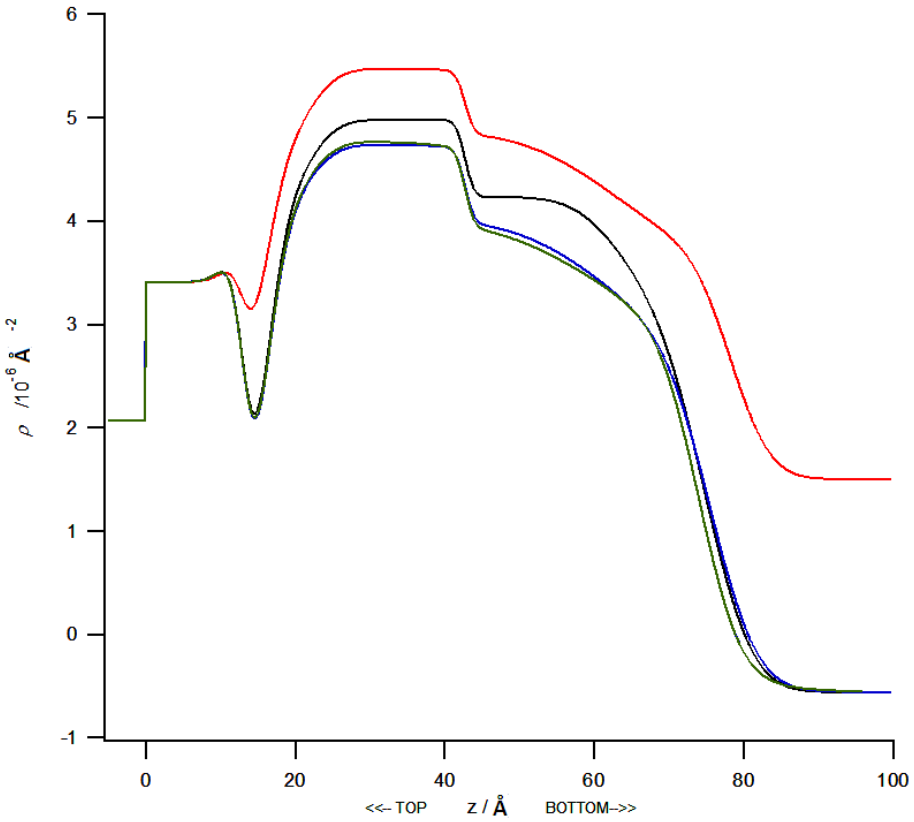

Figure 79: SLD profiles from the sample during the injection of the peptide. The black spectrum refers to the sample at 22°C after annealing, the red refers to the sample after the injection of the peptide, the blue to the sample washed with water, the green to the sample washed again with water and NaCl.

The red line in figure 79 refers to the sample before washing the peptide: the SLD of the solvent is higher than that of water because we injected a big amount of peptide, changing the whole solvent contrast profile. After the injection of the peptide, the roughness of the external layer of the membrane (that of the heads) enormously increases: from 1 to 10 Å. Moreover the solvent penetration of the external chains and heads increases of 3% in volume. No cholesterol migration between the leaflets occurs. Finally we don't observe an ulterior layer over the membrane. We could attribute the lowering of the SLD of external chains and heads of the membrane, instead of as consequence of an increase of the solvent penetration, as a consequence of the presence of the peptide. The peptide could distribute in the gaps of the polar heads of the lipids, without penetrating the membrane. It could both penetrating just the external leaflet, or expand the lipids chains while inserting among their heads.

3.4. FLOATING BILAYERS

In the previous section we presented the results of experiments performed on single membranes, investigated by X-rays and neutrons reflectivity.The coupling with the support could prevent the mobility of molecules between the two leaflets of the membrane[Schmitt et al. (2001)]. Moreover we could have charge interactions between the silicon support and the molecules constituting the membrane under study. In order to have an almost free membrane, away from the substrate, several methods can be considered:

- The first method is simply to make two membranes by four successive transfer of monolayers [Charitat et al. (1999)]. This sample is more fragile but has the advantage of being more symmetrical.
- A second possibility is to let vesicles disrupt over the support. In this way we cannot control the composition of each layer.
- It is also possible to deposit a layer of polymers on the substrate [Sinner and Knoll (2001)] and transfer over that two monolayers by the Langmuir-Blodgett technique.
- We can finally make a film of octadecyltrichlorosilane (OTS) hydrophobic covalently grafted to the substrate and transfer over it three monolayers lipid by the Langmuir-Blodgett technique [Hughes et al. (2002a)]. A first bilayer "mixed" OTS / lipid is get very "tough" and a second freer bilayer.

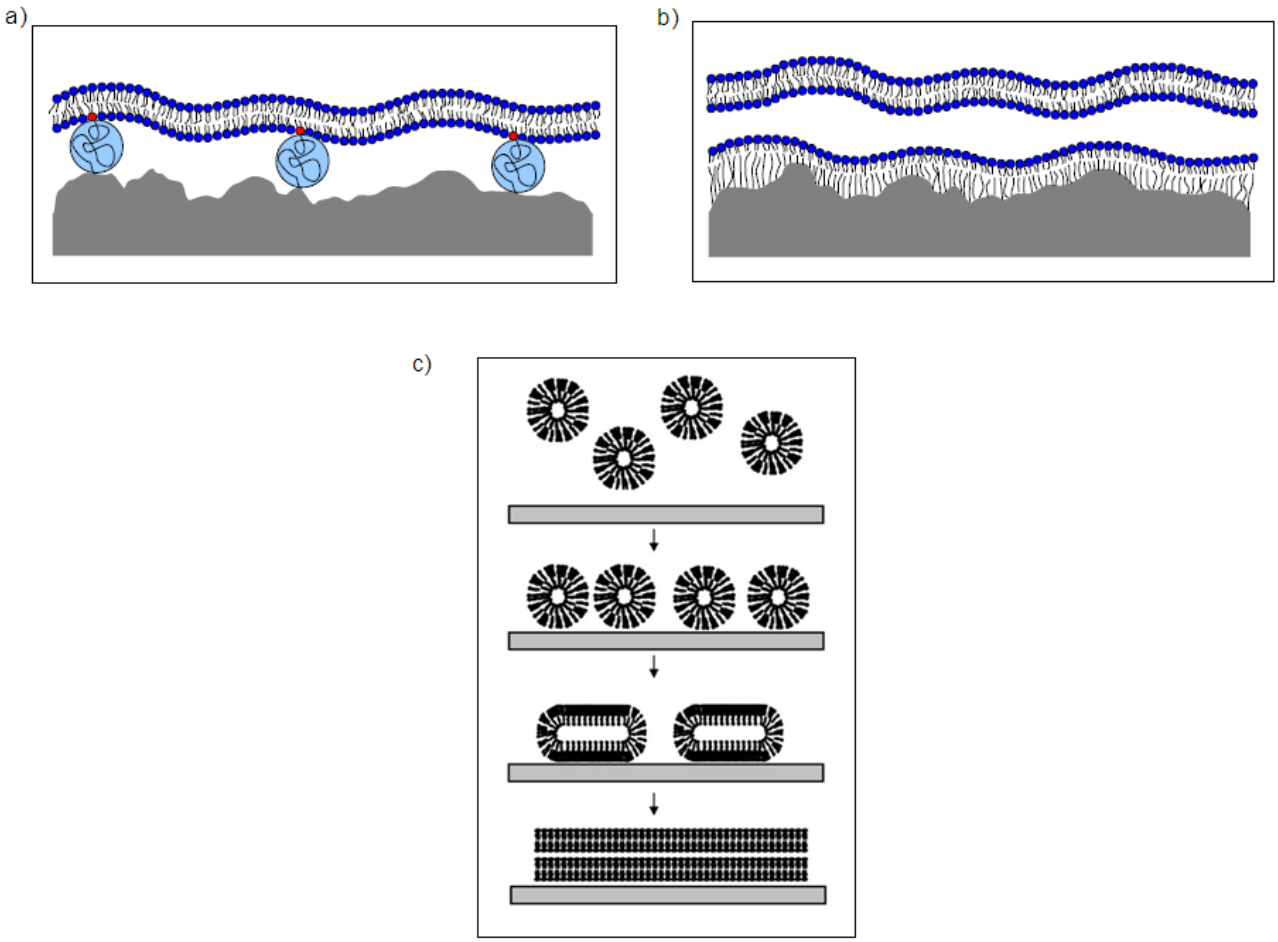

Figure 80: a schematic view of a) a tethered bilayer; b) a double OTS/lipids bilayer; c) the vesicles disruption technique.

We developed an experimental model with a single macroscopic bilayer floating at 1.5-2 nm on top of another adhering to a silicon flat surface, prepared, layer-by-layer, by combination of Langmuir-Blodgett (LB) and Langmuir-Schaefer(LS) techniques. The system so built has led in the past to stable and reproducible floating bilayers. With this technique the composition of each layer can be chosen suitably.

3.4.1. Neutron reflectivity from floating membranes: stability and main structural characteristics

We forced asymmetry in “adhering + floating” bilayers systems composed of phospholipids, gangliosides and cholesterol in bio-similar mole ratios, and we studied the samples by neutron reflectivity. The sample preparation procedure, measuring procedure and data analysis have been already explained.

As explained about supported bilayers measurements, before starting the experiment the silicon block has been characterized by three reflectivity measurements in three different solvents, to extract the features of the silicon oxide.

Double bilayer depositions were done in H_2O coupling three LB and one LS depositions.

For the bilayer adhering to the silicon support, we selected the long chain phospholipid DSPC, being in gel phase all over the investigated temperature range, from 22°C to 51°C. This guarantees the compactness and stability of the supporting bilayer. For the floating bilayer, DPPC was used as lipid matrix, being the lipid most likely to be found in membrane domains enriched in cholesterol and sphingolipids. Over it we deposited many bilayers starting by the simple DPPC matrix, which has been step by step complicated until the most complex sample: an asymmetric bilayer composed by DPPC, cholesterol and gangliosides. We used fully deuterated DPPC to highlight cholesterol and gangliosides. We performed measurements in different contrast solvents: H_20, D_2O, SMW.

A scheme of the first samples we studied is shown in figure 81.

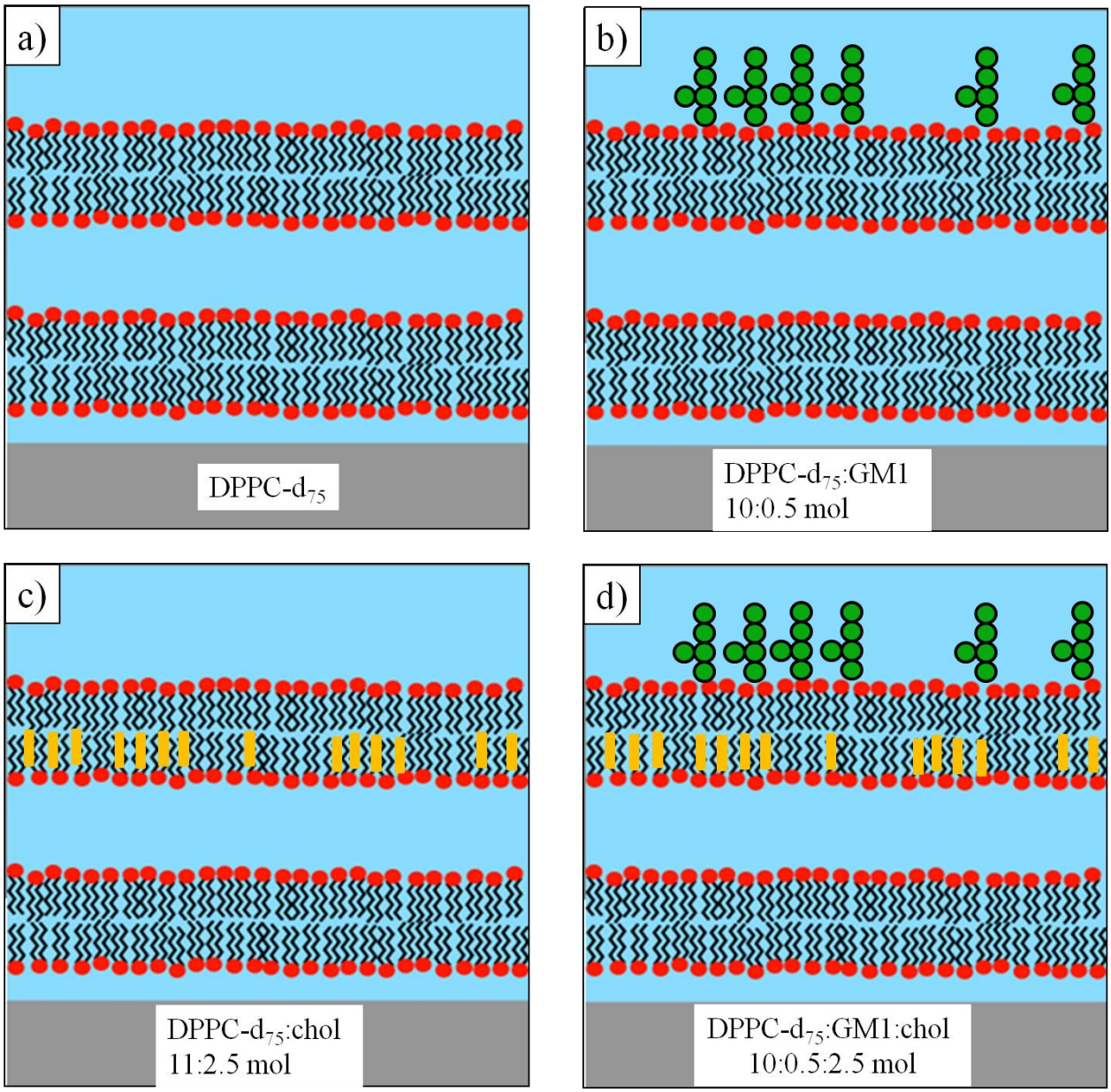

Figure 81: schematic view of the samples studied. The supported bilayer is DSPC in all cases.

In figure 82 neutron reflectivity spectra referred to the different samples are shown, and indicate that we are very sensible to the differences between the different samples, because all the spectra are very different the one to the other.

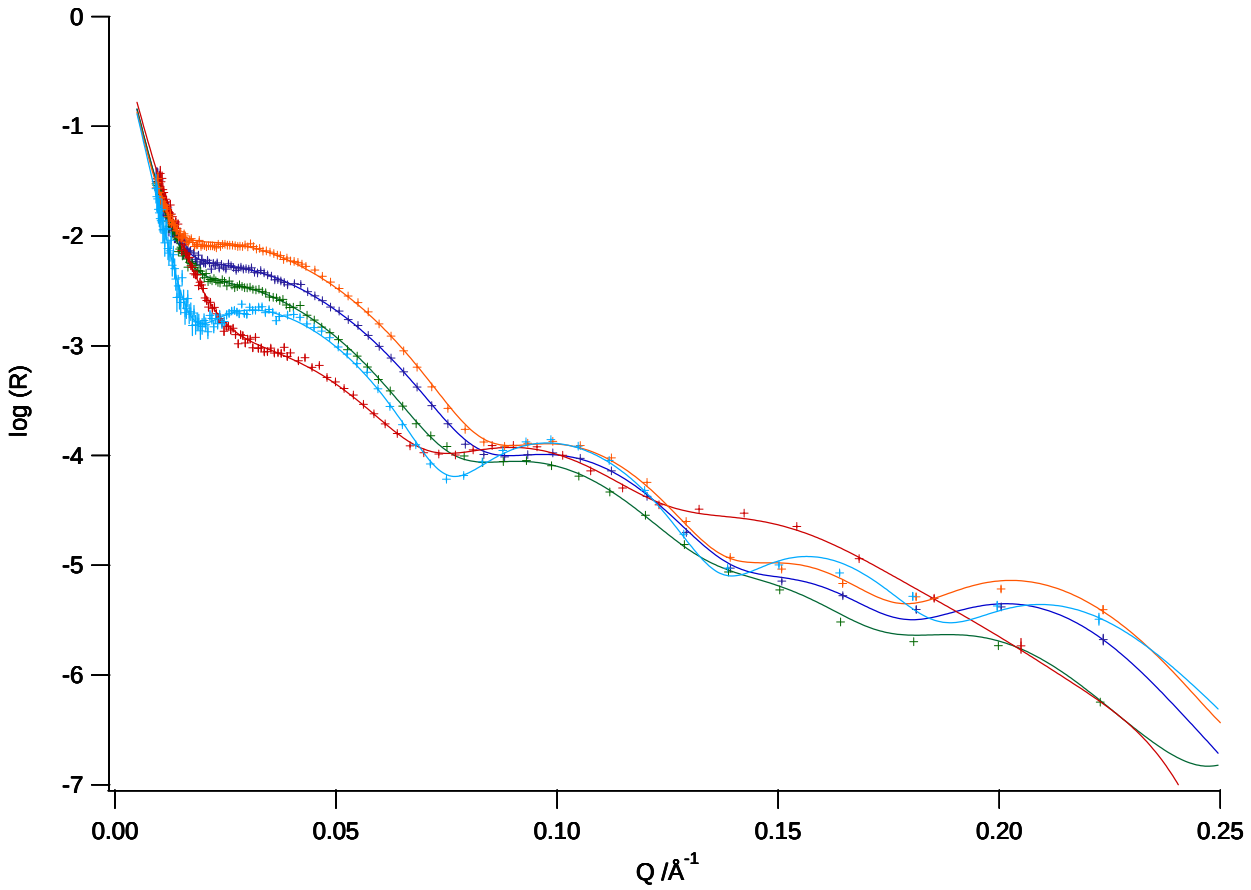

Figure 82: Neutron reflectivity from double membranes at 25°C in H_2O before annealing. The supported bilayer is DSPC in all cases. Spectra refer to the following studied floating membranes: pure DPPC (blue), DPPC+cholesterol symmetric (green), DPPC+cholesterol asymmetric (red), DPPC+asymmetric GM1 (orange), DPPC+asymmetric cholesterol+asymmetric GM1 (sky blue). Crosses are the experimental points, lines the fits.

In figure 83 a fitted (Motofit) spectrum is represented, with the relative SLD profile obtained, to show the goodness of our fits.

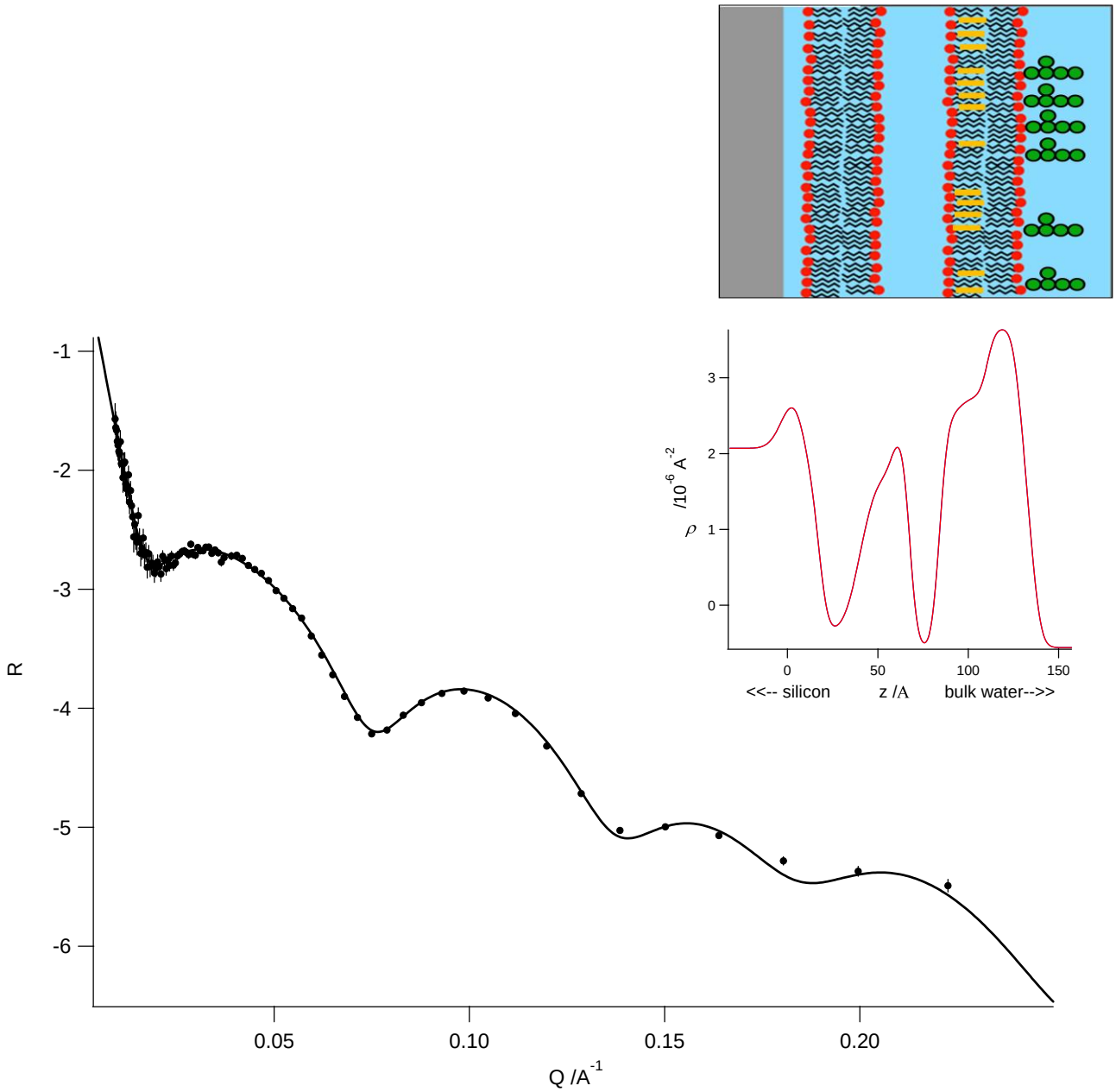

Figure 83: Fit (line) of the DPPC+cholesterol+GM1 sample spectra (dots) at 25°C in H2O. Insert: SLD profile of the sample.

Fit results are shown in table 11.

Table 11: Parameters obtained fitting the spectra referred to the studied samples.

d75DPPC	***DSPC adherent bilayer***		**FLOATING BILAYER**	
T (°C)	***1st bilayer thick (±1 Å)***	***1st bilayer solv p (±5%vol)***	**2nd bilayer thick (±1 Å)**	**2nd bilayer solv p (±5%vol)**
25	*61*	*12*	52	12
30	*59*	*12*	52	12
51	*59*	*12*	45	15
25 back	*62*	*10*	50	23
d75DPPC+ CHOL Asymm (inner layer)				
T (°C)	***1st bilayer thick (±1 Å)***	***1st bilayer solv p (±5%vol)***	**2nd bilayer thick (±1 Å)**	**2nd bilayer solv p (±5%vol)**
47	*62*	*12*	45	10
51	*57*	*14*	45	8
25 back	*61*	*19*	54	17
d75DPPC+ GM1 Asymm (outer layer)				
T (°C)	***1st bilayer thick (±1 Å)***	***1st bilayer solv p (±5%vol)***	**2nd bilayer thick (±1 Å)**	**2nd bilayer solv p (±5%vol)**
25	*61*	*8*	54	13
41	*60*	*15*	54	13
51	*57*	*13*	43	17
25 back	*58*	*4*	52	20
41 back	*60*	*17*	54	20
51 back	*58*	*13*	49	19
d75DPPC+ CHOL Asymm + GM1 Asymm				
T (°C)	***1st bilayer thick (±1 Å)***	***1st bilayer solv p (±5%vol)***	**2nd bilayer thick (±1 Å)**	**2nd bilayer solv p (±5%vol)**
25	*58*	*12*	52	16
41	*61*	*11*	53	15
51	*55*	*15*	44	15
25 back	*61*	*11*	56	30
41 back	*62*	*17*	55	30
51 back	*60*	*14*	52	21

Results agree with what we obtained by X-rays reflectivity on adherent bilayers.

The parameters obtained after annealing the samples show that, as expected, cholesterol thickens the bilayer (it varies from 50 to 54 Å), more than GM1 ganglioside (52 Å). The thickest membrane is the most complex, that is the one with all the

components: DPPC, cholesterol, GM1 (56 Å). This is probably due to the fact that the membrane is free to assume a curvature and so we see it thicker.
We also note that annealing the sample reduces the thickness and increases the solvent penetration, that is the sample is less compact.
We could not study the internal mechanisms of such membranes because of an unexpected but very important effect. A potentiality of the system has been in fact discovered.

3.4.2. Lipid exchange between two membranes

Lipid exchange between two membranes is a well known biological phenomenon.

We deposited the DSPC bilayer and the floating d_{75}DPPC bilayer and noted that the lipid exchange among the two membranes could be followed.

This means that it's possible to study the migration of molecules throughout different membranes, for example switching on or off the migration via the temperature of via the presence of a third component added.

At the beginning of the experiment we performed four subsequent measures to the system at room temperature, under the lipid chains melting temperature, and we observed the system to be very stable. No lipid exchange occurred. Then we raise the temperature and observed that lipid exchange took place between the adherent and floating membranes. This observation is possible thanks to the fact that neutrons distinguish very well normal and deuterated lipids.
So we observe that the SLD of DSPC chains ($-0.44*10^{-6}Å^{-2}$)was rising, going towards that of the deuterated chains of DPPC (SLD $7.66*10^{-6}Å^{-2}$), and vice versa for the floating membrane.
Results are reported in figure 84.

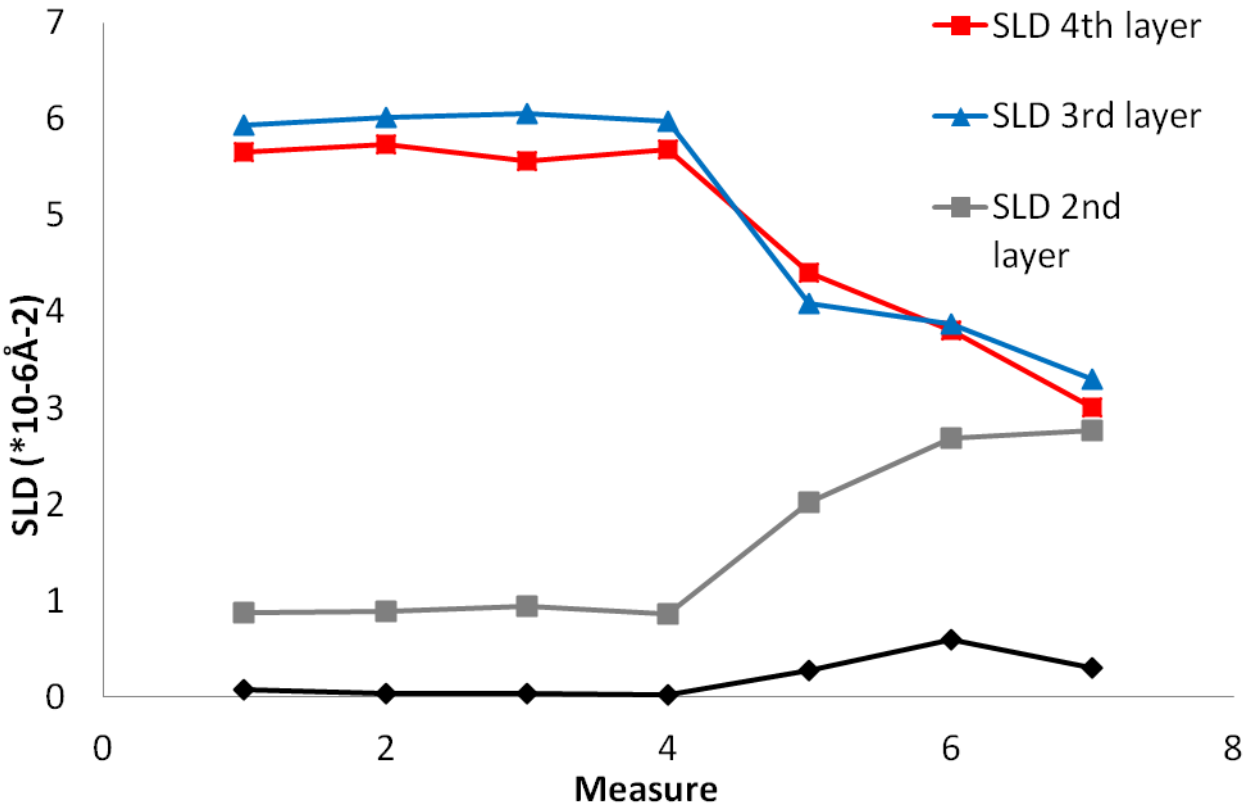

Figure 84: SLD variation of the fur deposited layers to form the DSPC+d75DPPC adherent+floating membranes system.

It is immediate to observe that the first deposited layer exchanges less than the others, being coupled with the support. Exchange tends to 50%, the equilibrium proportion.

We performed an equivalent analysis on the all the membranes to study whether the presence of additional components was preventing or slowing down lipid exchange.

Results, reported in figure 84, indicate that no big effect can be observed because of the presence of GM1 ganglioside or cholesterol.

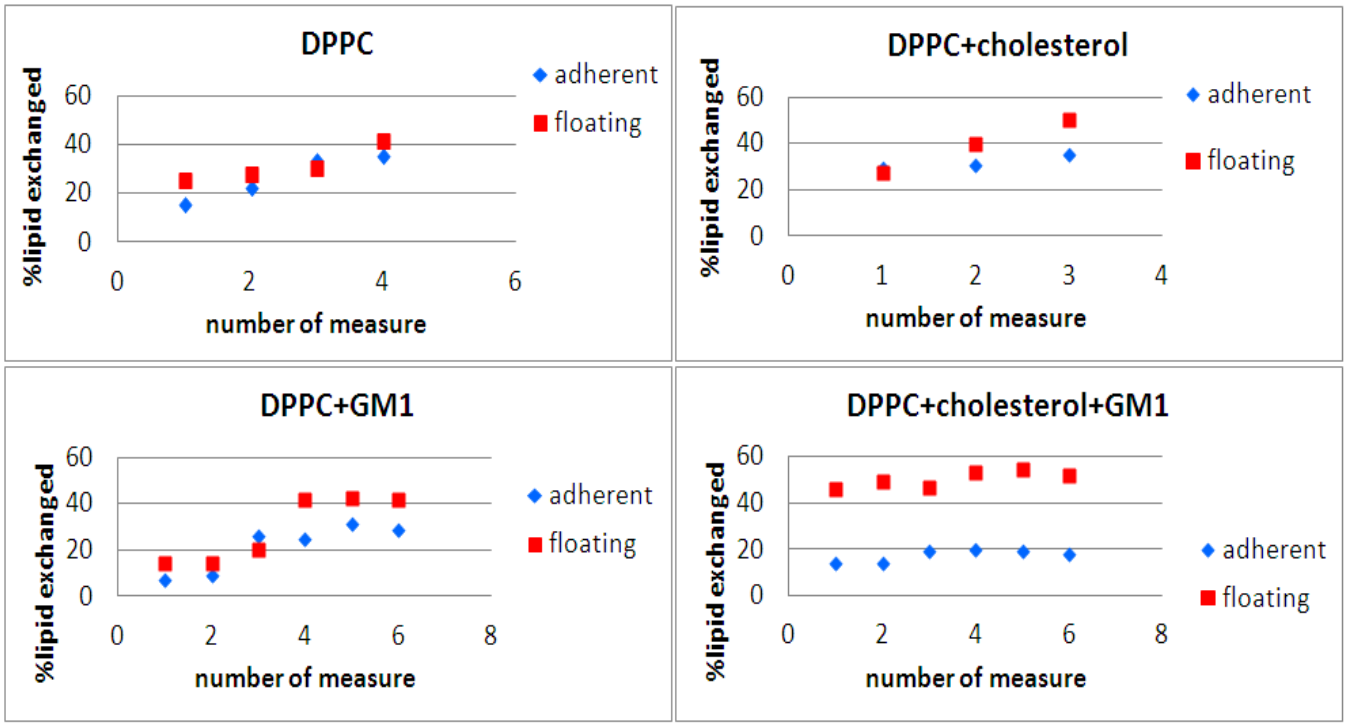

Figure 85: lipid exchange evolution in time on four different complicated double asymmetric bilayers systems.

In the four presented cases the floating bilayer exchanges lipids more than the adherent one, coupled with the silicon block. In all the presented cases, as expected, the exchange tends to 50%, the equilibrium proportion.

3.4.3. Cholesterol transverse disposition in a phospholipid floating membrane

To enhance our sensibility to cholesterol and gangliosides, and hide lipid exchange between the membranes, we decided to use as supporting bilayer a fully deuterated DSPC membrane.

The first complication for the membrane point of view, could be the presence of cholesterol.

On the way to more complex systems, containing lipids of different nature, we tested whether a simple imposed asymmetry was kept in time and whether it could stand some standard experimental protocols commonly employed when dealing with model membranes (i.e. annealing and solvent exchange).

Reflectivity from floating bilayers: can we keep the structural asymmetry?

V Rondelli [1], G Fragneto[2], S Motta[1], E Del Favero[1], L Cantù[1]

[1]Dept. of Chemistry, Biochemistry and Biotechnologies for Medicine, University of Milan, Segrate, Italy

[2]Institut Laue-Langevin, Grenoble Cedex, France

Abstract. To assess the structure of complex biomembranes, the use of asymmetric model systems is rare, due to the difficulty of realizing artificial membranes with desired heterogeneous composition and applicable for single membrane structural investigation. We developed an experimental model with a single macroscopic bilayer floating on top of another adhering to a silicon flat surface, prepared by Langmuir-Blodgett Langmuir-Schaefer technique, then investigated by neutron reflectivity. On the way to more complex systems, containing lipids of different nature, we tested whether a simple imposed asymmetry is kept in time and whether it can stand some standard experimental protocols commonly employed in treating model membranes. We focused on cholesterol, a basic component with a transverse distribution that is not symmetric in biomembranes, and may assume specific location in functional domains. So we forced different asymmetries in the “adhering + floating” bilayers system composed of phospholipids and cholesterol in bio-similar mole ratios. The neutron reflection accessible length-scale and its sensitivity, enhanced by the possibility to play with deuteration, allowed assessing the cross profile of the membrane and revealing that lipid redistribution can occur.

‘Journal of Physics, Congress proceedings’, in press.

3.4.4. A multicomponent floating membrane: the effect of a ganglioside

Going towards GEMs composition, we built up and studied the following system:

- 2 layers of d_{85}DSPC
- 3rd layer of d_{75}DPPC/Cholesterol 11/2.5 molar
- 4th layer of d_{75}DPPC/GM1 ganglioside 10.5/0.5 molar

We started with a relatively low amount of GM1 to avoid the membrane to assume a too big curvature and we put all the cholesterol in the inner leaflet of the membrane, to study eventual cholesterol redistribution.

We performed neutrons reflectivity measurements at 22°C, 30°C, 40°C, 45°C, 50°C, 55°C, and back to 45°C, 40°C, 35°C, 30°C, 22°C.

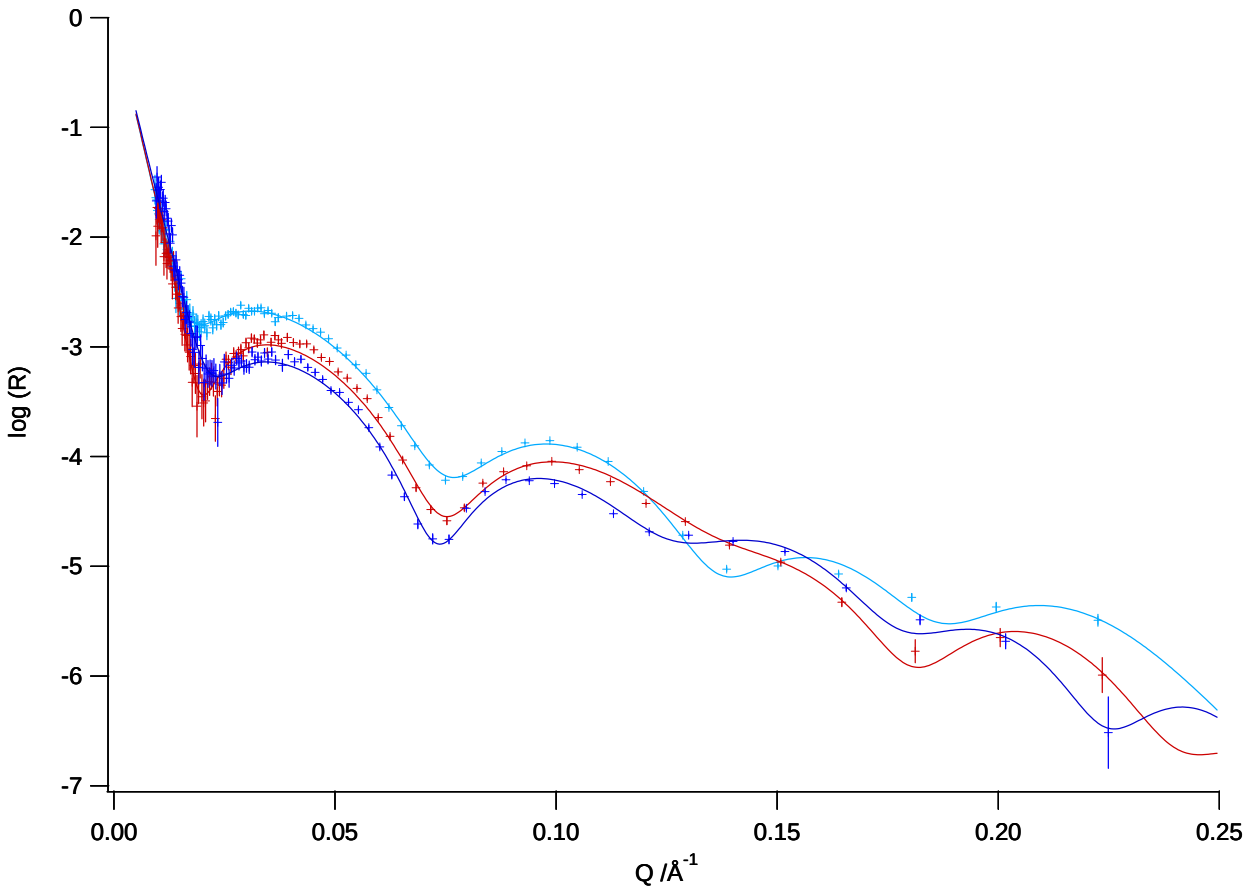

Figure 86: Neutron reflectivity from a DPPC+ asymmetric cholesterol + asymmetric GM1 floating membrane in H_2O before (25°C, sky blue), during (51°C, red) and after (25 °C back, blue) annealing. Crosses are the experimental points, lines the fits.

We performed many measurements to the system while crossing the gel-to-fluid chains transition and fluid-to-gel chains transition and figures 88 and 89 show our sensibility to the process.

The membrane is changing its tickness and density, in fact its contrast profile is different.

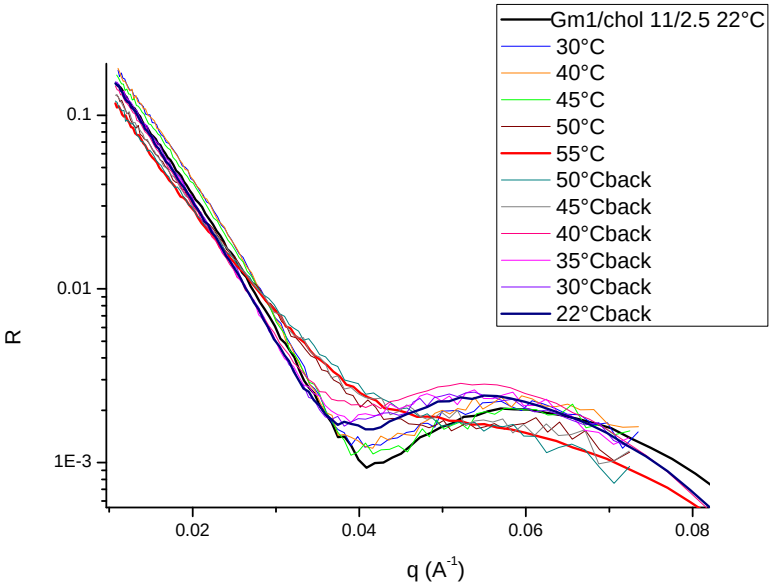

Figure 87: Neutrons reflectivity spectra referred to the DPPC+cholesterol+GM1 sample at various temperatures.

Heating the sample the chains gel-to-fluid transition is between 45 and 50°C as shown in figure 88.

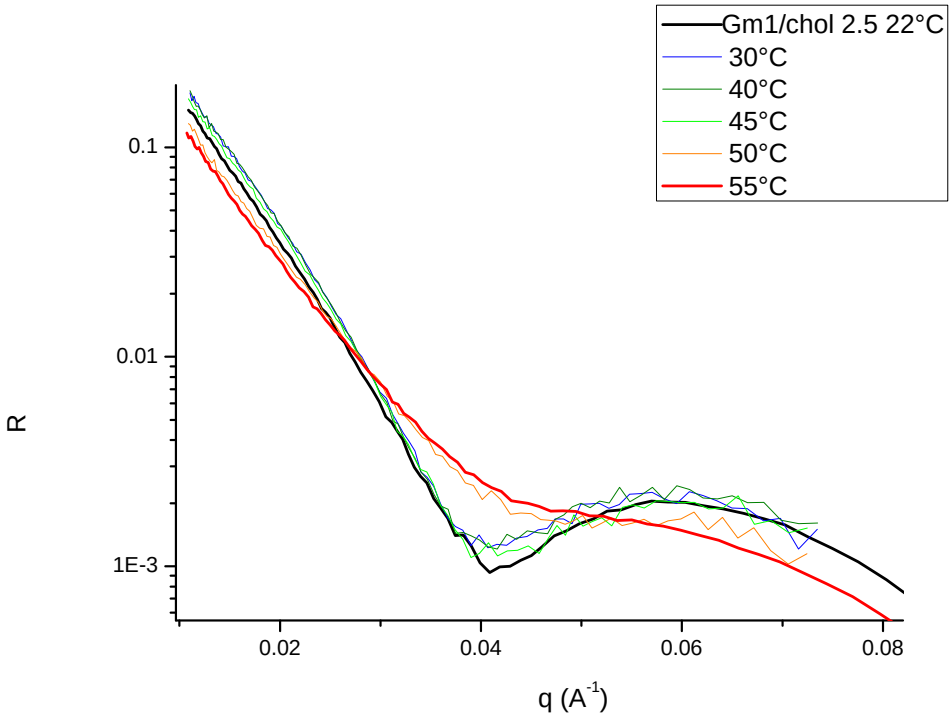

Figure 88: Spectra referred to the DPPC+cholesterol+GM1 sample at various temperatures heating the sample.

Figure 89 shows that cooling the sample the chains fluid-to-gel transition starts at about 40°C.

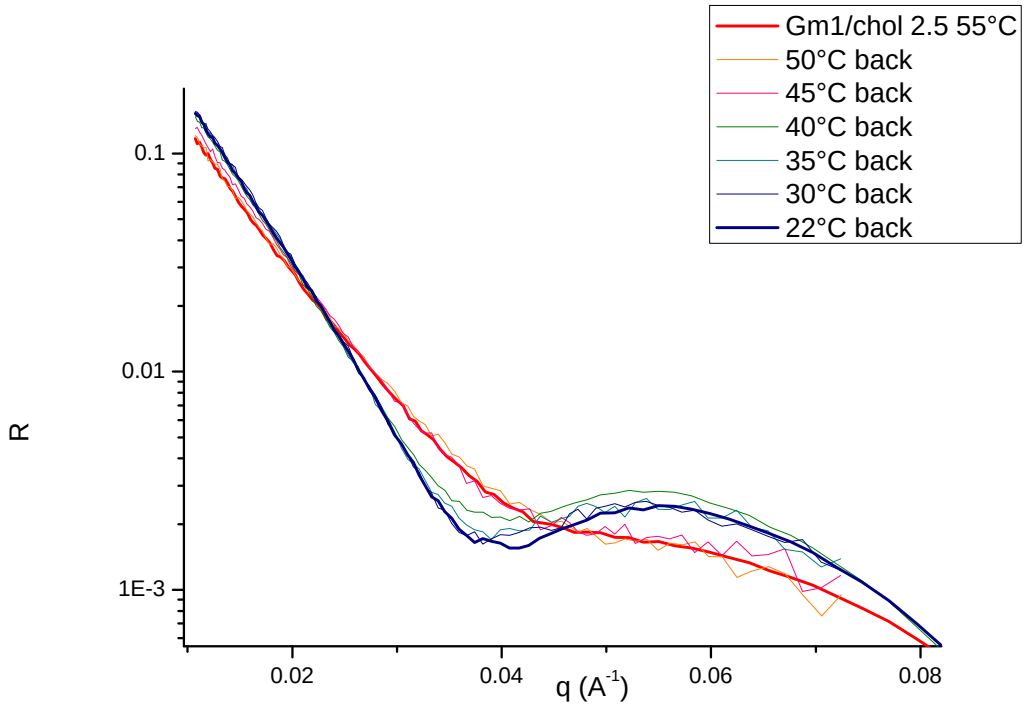

Figure 89: Spectra referred to the DPPC+cholesterol+GM1 sample at various temperatures cooling the sample.

The spectra have been fitted with Motofit. An example of fit quality is shown in figure and fit results are represented in table 12.

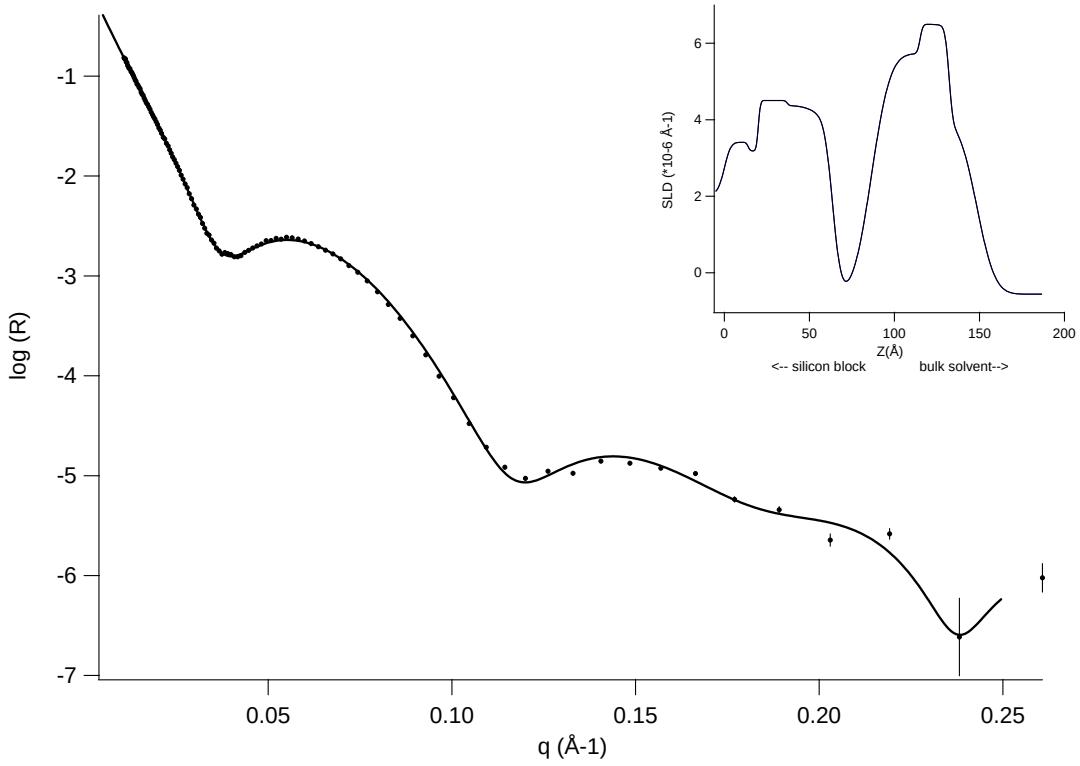

Figure 90: fit (line) of the neutrons reflectivity spectrum of the DPPC+cholesterol+GM1 floating bilayer annealed at 22°C. The solvent is water. the insert shows the SLD profile of the sample.

If comparing the inserts of figures 86 and 93 we note that the SLD difference between DSPC and d_{85}-DSPC is huge.

Table 12: parameters obtained fitting the data relative to the DPPC+cholesterol+GM1 floating bilayer.

	Thickness (±1Å)	SLD ($*10^{-6}$ Å^{-2})	Cholesterol content (%over the total)	Water content (%vol)	Roughness (±2Å)
water	22	-	0	100	4
heads 3	9	5.70	0	15	8
chains 3	21	**6.70**	81	14	7
chains 4	17	**7.05**	19	7	1
heads 4	16	5.30	0	16	2

Results show that on annealing the system, cholesterol redistributed inside the lipid chains to reach an asymmetric disposition: the 81% stay in the inner leaflet opposite to GM1, while the 19% migrates in the outer leaflet together with GM1.

3.4.5. Ganglioside GM1 forces the redistribution of cholesterol in a biomimetic membrane.

V Rondelli [1], G Fragneto[2], S Motta[1], E Del Favero[1], S Sonnino[1], L Cantù[1]

[1]Dept. of Chemistry, Biochemistry and Biotechnologies for Medicine, University of Milan, Segrate, Italy

[2]Institut Laue-Langevin, Grenoble Cedex, France

Abstract.

Aim of this work is the study of the structural effects brought by the presence of GM1 ganglioside to a cholesterol-containing lipid membrane, and the eventual coupling Cholesterol-GM1. In fact, it is often claimed that GM1 and Cholesterol constitute a pair affecting the structural properties of their environment in membrane microdomains. We realized different supporting+floating bilayers made of Phospholipid, Cholesterol and GM1 in biosimilar mole ratio, by the Langmuir-Blodgett Langmuir-Schaefer technique, to be investigated by the neutron reflectivity technique. Two important conclusions are drawn. First, it is experimentally shown that the presence of GM1forces asymmetry in Cholesterol distribution, opposite to what happens for a GM1-free membrane, submitted to a similar procedure, resulting in a full symmetrisation of Cholesterol distribution. Second, and most interesting, it is suggested from experimental that a *preferential* asymmetric distribution of GM1 and Cholesterol is realized in a model membrane with biomimetic composition, revealing that a true *coupling* between the two molecules occurs.

Work in progress.

3.4.6. Structural effects brought by salts in ganglisode-containing complex model membranes

We tested the stability of a sample containing GD1a ganglioside. GD1a ganglioside is more charged than GM1, and so it is supposed to further induce three dimensional modifications to the floating membrane.

The sample has been prepared as follows:

- 2 layers of d_{85}DSPC.
- 3rd layer of d_{75}DPPC/Cholesterol 11/1.75 molar
- 4th layer of d_{75}DPPC/Cholesterol/Gd1a ganglioside 10/0.75/1 molar

In particular we wanted to study the structure and stability of the membrane in salt solutions. To this scope neutrons reflectivity measurements have been performed on two samples at 22°C in pure water and one also in a NaCl 156 mM solution while the other in a RbCl 156 mM solution.

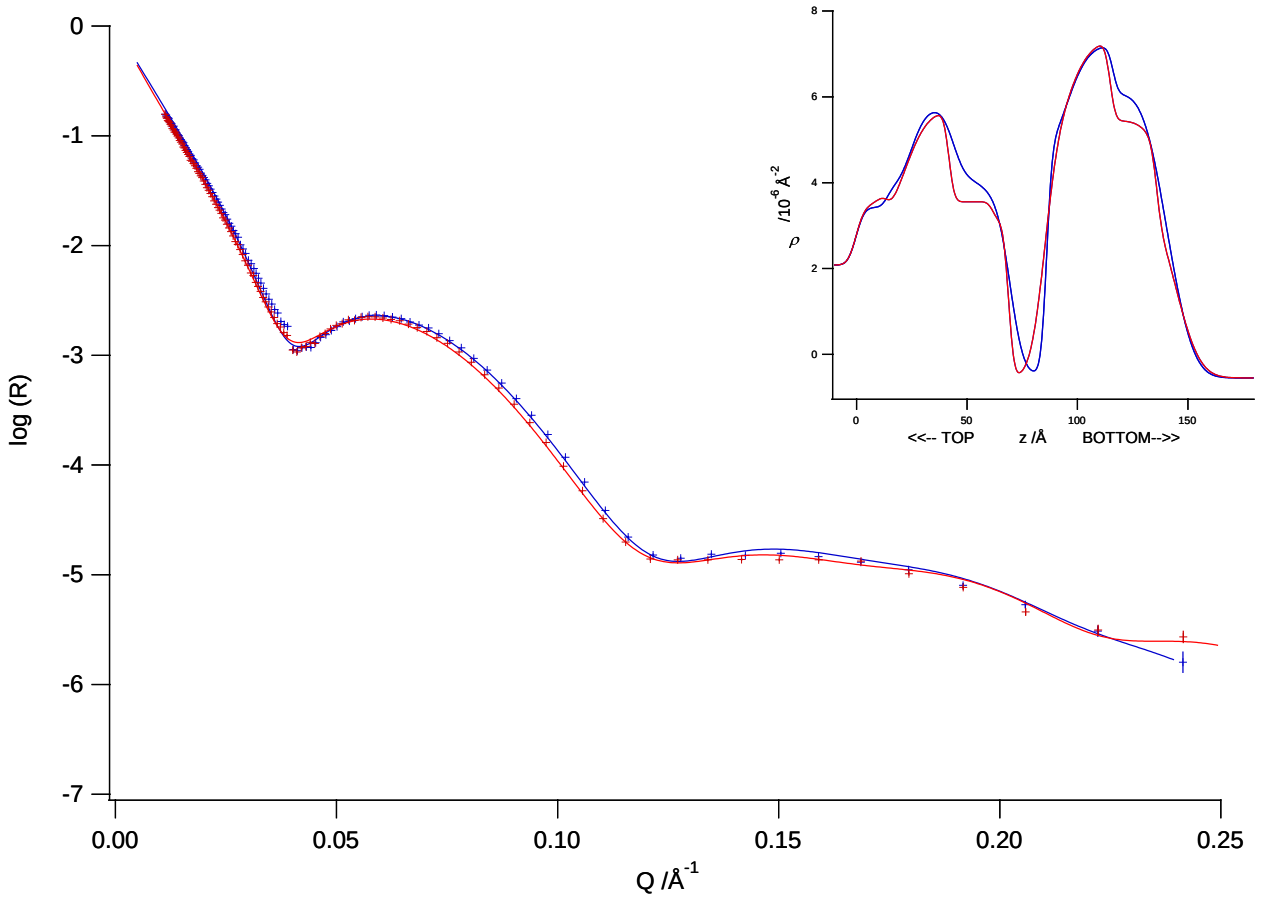

Figure 91: Neutron reflectivity spectra referred to the DPPC+cholesterol+GD1a sample at 22°C in H_2O (blue) and 156 mM NaCl solution (red). Crosses are experimental data, lines the fit. Insert shows the resulting SLD profiles obtained.

By adding NaCl we evidence a thickening of the floating membrane from 59 Å to 60 Å, and an increase in the solvent penetration from 9% to 15% in the hydrophobic chains.

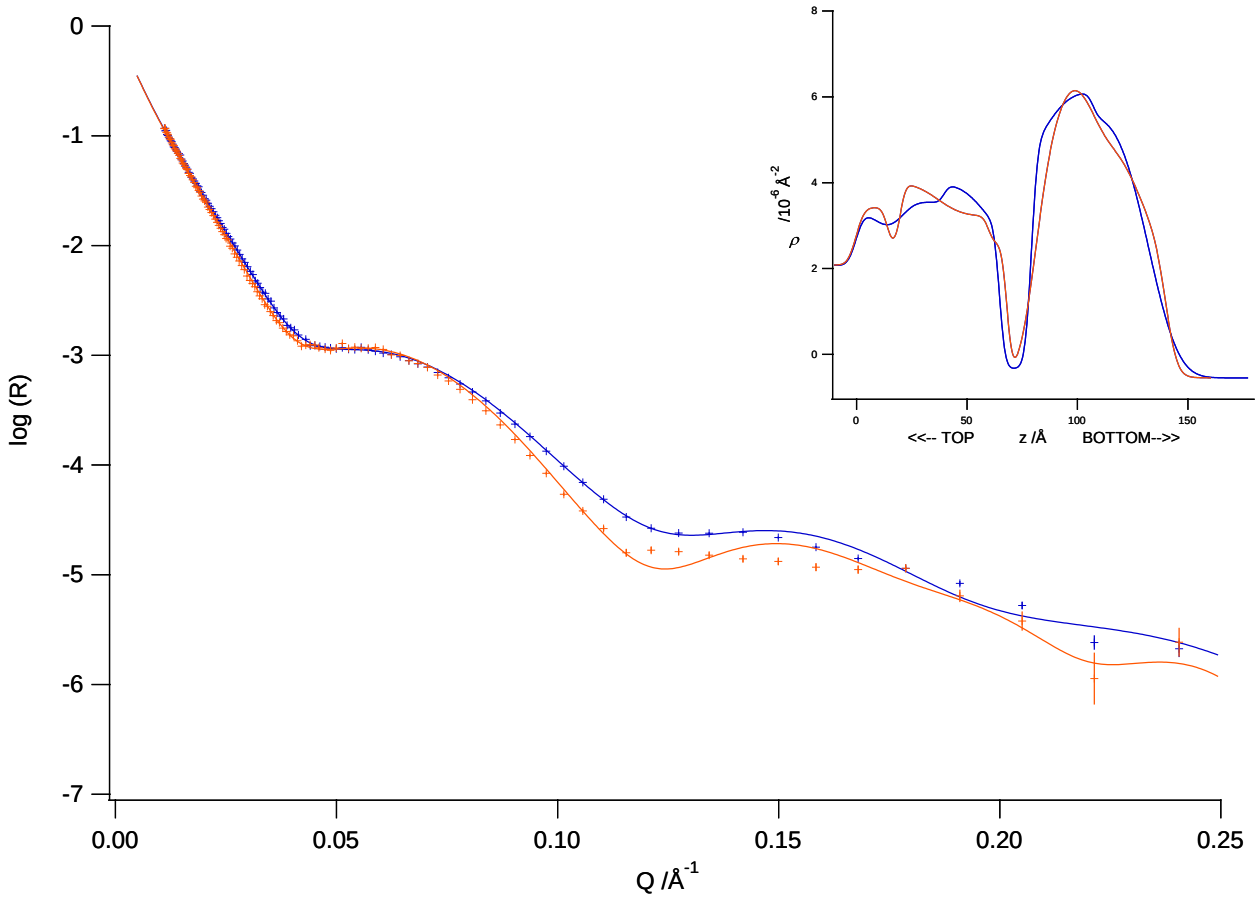

Figure 92: Neutron reflectivity spectra referred to the DPPC+cholesterol+GD1a sample at 22°C in H_2O (blue) and 156 mM RbCl solution (orange). Crosses are experimental data, lines the fit. Insert shows the resulting SLD profiles obtained.

Also RbCl salt acts on the membrane, and the changes brought are more evident: the membrane thickens from 59 Å to 61 Å, and the solvent penetration increases from 18% to 21% in chains volume.

Salts screen the electric charges of the glycolipid heads, slightly reducing the membrane compactness. However even in presence of salt the membranes keep their stability. This result is very important because it opens the way to the study of these model membranes in biosignificant solvents.

Once studied the main characteristics of biosimilar membranes and found the expected features in case of environmental modifications, we are interested in the study of the structural modifications brought by some surface event.

3.4.7. Structural effects brought by sialidase enzyme

About the action of sialidase, in the previous paragraphs we presented the results obtained about the consequent packing rearrangement occurring on the molecular scale , studied on curve aggregates by mean of X-Rays diffraction, and on the 'whole membrane scale' structural modifications brought to supported bilayers studied by X-rays reflectivity. We want now to study whether some structural phenomenon occurs inside the membrane, for example cholesterol redistribution, because of sialidase action, by mean of neutrons reflectivity on floating membranes.

The sample we built up to the study has been prepared as follows:

- 2 layers of d_{85}DSPC.
- 3rd layer of d_{75}DPPC/Cholesterol 11/1.75 molar
- 4th layer of d_{75}DPPC/Cholesterol/Gd1a ganglioside 10/0.75/1 molar

We performed the measures on this sample at 22°C, then in a NaCl 156 mM solution in water, and after the addiction of sialidase. In figure 98 the relative neutron reflectivity spectra are shown.

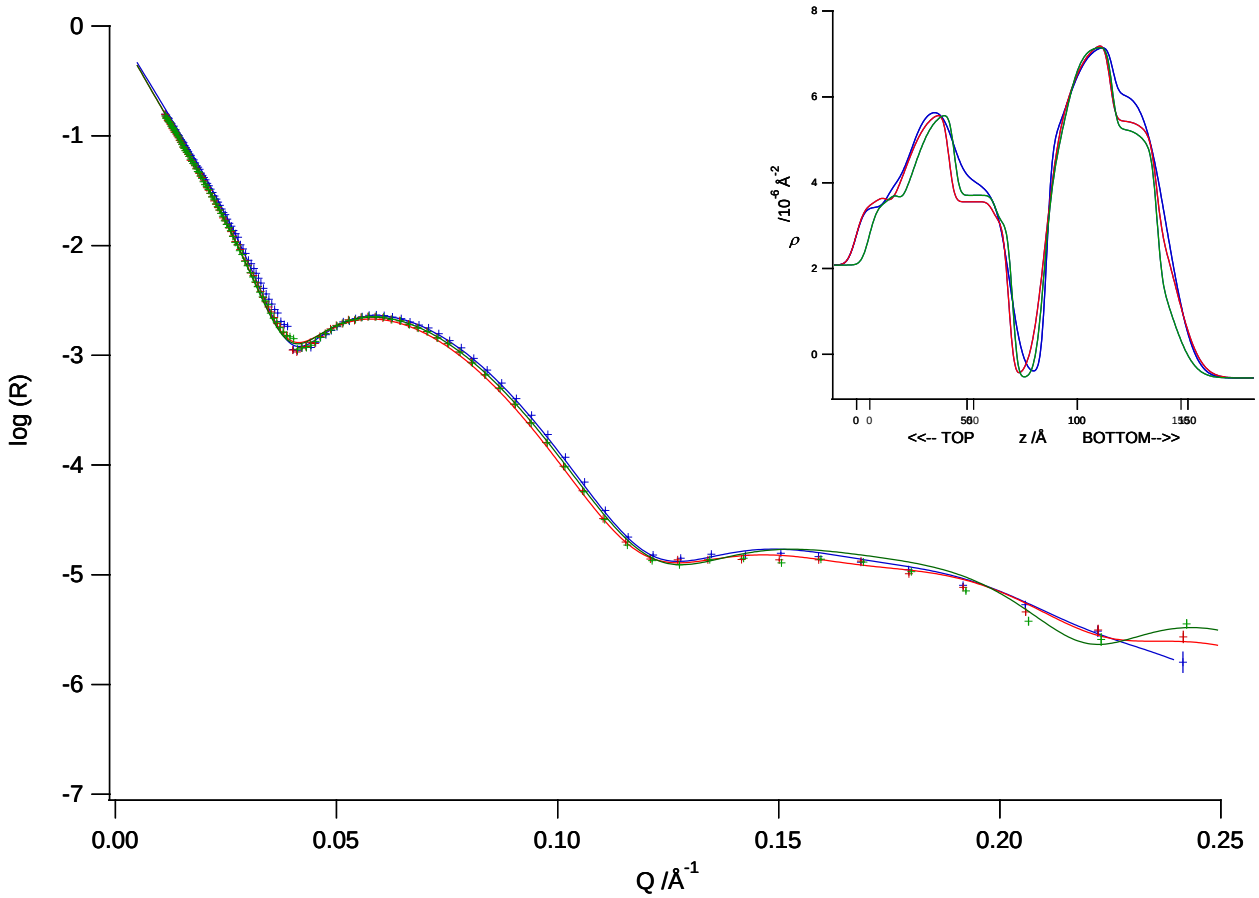

Figure 93: Neutron reflectivity spectra referred to a DPPC+cholesterol+GD1a sample at 22°C in H_2O (blue) and 156 mM NaCl solution (red), after the injection of sialidase (green). Crosses are experimental data, lines the fit. Insert shows the resulting SLD profiles obtained.

The supported bilayer is stable under all the conditions. No differences are evident from these data, being the spectrum referred to the sample after the action of the enzyme very similar to that of the sample in presence of NaCl. This means that no cholesterol migration occurs and no structural rearrangements, we are sensible to, occur. The differences we evidenced by X-Rays reflectivity measurements were in fact evident in the high-q region of the spectrum, not accessible to neutrons reflectivity, because of too low signal intensity.

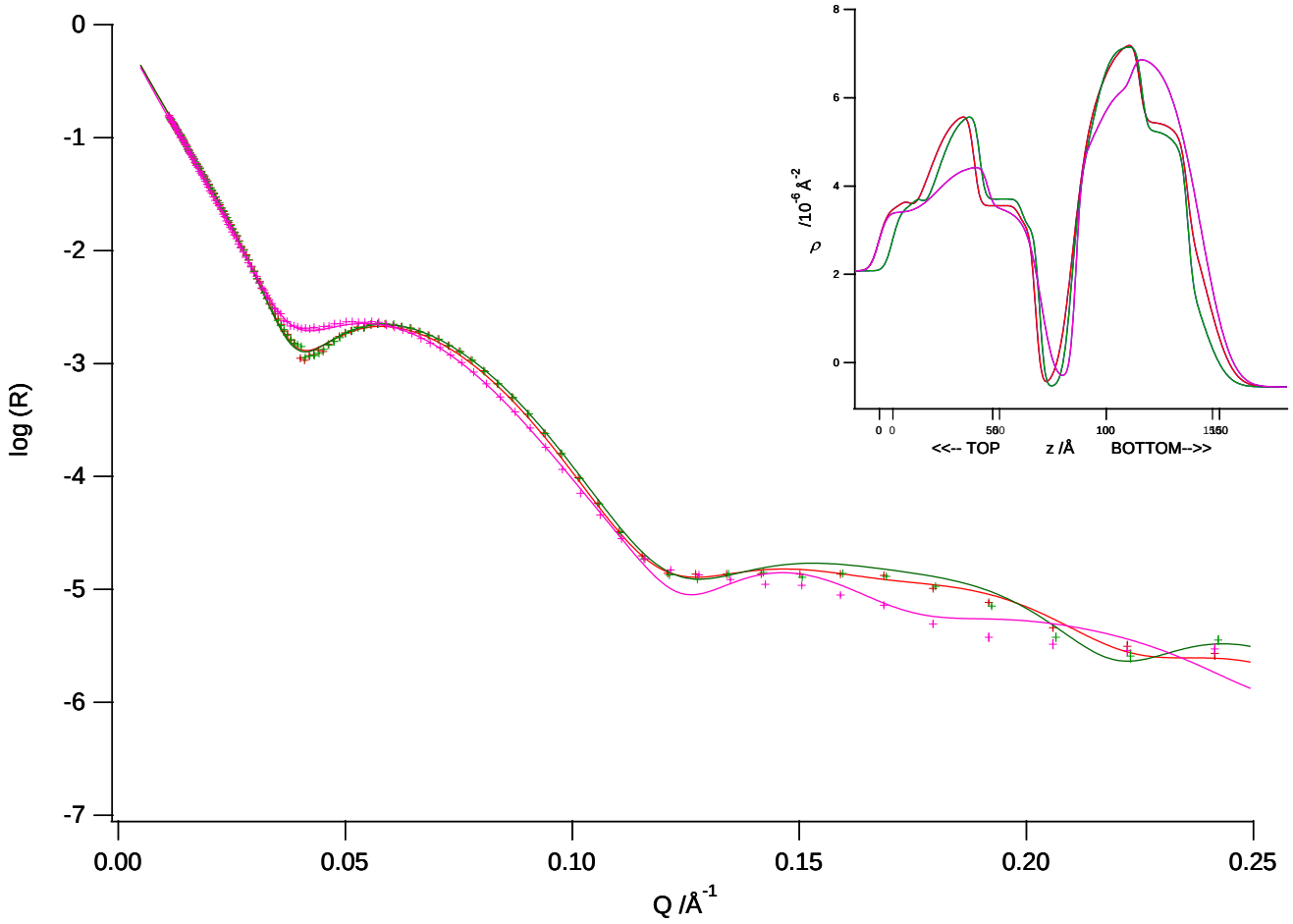

Figure 94: Neutron reflectivity spectra referred to a DPPC+cholesterol+GD1a sample in 156 mM NaCl solution (red), after the injection of sialidase (green) compared to a DPPC+cholesterol +GM1 one at in NaCl 156 mM solution (pink). T=22°C. Crosses are experimental data, lines the fit. Insert shows the resulting SLD profiles obtained.

This result does not mean that we are not sensible to the difference between membranes containing GM1 or GD1a gangliosides: in figure 94 it is possible to compare the systems and is evident that they are very different.

We finally performed X-rays reflectivity measurements from a floating membrane containing cholesterol and GD1a ganglioside to study whether we could obtain complementary information.

As before, over a DSPC membrane adhering to the silicon block, we deposited the membrane we are interested in. The final asymmetric (cholesterol and ganglioside) sample was made in this way:

- 2 layers of DSPC
- 3rd layer of DPPC/Cholesterol 11/1.75 molar
- 2nd layer of DPPC/Cholesterol/Gd1a 10/0.75/1 molar

After measuring the membrane in water at 22°C, we changed the solvent from pure water to a 150mM NaCl solution, and finally we added the sialidase enzyme.

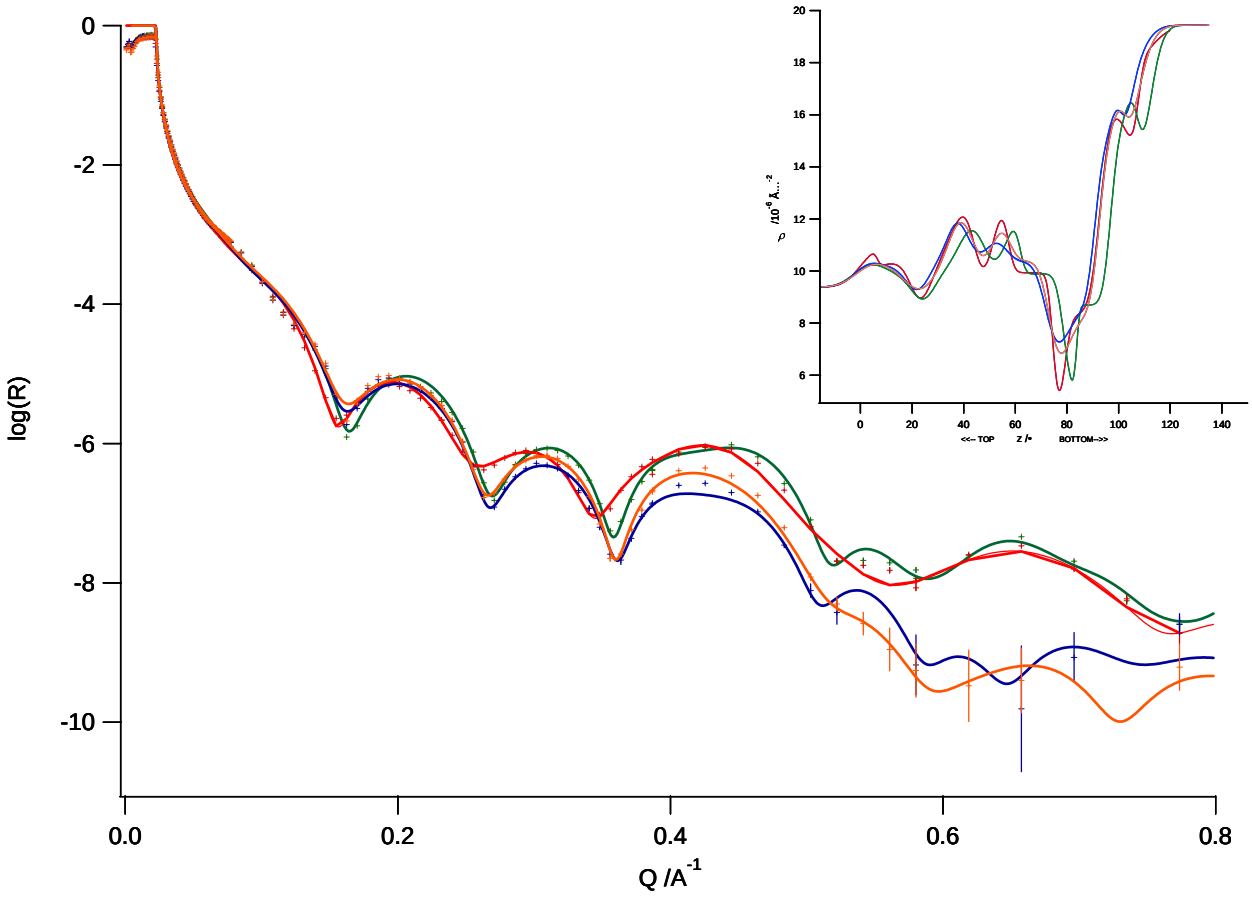

Figure 95: X-ray reflectivity from a floating bilayer containing cholesterol and GD1a at 22°C in water (green), NaCl 156 mM (red) and after the action of sialidase (blue and orange after 1 h). Crosses are the experimental points, lines the fit.

The presence of NaCl (red spectrum in Figure 95) 'destabilizes' the membrane changing the interactions among the charged heads, while the membrane seems to recover a new equilibrium by the action of sialidase. Different spectra refers to different samples, meaning that we are sensible to the differences we want to study. The enzyme action is visible also from the change in the SLD profile of the external heads (at z=0) in figure 95.

Unfortunately with this technique we are still not able to separate, in the SLD profiles, the contributes of water, cholesterol and lipid chains.

We built up another equal sample to see whether the measure was reproducible, but there was a bubble in the cell, so we may did not have a 100% coverage of the silicon block.

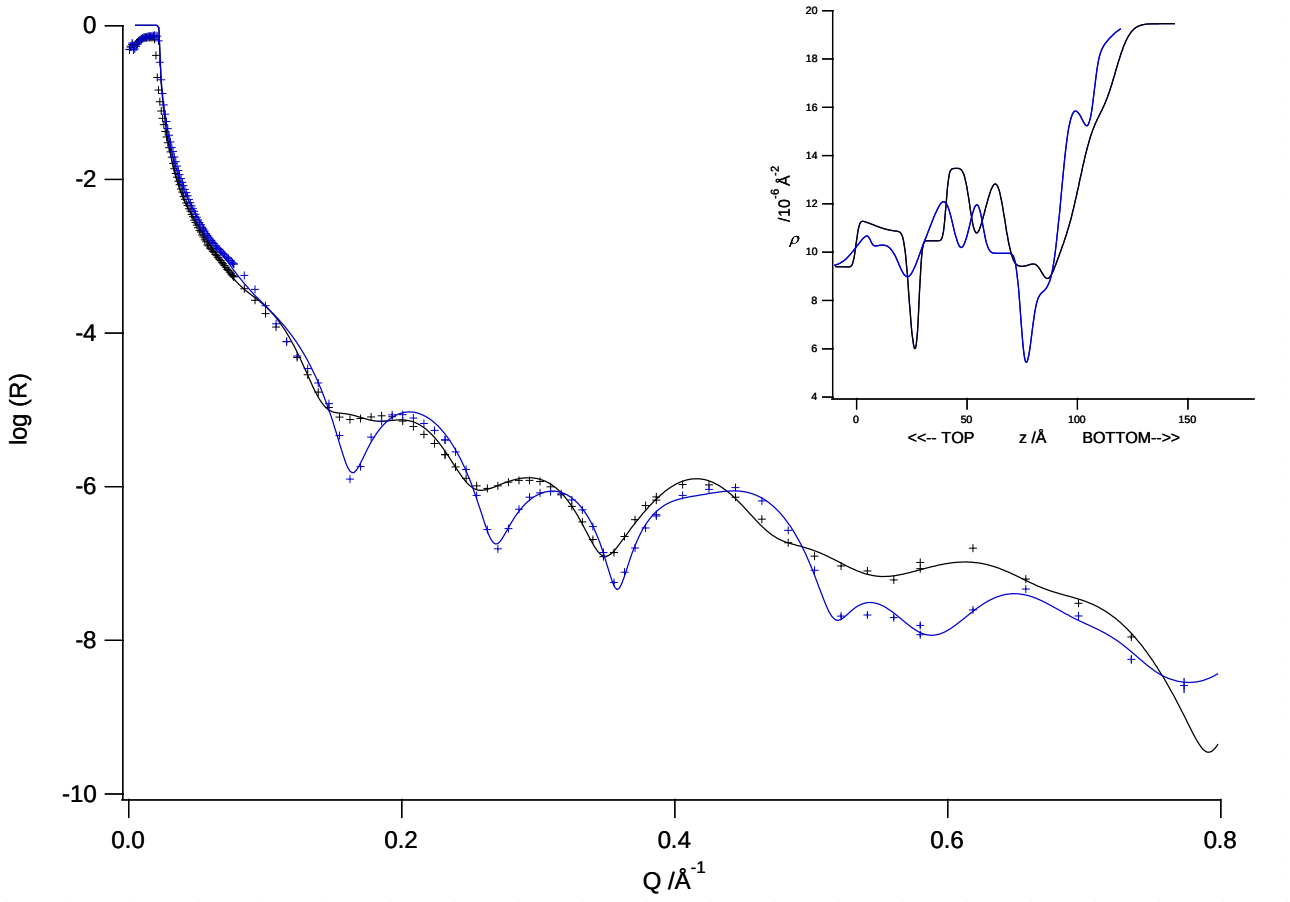

Figure 96: X-rays reflectivity from two floating membrane containing Gd1a ganglioside and cholesterol. The black one is not a good sample.

PERSPECTIVES

Many interesting results have been obtained and are presented in this work, and a lot of other possibilities can be explored, both from the technical point of view and from the phenomena investigated.

In this section some initial results are presented about technical improvements to develop the study of the morphology on the plane of membranes, surfaces characterization and samples preparation optimization, very interesting phenomena involving surfaces interactions.

Reflectivity from monolayers

Langmuir monolayers are an excellent model system for the investigation of interfaces between amphiphilic organic molecules and aqueous compartments, and are important as an intermediate step for the fabrication of model membranes. Neutron reflection experiments have been performed to establish the structure of monolayers formed at the air/water interface by two phospholipids, distearoylphosphatidylcholine (DSPC) and dipalmitoylphosphatidylcholine (DPPC), alone and mixed with cholesterol, at various surface pressures. Our aim was to build up Langmuir phospholipid-cholesterol mix monolayers and to study their behavior at various pressures.

Fully deuterated phospholipids were used (d_{75}-DPPC and d_{83}-DSPC from Avanti Polar Lipids Co.) to maximize the visibility of cholesterol. Cholesterol was purchased from Sigma-Aldrich Co.. For reflectivity measurements the contrast solutions were H_2O, D_2O and ZMW (Zero Matched Water, a mixture of 0.08 D_2O and 0.92 H_2O volume fractions with the same scattering length density of air, which is zero).

We performed neutron reflectivity measurements at the air- water interface of Langmuir monolayers to study whether we could obtain information about the cholesterol disposition inside the lipid chains. In fact DPPC chains length is comparable to cholesterol length, while DSPC chains are longer. We performed pressure to area isotherms also on d_{83}-DSPC and a d_{83}-DSPC:cholesterol 10:1.75 molar mixture to study eventual different phase behaviours.

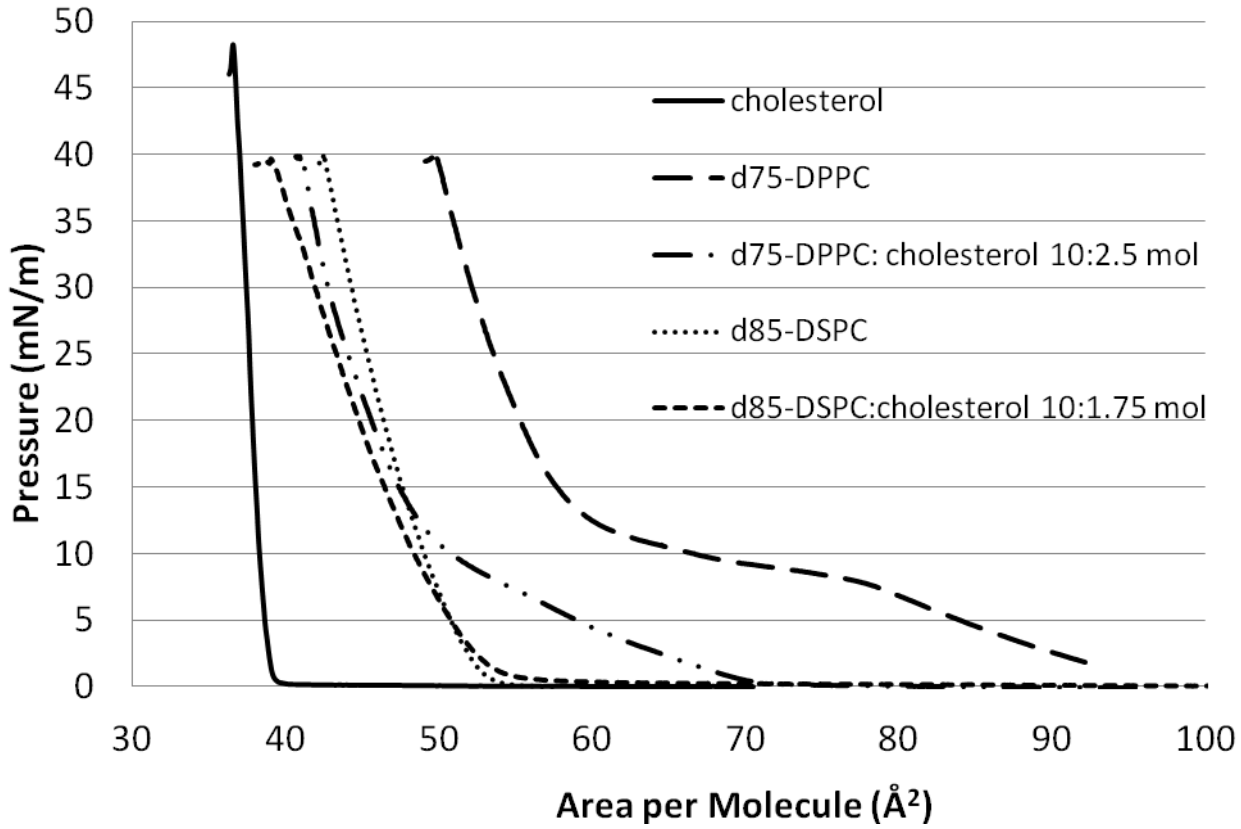

Figure 97: Pressure-area isotherms of various mixtures of d_{75}-DPPC, d_{85}-DSPC and cholesterol at 18°C. The subphase is water.

Neutron reflectivity measurements have been performed at the pressures of 14mN/m, 40mN/m, and back to 14mN/m opening back the barriers to verify if cholesterol protruded from lipid chains while compressing.

Reflectivity measurements were performed on the FIGARO [Wacklin et al. (2010)] reflectometer at ILL, Grenoble, France. Measurements were performed at 22°C.

Data were analyzed using the software Motofit, allowing simultaneous fit of data sets referred to the same sample in different contrast conditions, using the SLDs reported in table 5.

Table 13: properties of materials used

Material	SLD (10^{-6}Å^{-2})
air	0
H_2O	-0.56
D_2O	6.36
cholesterol	0.22
lipid D-heads	5.70
lipid D-chains gel phase	7.66
lipid D-chains fluid phase	6.13

An example of simultaneous fit is shown in figure 98 and fit results are reported in table 6.

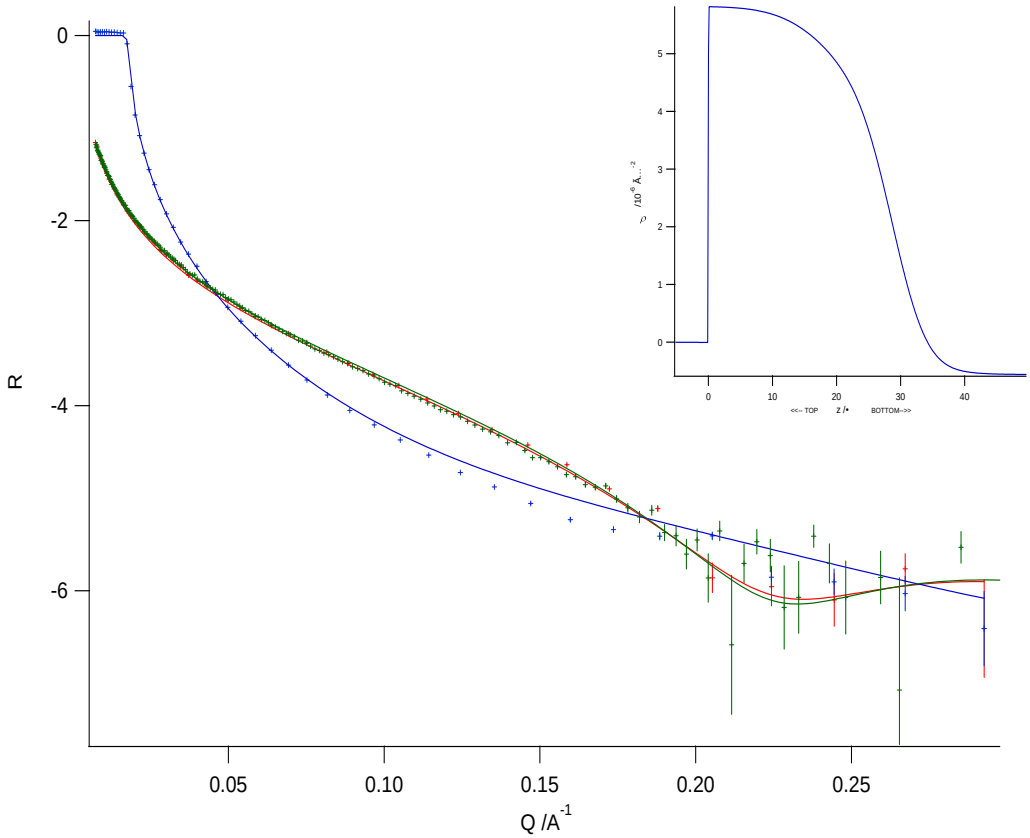

Figure 98: Simultaneous fit (lines) of a d_{75}-DPPC-cholesterol monolayer at the air-water interface at 40mN/m pressure at 22°C in different solvents. Dots are the experimental points. Blue: the solvent is D2O; Green: the solvent is H2O; Red: the solvent is ZMW. In the insert the SLD profile is shown.

Table 14: parameters obtained fitting the neutron reflectivity data.

		CHAINS				HEADS				
	P (mN/m)	*THICK (±1 Å)*	*SLD (10^{-6} Å^{-2})*	*SOLV. P. (±5 %vol)*	*ROUGH (±2 Å)*	*THICK (±1 Å)*	*SLD (10^{-6} Å^{-2})*	*SOLV. P. (±5 %vol)*	*ROUGH (±2 Å)*	*ROUGH HEADS-WATER*
D_{75}DPPC	40	16	7.66	0	0	9	5.70	0	5	5
D_{75}DPPC-chol 11-2.5	14	17	6.3	23	5	9	5.70	5	0	0
	40	20	6.3	0	0	9	5.70	40	8	3
	14	16	6.3	0	2	9	5.70	30	0	8
D_{85}DSPC	14	16	7.66	2	0	9	5.70	9	1	4
	40	18	7.66	1	0	9	5.70	8	6	4
	14	16	7.66	0	0	9	5.70	5	0	6
D_{85}DSPC-chol 11-2.5	14	19	6.3	1	0	9	5.70	31	0	7
	40	22	6.3	0	2	9	5.70	35	4	5
	14	19	6.3	0	0	9	5.70	20	5	0

Unfortunately we don't have the measurements referred to the DPPC-d_{75} at 14mN/m, but information can be obtained by the other measurements performed.

Interaction of MENS with a complex biomimetic membrane

Gene therapy, the genetic modification of cells for therapeutic benefits, is one of the most promising approaches for the treatment of genetic diseases and cancer. It requires exogenous genes to be delivered to target cells and to reach endogenous DNA within the nucleus, after crossing the different cell membranes without being addressed to the lysosomial degradation pathway. DNA-phospholipids complexes (MC), are very promising vectors, due to their safety, ease of preparation and lack of immunogenicity [Koynova R. et al., (2006)]. The most critical obstacle to the clinical application of MCs is their low transfection efficiency (the amount of exogenous DNA transferred into cells followed by gene expression). Recently, a variant of MC has also been proposed, namely Multicomponent Envelope-type Nanoparticle System (MENS) [G. Caracciolo (2007)]. In MENS, a plasmid DNA core is condensed with protamine sulfate. Such a core is complexed with highly-fusogenic multicomponent liposomes (M) that have intrinsic endosomal rupture properties. Supported bilayers are the right system to study the eventual interaction between lipoplexes and model membranes.

We built up a floating membrane as follows:

- 2 layers of d_{85}DSPC.
- 3rd layer of d_{75}DPPC/Cholesterol 11/1.75 molar
- 4th layer of d_{75}DPPC/Cholesterol/Gd1a ganglioside 10/0.75/1 molar

And we injected directly in the cell 50 μl of MENS solution 1mg/ml.

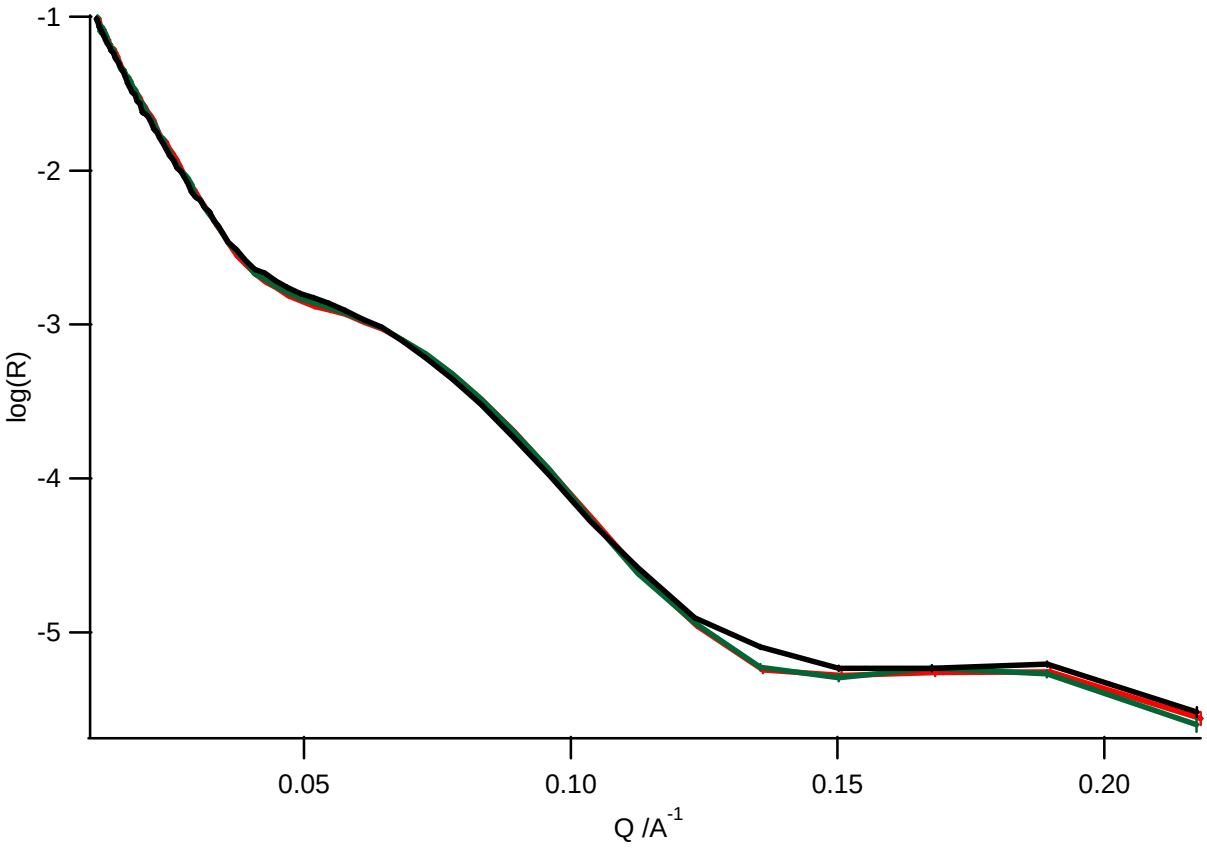

Figure 99: Neutron reflectivity from a floating membrane with an asymmetric content of both cholesterol and GD1a ganglioside. Spectra refer to the system before(black) and after(red) the incubation of MENS. Green spectrum refers to the system after solvent exchange. T=22°C, the solvent is H2O.

The little variations observed in the spectra referred to the system before (black spectrum in figure 99) and after the injection of MENS could be due to a minimal monomeric exchange between the membrane and the MENS, but it is clear that no relevant phenomena implying DNA membrane crossing or MENS interaction with the prepared model membrane happen.

The same experiment has been performed on FIGARO beamline, on a supported asymmetric bilayer composed by DSPC-d_{85}, cholesterol and GM1. In fact MENS hare big

heavy aggregates and, being on D17 beamline the sample in vertical position, while on FIGARO it is kept horizontal, we wanted to be sure that the molecules did not precipitate without interacting with the membrane. Also in this case non structural changes occur in the membrane (figure 100).

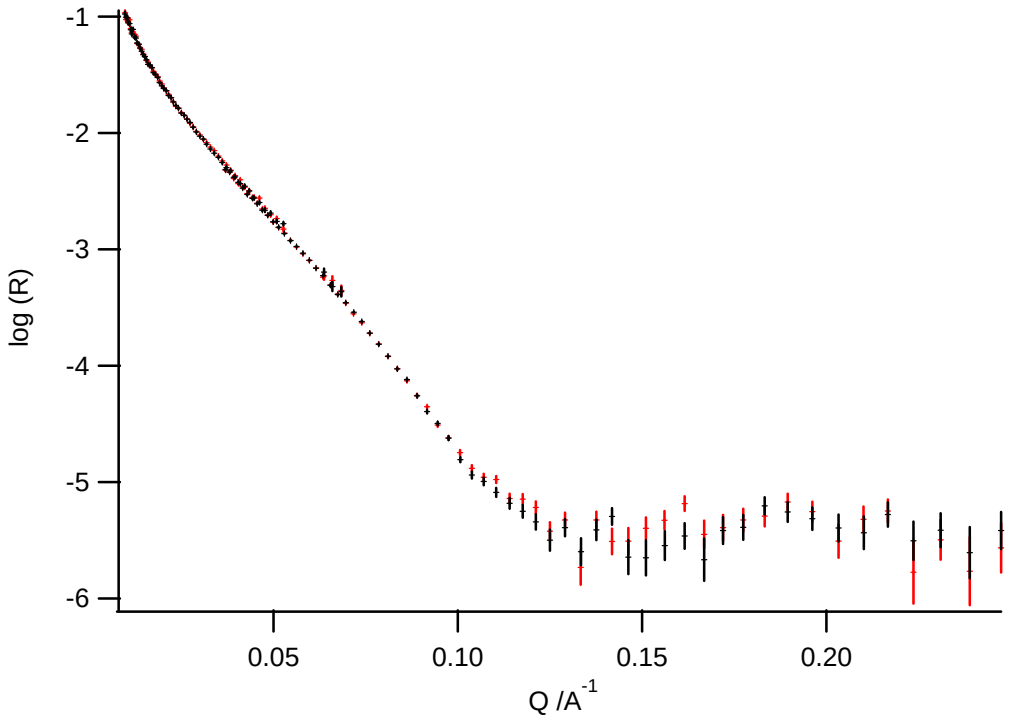

Figure 100: Neutron reflectivity spectra from a supported bilayer containing cholesterol and GM1 before (black) and after (red) the injection of MENS. The system are indistinguishable.

Morphological study of complex biomimetic membrane

By radiation reflectivity we access the internal structure of the deposited membranes, but also the study of their surface could bring interesting information. Many surface imaging techniques could be applied to the study of complicated systems built up over large areas from atomic force microscopy (AFM) to fluorescence microscopy, but also the off-specular signal we have in a reflectivity experiment could be studied and gives interesting information about the topology of the membrane surface. We intend, in the future, to apply AFM to the study of such complex membranes and we are opening the way for new forefront studies. In fact we build up and we are now optimizing a cell for AFM in liquid studies on floating membranes (figure 101).

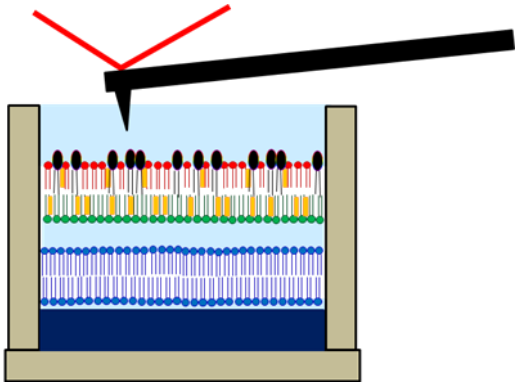

Figure 101: Schematic view of the cell we built up to do AFM measures on floating membranes in liquid.

The difficulties we have faced are many. First the fact that we are dealing with a very delicate system. Second we had to prepare the sample ‘closing’ it in a cell to transport it to the Microscopy lab, far away from the chemistry lab, and then to turn it over for the measure (We remember that to deposit the fourth layer the Langmuir-Schaefer technique is used, consisting in ‘closing’ the turned block over the deposited and compressed surface). Finally we needed a layer of water over the membrane, but maximum 2mm thick not to wet the electronic components of the AFM tip.

The cell is realized and liquid AFM studies on floating membranes are planned for the next year.

CONCLUSIONS

We focused on the study of the surface structuring of biomimetic membranes in connection to the presence and disposition of components and as a result of their interactions, side-to-side, back-to-back and with the external world. Moreover, their interplay gives rise to a dynamic response of the structure of a membrane, induced by interactions taking place at its surface.

To access these fine structures and dynamics, we started from simple models with controlled composition and environmental conditions. Model systems of different geometries were chosen, where a membrane patch is embedded with different constraints, in order to enhance different properties, so giving peculiar information.

1) **Micelles and Vesicles**

We started our study from model membranes constituted by lipid micelles and vesicles in water solution. We focused on asymmetry, an aspect found in natural membranes, where gangliosides reside only in the external layer.

We built up an asymmetric model membrane by incubating GM1 and GD1a gangliosides micelles on preformed DMPC vesicles, in the proportion 10:1 lipid:ganglioside. In few-hours times and via monomer exchange, ganglioside molecules enter the phospholipid vesicles and, being the flip-flop process prevented by their huge hydrophilic headgroup, they remain confined into the outer layer of the vesicle. Together with phospholipid and ganglioside, we added cholesterol, alternatively premixed with the preformed micelle or with the preformed vesicle in different proportions. We tested 10:1:1 lipid:cholesterol:ganglioside molar proportion systems and 10:0.5:0.5 lipid:cholesterol:ganglioside systems. We studied the structure of the resulting systems by the Small Angle X-ray Scattering (SAXS) technique.

Cholesterol affects the structure of both the micelles, modifying their shape and their structuring in the solvent, and the final aggregates were found to be different if cholesterol was in the starting micelles or in the starting vesicles.

Moreover, thanks to the slow exchange process and to the fast and powerful technique, we have been able to follow on the way the structural rearrangement due to gangliosides entry in DMPC vesicles.

The typical mixing times have been extracted and ***while the typical times referred to the incubation of GM1 and Gd1a micelles in DMPC are very similar, around 6***

hours, the process takes longer in case of mix between DMPC and micelles of GM1:Gd1a 1:1 molar.

Furthermore cholesterol has been found to fasten the incubation process, the more if originally embedded in the ganglioside micelles.

An exception is the mixing of (DMPC vesicle) : (cholesterol+GM1 micelle) solutions in molar proportion 10:0.5, taking longer than in absence of cholesterol.

Then we observed the structural changes induced in model aggregates, pure or mixed micelles or vesicles containing ganglioside GD1a, following the action of the enzyme sialidase.

Sialidase detaches the external sialic acid from GD1a sugar head, turning it into GM1. We applied Small-Angle X-ray and Neutron scattering techniques to follow the time evolution of the aggregate structures while chemically undergoing the enzymatic action. ***We found that the aggregates could be either very stable,*** in single component micellar systems such as GD1a micelles, ***or structurally responsive***, in mixed model systems, as GD1a+C_{12}PC and GD1a+DMPC. Moreover, while in progress, ***the sialidase–ganglioside interaction seems to define a time lag where the system is structurally off the smooth route between the initial and the final states***.

2) **Extended single membranes deposited on a macroscopic support.**

In the last few years a considerable effort has been put in developing protocols to prepare model systems that, although still extremely simple to allow for structural studies, could reproduce some clue features of natural ones. One of them is asymmetry.

Asymmetric model membranes are rare, due to the difficulty of realizing hydrated artificial membranes with well defined heterogeneous composition and applicable for non-average structural investigation. Reflectivity technique is currently being developed to respond to this challenge. In collaboration with the Institut Laue-Langevin (ILL) in Grenoble, ***we developed and tested an experimental model bearing forced membrane asymmetry in a macroscopic single bilayer, to be investigated by X-ray and neutron reflectivity.*** The sample preparation protocol involves the ‘Langmuir-Blodgett film deposition’ technique to build asymmetric floating single or double bilayers. The LB-technique is one of the most promising techniques for preparing thin films as it enables the precise control of the monolayer thickness, homogeneous deposition of the monolayer over large areas and the possibility to make multilayer structures with varying

composition of the layers. ***The sample preparation takes at least 4 hours and enables the preparation of 2500mm^2 big membranes***.

Then, the Angstrom scale of X-rays and neutrons accessibility is able to scan the membrane in the cross direction and describe its structural properties. The incoming beam crosses the membrane as a stack of semireflecting mirrors: the water layers, the polar heads, the hydrophobic chains. Due to the different composition and thickness of the layers, the intensity reflected or diffracted by each of them is different. The measured intensity spectrum is the sum of the radiation waves diffracted from each layer of the sample. ***The technique, then, gives information about the transverse structure of the sample, layer by layer: thickness, composition, compactness, surface roughness***.

Before starting our studies on single or double model membranes, we studied monolayers on water surface.

Pure lipids or lipid mixtures were spread on a water surface, where they float, headgroups dipped in, to form a film. We compressed the film until its compression limit, meanwhile performing isotherm measurements in the form of surface pressure (mN/m) versus area per lipid molecule (A^2/molecule). This technique provides information about the phase behaviour of each monolayer as a function of its packing density. First, we verified the effect brought about by addition of cholesterol to DPPC, by recording the (π-A) curves of the mixed Langmuir monolayers at the air-water interface as a function of different molar ratios between DPPC-d$_{75}$ and cholesterol. Progressive addition of cholesterol to DPPC-d$_{75}$ results in progressively decreasing the occupied area per average molecule. ***We assessed that for all of the investigated mixed systems, at a given pressure, the measured area per molecule is lower than expected for ideal mixing***. In fact, the effect of cholesterol is to rigidify and order the lipid chains, with a consequent reduction of the occupied area per average molecule at the air-water interface. Moreover, ***by surface study we could establish the optimal conditions to deposit the layers, in order to have compact and stable samples to be investigated by reflectivity.*** We performed in fact neutron reflectivity studies on various mixed systems at the air-water interface, at different pressures.

X-rays and neutrons reflectivity measurements were performed on single and double bilayers systems to get the main structural properties of model membranes formed by DPPC, cholesterol and gangliosides.

The molar ratio lipid: ganglioside: cholesterol was the biosimilar 10:1:2.5. The use of fully deuterated (D-isotope) phospholipids makes the lipid matrix 'transparent' for neutrons, exalting the contrast profile of cholesterol and gangliosides, while X-rays reflectivity experiments have been carried on normal (H-isotope) lipid membranes and are more sensible to gangliosides polar heads.

We started our studied by investigating the characteristics of single supported membranes, mainly by X-rays reflectivity. By the reconstruction of the contrast profile the known characteristics of a lipid membrane such as the variation of the thickness at various temperatures have be addressed.

Comparing the spectra referred to DPPC and DPPC-d_{75}we observed that the fully deuterated DPPC membrane is 1 Å thicker than the DPPC one (54 Å versus 53 Å), but all the other characteristics are unchanged. Moreover we observed that while the presence of cholesterol thickens the membrane, gangliosides do not.

We studied the effects brought by the presence of the sialidase enzyme on model membranes composed by DPPC, cholesterol and gangliosides. Sialidase action results in an increase of the bilayers thickness both in GD1a and GM1 containing membranes. From the spectra comparison presented we see that big differences have been found among different samples, but by X-rays we are not sensible to the exact content of water and to the transverse position of cholesterol.

By neutrons reflectivity we first verified to find the same characteristics observed by X-rays reflectivity and then we studied the interaction between a B peptide and a GM1-containing membrane. We observed that, as predicted, the peptide distributes over the membrane surface, in the gaps of the polar heads of the lipids, without penetrating the membrane.

The most complex studies we could perform have been carried on membranes free to fluctuate over a water layer, in a solvent. Also in this case we verified the main characteristics expected to be found about membranes, and the stability of the system. Experiments suggest new guidelines for protocols to be used with asymmetric samples, both for lipid redistribution and for macroscopic bilayer integrity. We carried the measurements both in water and in physiological 156 mM salt (NaCl, RbCl) solution. ***Salts act in slightly increasing the membrane thickness but do not destabilize it***, opening the way to the study of membranes in biosignificant solvents.

We realized a double bilayers system useful to the study of single lipid migration between two membranes.

We studied the effects brought by the action of sialidase enzyme on floating membranes and we observe that no cholesterol migration is caused by it, and the membrane is not finally destabilized by its action.

We found that ***in an originally asymmetric only-DPPC-cholesterol membrane***, submitted to annealing, ***cholesterol migrates between layers, assuming a symmetric disposition in the two leaflets of the membrane.***

On the contrary, ***in a DPPC-(one-side-GM1)-cholesterol membrane, redistribution results in a preferred asymmetric disposition of cholesterol***: the majority resides in the ganglioside-free leaflet, and the minority (about 20%) in the ganglioside-rich leaflet. ***The same preferred distribution of cholesterol is realized whatever the initial distribution of cholesterol and the modality of GM1 insertion,*** either spread with the film during the deposition procedure or incubated onto an existing DPPC+cholesterol symmetric membrane. ***This is an important finding, as ganglioside-cholesterol structural coupling has been widely indicated to be determinant for membrane GEMs structure, but never experimentally confirmed before.***

Actually this experimental proof was made possible thanks to the cutting-edge neutron reflection technique applied to the asymmetric LB deposition protocol, newly developed in this thesis work. This combination of techniques is extremely promising, as it gives the opportunity to create biologically interesting model membranes with distinctive features such as asymmetry, and allow a fine study of their internal structure through a unique detailed insight on the nanometric scale.

REFERENCES

Anianssonn E., Wall S., Algren N., Hoffmann H., Kielmann I., Hulbricht W., Zana R., Lang J. and Tondre C. (1976) J. Phys. Chem. 80,905.

Aragon S., Pecora R. (1977) J. Chem. Phys. 66.

Aragon S., Pecora R. (1982) J. Coll. Int. Sci. 89/1,170.

Bach D., Miller I. R., and Sela B.-A.. 1982. Calorimetric studies on various gangliosides and ganglioside-lipid interactions. Biochim. Biophys. Acta. 686:233–239.

Basu A., Glew R. H.. 1985. Characterization of the activation of rat liver b-glucosidase by sialosylgangliotetraosylceramide. J. Biol. Chem. 260:13067–13073.

Baumgart T., Hess S.T., Webb W.W., 2003. Imaging coexisting fluid domains in biomembrane models coupling curvature and line tension. Nature 425, 821–824.

Berne B.J., Pecora R. (1975) Dynamic Light Scattering, Wiley.

Blodgett K B, Langmuir I 1937 Built-Up Films of Barium Stearate and Their Optical Properties *Phys. Rev* 51, 964-982.

Blodgett K.B.. Films built by depositing successive monomolecular layers on a solid surface. *Journal of the American Chemical Society*, 57 :1007–1022, 1935.

Boretta M, Cantù L, Corti M, Del Favero E., 1997 , Cubic phases of gangliosides in water: Possible role of the conformational bistability of the headgroup, Physica A 236: 162-176.

Born M, Wolf E 1959 Principles of Optics *Pergamon Press Ltd, London.*

Bradshaw J., Phase behavior of dmpc free supported bilayer studied by neutron reflectivity. *Langmuir*, 18 :8161–8171, 2002b.

Brocca P, Cantù L, Corti M, Del Favero E, Motta S, 2004, Shape Fluctuations of Large Unilamellar Vesicles Observed by Laser Light Scattering: Influence of the Small-Scale

Structure *Langmuir* 20(6) 2141-2148.

Brochard F., Lennon J.F. (1975) J. Phys. France 36, 1035.

Brown D.A, London E., 2000. Structure and function of sphingolipid- and cholesterol-rich membrane rafts. J. Biol. Chem. 275, 17221–17224.

Cantù L., Corti M., Del Favero E., Muller E., Raudino A., and Sonnino S. 1999.

Cantù L., Corti M. and Degiorgio V. (1987) Faraday Discuss. Chem. Soc. 83,287

Cantù L., Corti M., Musolino M. and Salina P. (1990) Europhys. Lett. 136,561.

Cantù L., Corti M. and Degiorgio V. (1990) J. Phys. Chem. 94,793.

Cantù L., et al., Structural aspects of ganglioside-containing membranes, Biochim. Biophys. Acta (2008).

Cantù L., Corti M., Lago P., Musolino M. (1991) SPIE 1430,144.

Cantù L., Corti M., Degiorgio V., Piazza R. and Rennie A. (1988) Progr. Coll. Pol. Sci. 761,216.

Cantù L., Mauri M., Musolino M., Tomatis S., Corti M. (1993) Progr. Coll. Polym. Sci. 93,30.

Cantù, L., Corti M., Del Favero E., Raudino, A., 2000. Tightly packed lipid lamellae with large conformational flexibility in the interfacial region may exhibit multiple periodicity in their repeat distance. A theoretical analysis and X-ray verification. Langmuir 16, 8903–8911.

Cantù L., Corti M., DelFavero E., 1997a. Selfaggregation of glyco-lipids in water: vesicle to micelle transition. J. Mol. Liq. 71, 151–161.

Cantu L., Corti M., DelFavero E., Raudino A., 1997b. Physical aspects of non-ideal mixing of amphiphilic molecules in solution: the interesting case of gangliosides. J. Phys.-

Condensed Matter 9, 5033–5055.

Caracciolo G., Marchini C., Pozzi D., Caminiti R., Amenitsch H., Montani M., and Amici A., Langmuir 23, 4498 (2007).

Cecchi C., Nichino D., Zampagni M., et al., 2009. A protective role for lipid raft cholesterol against amyloid-induced membrane damage in human neuroblas- toma cells. Biochim. Biophys. Acta 1788, 2204–2216.

Charitat T., Bellet-Amalric E., Fragneto G., Graner F.. Adsorbed and free lipid bilayers at the solid-liquid interface. *European Physical Journal B*, 8 :583–593, 1999.

Chiu S W, Jakobsson E, Mashl R J, Scott H L 2002 Cholesterol induced modifications in lipid bilayers: A simulation study *Biophys. J.*, 83, 1842-1853.

Clint J.H. (1975) J. Chem. Soc. 71,1327.

Corti M, Degiorgio V, Sonnino S, Ghidoni R, 1982 J, Pys Chem. 86, 2533-2537.

Degiorgio V. and Corti M. (Eds.), Physics of Amphiphiles: Micelles, Vesicles and Microemulsions, North Holland, Amsterdam.

Corti M. and Cantù L. (1990) Adv. Coll. Int. Sci. 32,151.

Corti M., Cantù L. (1996) in Nonmedical Applications of Liposomes, D.D. Lasic, Y. Barenholz (eds.), CRC Press, Boca Raton.

Corti M., Cantù L. and Salina P. (1991) Adv. Coll. Int. Sci. 36,153.

Corti M., Brocca P., Cantu L., Del Favero E., Motta S., Nodari M.C., 2006. Curved single-bilayers in the region of the anomalous swelling: effect of curvature and chain length. Colloids Surf. a-Physicochem. Eng. Aspects 291, 63–68.

Cubitt R , Fragneto G 2002 D17: The new reflectometer at the ILL *Applied Physics A* 74, S329-S331.

Daillant J., Bellet-Amalric E., Braslau A., Charitat T., Fragneto G., Graner F., Mora S., Rieutord F., et Stidder B.. Structure and fluctuations of a single floating lipid bilayer. *The Proceding of the National Academy of Sciences USA*, 102 : 11639–11644, 2005.

Daillant J. et A. (Eds.) Gibaud. *X-ray and Neutron Reflectivity, second edition*. Lecture Notes Phys. 770, Springer Verlag, Heidelberg, 2009.

De Bergevin F.. *X-ray and Neutron Reflectivity : Principles and Applications*, Springer, 2009.

Del Favero, E.Tesi di dottorato, 1998.

Deme B, Lay-Theng L, 1997 *J. Phys. Chem. B*, 101, 8250.

Devlin T. M., Membrane biologiche: Struttura e Generalità in Manuale di Biochimica con Aspetti Clinici, Liviana Università, Padova 1989.

Engel J.; Schwarz G. “Cooperative conformational transitions of linear biopolymers” Angew.Chem., Int. Ed. Engl. 1970, 9, 389.

Evans E.A., R. Waugh (1981) Biophys. J. 54, 495.

Fantini J., Barrantes F.J., 2009. Sphingolipid/cholesterol regulation of neurotransmitter receptor conformation and function. Biochim. Biophys. Acta 1788, 2345–2361.

Farago B., D. Richter, J.S. Huang, S.A. Safran, S.T. Milner, Phys. Rev. Lett. 65 (1990) 3348.

Faucon J., M. Mitov, P. Méléard, I. Bivas, P. Bothorel, J. Phys. France, 50 (1989) 2389.

Felgner P.L., E. Freire, Y. Barenholz, T.E. Thompson, Asymmetric incorporation of trisialoganglioside into dipalmitoylphosphatidylcholine vesicles, Biochemistry (1981) 2168–2172.

Ferraretto A., Pitto M., Palestini P., Masserini M., 1997. Lipid domains in the membrane: thermotropic properties of sphingomyelin vesicles containing GM1 ganglioside and

cholesterol. Biochemistry 36, 9232–9236.

Fragneto G, Charitat T, Graner F, Mecke K, Perino-Gallice , Bellet-Amalric 2001 A fluid floating bilayer *Europhys Lett* 53 (1) 100–106.

Fragneto G, Graner F, Charitat T, Dubos P, Bellet-Amalric E 2000 *Langmuir*, 16, 4581.

Fragneto G., Charitat T., Bellet-Amalric E., Cubitt R., et Graner F.. Swelling of phospholipid floating bilayers : the effect of chain length. *Langmuir*, 19 :7695– 7702, 2003.

Fromhertz P. (1991) Chem. Phys. Lett. 94,259.

Fujime S., K. Kubota (1985) Biophys. Chem. 23,1.

Gibaud A.. *X-ray and Neutron Reflectivity :Principles and Applications*, Springer, 2009.

Goldschmidt-Arzi M., Shimoni E., Sabanay H., Futerman A.H., Addadi L., 2011. Intracellular localization of organized lipid domains of C16- ceramide/cholesterol. J. Struct. Biol. 175, 21–30.

Gordon, Beales, Zhao, Blake, MacKintosh, Olmsted, Cates, Egelhaaf, Poon, ‘Lipid organization and the morphology of solid-like domains in phase-separating binary lipid membranes’, J. Phis. Condensed Matter, 2006.

Gradzielski M., D. Langevin, B. Farago (1996) Phys. Rev. E 53, 3900.

Greenwood Alexander I., Tristram-Nagle Stephanie, Nagle John F. 2006 Chemistry and physics of lipids, 143, 1-10.

Hakomori Sen-itiroh, Handa Kazuko, Iwabuchi Kazuhisa, Yamamura Soichiro and Prinetti Alessandro .New insights in glycosphingolipid function:“glycosignaling domain, a cell surface assembly of glycosphingolipids with signal transducer molecules,involved in cell adhesion coupled with signaling. Glycobiology vol. 8 no. 10 pp. xi–xix, 1998

Hayakawa Tomohiro and Hirai Mitsuhiro, ‘Bilayer structure of ganglioside/cholesterol

mixed system in the presence of Ca2+, J. Appl. Cryst. (2003). 36, 489-493.

Heinburg, ‘A model for the lipid pretransition: coupling of ripple formation with the chain-melting transition’, Biophysical J., 2000.

Helfrich W. (1973) Naturforsch 28,693.

Helfrich W. (1986) J. Phisique 47,321.

Helfrich W. (1990) Les Houches, Liquids at Interfaces, Elsevier Science Publishers B.V.

Hofsass C, Lindahl E, Edholm O 2003 Molecular dynamics simulations of phospholipid bilayers with cholesterol. *Biophys. J*., 84, 2192-2206.

Hughes A. V., Goldar A., Gestenberg M. C., Roser S. J., Bradshaw J. A hybrid sam phospholipid approach to fabricating a free supported lipid bilayer. *Physical Chemistry Chemical Physics*, 4 :2371–2378, 2002a.

Israelachvili J.N., Mitchell D.T. and Ninham B.W. (1976) J. Chem. Soc. Faraday Trans. II 72,1525.

Israelachvili J.N., Mitchell D.T. and Ninham B.W. (1977) Bioch.Biophys.Acta 470.

Israelachvili J.N., Marcelia S., Horn R.G. (1980) Quartely Reviews Biophys. 13,121.

Jain M.K., White 3rd H.B., 1977. Long-range order in biomembranes. Adv. Lipid Res. 15, 1–60.

Jorgensen K., Mouritsen O.G., 1995. Phase separation dynamics and lateral organi-zation of two-component lipid membranes. Biophys. J. 69, 942–954.

Kakio A., Nishimoto S., Yanagisawa K., Kozutsumi Y., Matsuzaki K., 2002. Interactions of amyloid beta-protein with various gangliosides in raft-like membranes: importance of GM1 ganglioside-bound form as an endogenous seed for Alzheimer amyloid. Biochemistry 41, 7385–7390.

Karnovsky M.J., Kleinfeld A.M., Hoover R.L., Klausner R.D., 1982. The concept of lipid domains in membranes. J. Cell Biol. 94, 1–6.

Knoll W., Schmidt G., Rotzer H., Henkel T., Pfeiffer W., Sackmann E., Mittler- Neher S., Spinke J., 1991. Lateral order in binary lipid alloys and its coupling to membrane functions. Chem. Phys. Lipids 57, 363–374.

Komura S. (1996) in M. Rosoff (ed.) Vesicles, Dekker, New York.

Koynova R. et al., Proc. Natl. Acad. Sci. USA 2006, 103, 14373-14378.

Kucerka, Nieh, Pencer, Harroun, Katsaras, 'The study of liposomes, lamellae and membranes using neutrons and X-rays', C. Opinion in Colloid S., 2007.

Langmuir L. The mecanism of surface phenomena of flotation. *Transactions of the Faraday Society*, 15 :62–74, 1920.

Lee A.G., Birdsall N.J., Metcalfe J.C., Toon P.A., Warren, G.B., 1974. Clusters in lipid bilayers and the interpretation of thermal effects in biological membranes. Bio- chemistry 13, 3699–3705.

Lipowsky R., Richter D., Kremer Eds K.., The Structure and Conformation of Amphiphilic Membranes, Springer- Verlag berlin 1992.

Malaquin L:. These de Doctorat, 2009.

Martin D.K.. Nanobiotecnology of Biomimetic membranes, 2207, Springer SBM, LLC.

Matsuzaki, K., Kato K., Yanagisawa K., 2010. Abeta polymerization through inter- action with membrane gangliosides. Biochim. Biophys. Acta 1801, 868–877.

Matsuzaki K., Kato K., Yanagisawa K., 2010. Abeta polymerization through inter- action with membrane gangliosides. Biochim. Biophys. Acta 1801, 868–877.

Mayer L.D., Hope M.J., Cullis P.R., Vescicles of variable sizes produced by a rapid

extrusion procedure, BBA 858 (1986) 161-168.

Mayor S., Rao M., 2004. Rafts: scale-dependent, active lipid organization at the cell surface. Traffic 5, 231–240.

McMahon H.T., Gallop J.L., 2005. Membrane curvature and mechanisms of dynamic cell membrane remodelling. Nature 438, 590–596.

Milner S.T., Safran S.A., Phys. Rev. A 36 (1987) 4371.

Mizuno T., Nakata M., Naiki H., Michikawa M.,Wang R., Haass C., Yanagisawa K., 1999. Cholesterol-dependent generation of a seeding amyloid beta-protein in cell culture. J. Biol. Chem. 274, 15110–15114.

Mouritsen O.G., 2010. The liquid-ordered state comes of age. Biochim. Biophys. Acta 1798, 1286–1288.

Murray R., Granner D., Mayes P., Rodwell V., Membranes: Structure, Assembly & Function in Harper's Biochemistry, Appleton & Lange, New York 1988.

Nelson A 2006 Co-refinement of multiple contrast neutron/X-ray reflectivity data using MOTOFIT *Journal of Applied Crystallography* 39, 273-276.

Pasenkiewicz-Gierula M, Rog T, Kitamura K, Kusumi A 2000 Cholesterol effects on the phosphatidylcholine bilayer polar region: A molecular simulation study *Biophys. J.*, 78, 1376-1389.

Penfold J, Thomas R K 1990 *JPCM* 2, 1369.

Picot C., Weill G., Benoit H. (1968) J. Coll. Int. Sci. 27/3,300.

Prinetti A, Chigorno V, Tettamanti G, Sonnino S, 2000, J.Biol Chem 275, 11658-11665.

Prinetti A., Chigorno V., Tettamanti G., Sonnino S., 2000. Sphingolipid-enriched membrane domains from rat cerebellar granule cells differentiated in culture. A compositional study. J. Biol. Chem. 275, 11658–11665.

Quinn P.J., 2010. A lipid matrix model of membrane raft structure. Prog. Lipid Res. 49, 390–406.

Rahmann H. (ed.), (1987) Gangliosides and Modulation of Neuronal Functions, Springer-Verlag, Berlin.

Raudino A. (1991) Colloid Polym. Sci. 269,1263.

Richter, Finegold, Rapp, 'Sterols sense swelling in lipid bilayers', Physical Review, 1999

Roberts G 1990 Langmuir Blodgett films *Plenum press* New York.

Rondelli V, Fragneto G, Motta S, Del Favero E, Cantù L, 'Reflectivity from floating bilayers: can we keep the structural asymmetry?' J Phys Congress proceedings, in press.

Sackmann E.. *Handbook of Biological Physics*, chapter Physical Basis of Self-Organization and Function of Membranes : Physics of Vesicles, pages 213–303. Elsevier Science B.V., 1995.

Sackmann E., Membrane Bending Energy Concept of Vescicle- and Cell-Shapes and Shape-transitions, FEBS Letters 346 (1994) 3-16.

Sankaram M.B., Thompson T.E., 1990. Interaction of cholesterol with various glycerophospholipids and sphingomyelin. Biochemistry 29, 10670–10675.

Scheffer L., Futerman A.H., Addadi L., 2007. Antibody labeling of cholesterol/ceramide ordered domains in cell membranes. Chembiochem 8, 2286–2294.

Scheffer L., Solomonov I., Weygand M.J., Kjaer K., Leiserowitz L., Addadi L., 2005. Structure of cholesterol/ceramide monolayer mixtures: implications to the molecular organization of lipid rafts. Biophys. J. 88, 3381–3391.

Schmitt J., Danner B., Bayerl T.M. Polymer cushions in supported phospholipid bilayers reduce significantly the frictional drag between bilayer and solid surface. *Langmuir*, 17 :244–246, 2001.

Schneider M.B., J.T. Jenkins, W.W. Webb, J. Phys. France 45 (1984) 1457.

Schroeder F., Jefferson J.R., Kier A.B., Knittel J., Scallen T.J., Wood W.G., Hapala I., 1991. Membrane cholesterol dynamics: cholesterol domains and kinetic pools. Proc. Soc. Exp. Biol. Med. 196, 235–252.

Simons K., and Ikonen E.. 1997. Functional rafts in cell membranes. Nature. 387:569–572.

Simons K., van Meer G., 1988. Lipid sorting in epithelial cells. Biochemistry 27, 6197–6202.

Singer SJ, Nicolson GL Science. The fluid mosaic model of the structure of cell membranes 1972 ,Feb 18;175(4023):720-31.

Sinner E., Knoll W. Functional tethered membranes. *Curr. Op. Chem. Biol.*, 5 : 705–711, 2001.

Smondyrew A M, Berkowitz M L 1999 Structure of dipalmitoylphosphatidylcholine / cholesterol bilayer at low and high cholesterol concentrations: Molecular dynamics simulation *Biophys. J.* 77, 2075-2089.

Snyder B., Freire E., 1980. Compositional domain structure in phosphatidylcholine–cholesterol and sphingomyelin–cholesterol bilayers. Proc. Natl. Acad. Sci. U.S.A. 77, 4055–4059.

Sonnino S., Prinetti A., Mauri L., Chigorno V., Tettamanti G., Dynamic and structural properties of sphingolipids as driving forces for the formation of membrane domains, Chem. Rev. 106 (6) (2006) 2111–2125.

Sonnino S., Cantù L., Corti M., Acquotti D., Venerando B. (1994) Chem. Phys. Lipids 71,21.

Sonnino S., L. Cantu, M. Corti, D. Acquotti, B. Venerando, Aggregative properties of gangliosides in solution, Chem. Phys. Lipids 71 (1994) 21–45.

Sonnino S., Cantù L., Corti M., Acquotti D., Kirschner G. and Tettamanti G. (1990) Chem. Phys. Lipids 52,231.

Sonnino S., Prinetti A., 2008. Membrane lipid domains and membrane lipid domain preparations: are they the same thing? Trends Glycosci. Glycotechnol., 20.

Sonnino S., Prinetti A., Mauri L., Chigorno V., Tettamanti G., 2006. Dynamic and structural properties of sphingolipids as driving forces for the formation ofmem- brane domains. Chem. Rev. 106, 2111–2125.

Spiegel S., Schlessinger J., and Fishman P. H.. 1984. Incorporation of fluorescent gangliosides into human fibroblasts: mobility, fate, and interaction with fibronectin. J. Cell Biol. 99:699–704.

Sprong H., van der Sluijs P., and van Meer G.. 2001. How proteins move lipids and lipids move proteins. Nat. Rev. Mol. Cell Biol. 2:504–513.

Squires G.L.. Introduction to the theory of Thermal Neutron Scattering, 1978. Cambridge Universitu press.

Stewart J.C.M. (1980) Anal. Biochem. 104, 10-14.

Stidder B, Fragneto G, Cubitt R, Hughes A V, Roser S J 2005 Cholesterol Induced Suppression of Large Swelling of Water Layer in Phosphocholine Floating Bilayers *Langmuir* 21, 8703-8710.

Stidder B, Fragneto G, Roser S J 2005 Effect of Low Amounts of Cholesterol on the Swelling Behavior of Floating Bilayers *Langmuir* 21, 9187.

Stryer L., Introduction to Biological Membranes in Biochemistry, W. H. Freeman & C., New York 1988.

Svennerholm L. (1957) BBA 24, 604-611.

Tamm L K, McConnell H M 1985 *Biophys J* 47, 105 1985.

Tanford C. (1963) Physical Chemistry of Macromolecules, Wiley, New York, London.

Tanford C. (1980) The Hydrophobic Effect, Wiley, New York.

Tetrahymena, An X-ray diffraction study. Biochemistry 17, 2005– 2010.

Tettamanti G, Bonali F, Marchesini S, Zambotti V, Biochim Biophys Acta 296, 160 (1973).

Thilo (1977) Biochim. Biophys. Acta 469,326.

Tian A., Baumgart T., 2009. Sorting of lipids and proteins in membrane curvature gradients. Biophys. J. 96, 2676–2688.

Tinker D.O. (1972) Chem. Phys. Lipids 8.

Tokumasu, Jin, Dvorak, 'Lipid membrane phase behaviour elucidated in real time by controlled environment atomic force microscopy', J. of Elecron Microscopy, 2002

Townsend R.R. (ed.), (1996) Techniques in Glycobiology, Marcel Dekker New York.

Tu K C, Klein M L, Tobias D J 1998 Constant-pressure molecular dynamics investigation of cholesterol effects in a dipalmitoylphosphatidylcholine bilayer *Biophys. J*., 75, 2147-2156.

Van Meer G., 2011a. Dynamic transbilayer lipid asymmetry. Cold Spring Harb. Perspect. Biol., 3.

Van Meer G., Voelker D.R., Feigenson G.W., 2008. Membrane lipids: where they are and how they behave. Nat. Rev. Mol. Cell Biol. 9, 112–124.

Vid J R 1985 *Vac. Sci. Tecnol. A* 3, 3, 1027.

Wacklin H, Tiberg F, Fragneto G, Thomas R 2005 Composition of supported model membranes determined by neutron reflection *Langmuir* 21, 2827-2837.

Wacklin Hanna P. , Campbell Richard A. , Cubitt Robert, Fragneto Giovanna ‘Scientific Highlights from FIGARO's First Year’ Neutron News Volume 21, Issue 2, 2010.

Wang R., Shi J., Parikh A. N., Shreve A. P., Chen L., and Swanson B. I.. 2004. Evidence for cholera aggregation on GM1-decorated lipid bilayers. Colloids Surf. B Biointerfaces. 33:45–51.

Wood W.G., Igbavboa U., Muller W.E., Eckert G.P., 2011. Cholesterol asymmetry in synaptic plasma membranes. J. Neurochem. 116, 684–689.

Wunderlich F., Ronai A., Speth V., Seelig J., Blume A., 1975. Thermotropic lipid clustering in tetrahymena membranes. Biochemistry 14, 3730–3735.